Universität Rostock Traditio et Innovatio

Annexin A1 as a new functional linker between actin filaments and phagosomes during phagocytosis

Dissertation
zur
Erlangung des akademischen Grades
doctor rerum naturalium (Dr. rer. nat.)
der Mathematisch-Naturwissenschaftlichen Fakultät
der Universität Rostock

vorgelegt von
Devang Patel
aus Ahmedabad, India

Rostock, September 2010

urn:nbn:de:gbv:28-diss2011-0019-0

Gutachter:

PD Dr. Sergei A. Kuznetsov, University of Rostock, Germany

Prof. Dr Gareth Griffiths, University of Oslo, Norway

Datum des Wissenschaftlichen Kolloquium: 10.01.2011

મારા પરિવાર ને અર્પણ

(To my Family)

Table of Contents

1. Summary

Remodelling of the actin cytoskeleton plays a key role in particle internalisation and phagosome maturation processes. Actin binding proteins (ABPs) are the main players in actin remodelling, but the precise role of these proteins in phagocytosis needs to be investigated. Annexins, a group of ABPs, are found to be present on phagosomes.

In the current study I identified annexin A1 as a factor, which binds to isolated latex bead phagosomes (LBP) in the presence of Ca^{2+} and facilitates F-actin-LBP interaction *in vitro*. In macrophages the association of endogenous annexin A1 with gelatin-LBP membranes is strongly correlated with the spatial and temporal accumulation of F-actin at the gelatin-LBP. Annexin A1 was found on phagocytic cups and around early phagosomes, where the F-actin prominently concentrated. After uptake was completed, annexin A1 along with F-actin dissociated from the nascent LBP surface. At later stages of phagocytosis annexin A1 transiently concentrated only around those gelatin-LBP, which showed transient F-actin accumulation ("flashing"). Reduction of annexin A1 expression resulted in impaired phagocytosis and actin flashing. These data identify annexin A1 as an important component of phagocytosis that appears to link actin accumulation to different steps of phagosome formation.[1]

Moreover, I also proved that receptor signalling regulates annexin A1 recruitment on different phagosomes. Annexin A1 was present on Fc-LBP but not on man-LBP. Although in *in vitro* condition annexin A1 was able to stimulate F-actin-LBP interaction for all tested LBP, knockdown experiments reviled that annexin A1 is important for well defined FcRs mediated phagocytosis but not in mannose receptor mediated phagocytosis. Furthermore, extracellular annexin A1 also had distinct effect on different receptor mediated phagocytosis. Extracellular annexin A1 strongly reduces Fc-beads internalisation but equally stimulates man-beads phagocytosis.

Obtained results demonstrate that annexin A1 is important for different stages phagocytosis and have different role in different receptors mediated phagocytosis.

[1] Paper submitted to Journal of Cell Sci. and currently in press

2. Introduction

2.1. Phagocytosis

Eukaryotic cells internalise a variety of particles during their lifetime. Cells have evolved a variety of strategies to internalise particles and solutes, including pinocytosis, receptor-mediated endocytosis and phagocytosis (Underhill and Ozinsky, 2002; Vieira et al., 2002)). The uptake of particles >0.5 μm in size is termed phagocytosis (Greek: *phago*-eating, *cyte*-vessel and *osis*-process), whereas particles <0.5 μm are taken up by receptor-mediated endocytosis or pinocytosis. Receptor mediated endocytosis is a specific process through which macromolecules, viruses and small particles are internalised in the cells. Pinocytosis usually refers to the uptake of fluid and solutes. Pinocytosis and receptor-mediated endocytosis share a clathrin-based mechanism and usually occur independently of actin polymerisation. By contrast, phagocytosis occurs by an actin-dependent mechanism and is usually independent of clathrin.

Although primitive organisms use phagocytosis primarily for acquisition of nutrients, phagocytosis in metazoans occurs in specialised phagocytic cells, such as macrophages, dendritic cells and neutrophils. Although a large number of mammalian cell types are capable of phagocytosis, their phagocytic efficiency varies greatly. To distinguish this varying ability, terms non-professional phagocytes, para-professional phagocytes and professional phagocytes used which referring to cells with low, average and high phagocytic competence respectively (Rabinovitch, 1995). Professional phagocytes include mainly neutrophils and cells of the monocytic/macrophage lineage, sentinels of the immune system that hunt and destroy any foreign particles, apoptotic or defective host cells. Professional phagocytes have evolved into an extraordinarily complex process underlying a variety of critical biological phenomena. In addition to internalisation and degradation of pathogenic microbes, professional phagocytes trigger activation of the innate and adaptive immune response after antigen presentation at the surface of the phagocytic cell.

In mammals professional phagocytes can be divided in to two groups: mononuclear phagocytes and polymorphonuclear phagocytes. Mononuclear cells include macrophages, monocytes and dendritic cells, while second group includes neutrophils which are short living cells. Macrophages are long-living cells that can be located in different tissues, such as the connective tissue, the sub-mucosa of the gastro-intestinal tract, the lungs, the liver, the central nervous system, bones and throughout the spleen, where they remove senescent blood cells (Janeway et al. 2004). All those cell types originate from pluripotent stem cells

present in the bone marrow that differentiate in response to hematopoietic factors. After differentiation, mononuclear phagocytes are released in the blood and remain circulating as monocytes, unless they are recruited to sites of inflammation by chemotactic signals and become macrophages which enter the tissues.

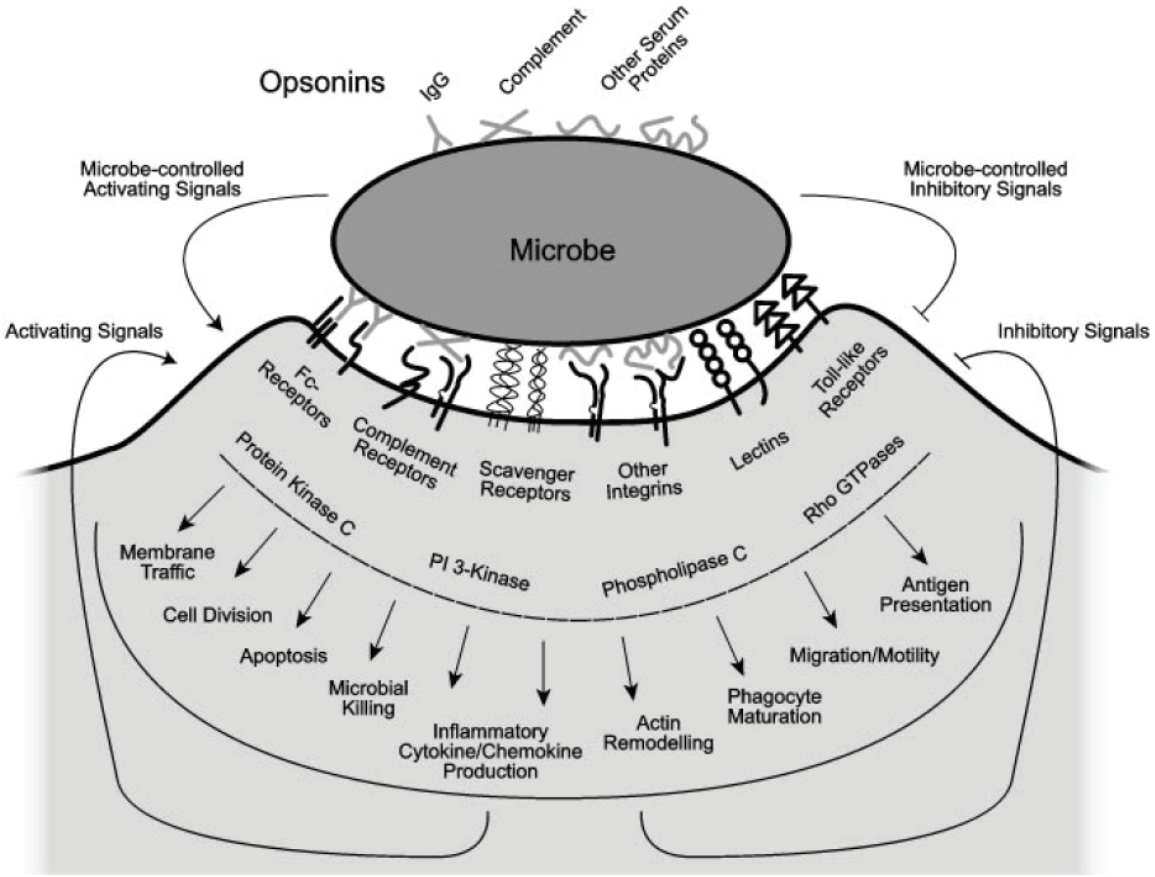

Figure 1 Receptor and signalling interactions during phagocytosis of microbes. Multiple receptors simultaneously recognise microbes both through direct binding and by binding to opsonins on the microbe surface. Receptor engagement induces many intracellular signals, and several molecules are utilised in many pathways. Signalling during phagocytosis may subsequently serve to activate or inhibit further phagocytosis and microbe-induced responses. adapted from (Underhill and Ozinsky, 2002)

2.1.1. Phagocytic receptors

Phagocytosis is initiated by the interaction of surface receptors with their cognate ligand. Ligands can be endogenous components of the particle, exemplified by lipopolysaccharides of bacteria and phosphatidylserine in apoptotic cells. Internalisation triggered by endogenous ligands of the particle is known as non-opsonic (Ofek et al., 1995). The immune system is equipped with a variety of receptors that recognise non-opsonic ligands, including CD14 that binds to lipopolysaccharides, as well as receptors that recognise specifically phosphatidylserine, mannose or fucose residues (Schutt, 1999). Other

class of the ligands are known as opsonins, which are host-derived proteins that coat the surface of a particle. The best characterised opsonins are the complement fragment C3b, iC3b and IgG antibodies. C3b and iC3B bind relatively non-specifically to the surface of foreign particles, whereas IgG molecules attach to the phagocytic target by recognising specific surface epitopes. C3b or iC3b-opsonised particles are recognised by complement receptors members of the integrin super family, while IgG-opsonised particles engage FcγRs (Kwiatkowska and Sobota, 1999). In any case, receptor engagement leads to internalisation of the particle into a phagosome by a complex sequence of events that require kinase activation, alterations in phospholipids metabolism, remodelling of the actin cytoskeleton and acceleration of membrane traffic (Kwiatkowska and Sobota, 1999).

2.1.1.1. Fc receptors

In mammals, binding of immunoglobulins (Igs) to foreign particles (opsonisation) leads to the prompt clearance of those particles from the organism. The conserved Fc-domains of the Igs are recognised by Fc receptors (FcRs) present on professional phagocytes, such as macrophages and neutrophils. An opsonised particle binds to Fc-receptors and is rapidly internalised by an actin-dependent extension of the plasma membrane around the opsonised particle. This process is accompanied by the production of proinflammatory and toxic molecules, such as the production of superoxide and the release of cytokines from the phagocytic cell (Garcia-Garcia and Rosales, 2002). The major Ig opsonin is IgG, which binds to the corresponding Fc-gamma-receptors (FcγRs), although IgA and IgE also have cognate Fc receptors (FcαRs and FcεRs, respectively) that are involved in phagocytosis (Swanson and Hoppe, 2004). There are three classes of FcγRs: FcγRI, FcγRII and FcγRIII. Each class consists of several receptor isoforms which are the product of different genes and splicing variants (Ravetch and Bolland, 2001). Except FcγRIIIA and all the other FcRs, FcγRIIIB lacks a transmembrane region and a cytoplasmic tail. This receptor is anchored to the membrane by a glycol-phosphatidylinositol moiety (Garcia-Garcia and Rosales, 2002; Ravetch and Bolland, 2001; Swanson and Hoppe, 2004).

2.1.1.2. Complement receptors

Another major group of receptors that mediate phagocytosis by professional phagocytes is the complement receptors. Complement-receptor-mediated phagocytosis is morphologically distinct from that mediated by FcRs, although both processes require actin

polymerisation. Complement-opsonised particles get internalised, with minimal membrane disturbance and this does not usually lead to an inflammatory response or the generation of superoxide (Ofek et al., 1995; Smith et al., 1999).. The complement system is evolutionarily much older than adaptive immunity and is present even in simple organisms such as sea urchins and yet still represents an important part of the innate immune system in higher organisms, including humans (Smith et al., 1999). C3b is well characterised molecule that can bind to molecules on microbial surfaces and acts like an opsonin and is recognised by the complement receptor 1 (CR1). C3b can be further modified by plasma factors H and I, which convert it to iC3b. iC3b is a very potent opsonin that can be recognised by the CR3 and CR4. The complement receptors CR1, CR3 and CR4, are expressed on macrophages and neutrophils and are capable of mediating phagocytosis (Ofek et al., 1995; Smith et al., 1999).

2.1.1.3. Mannose receptor

The mannose receptor (MR) (CD206) is a type-I transmembrane protein that is characterised as a Group VI C-type lectin. It shares the same overall structure with three other receptors (phospholipase A2 receptor, ENDO 180 and DEC205) which together are known as the MR family (Stahl and Ezekowitz, 1998). The MR on macrophages recognises mannose and fucose on the surfaces of pathogens and mediates phagocytosis of the organisms. The high affinity of this receptor for branched mannose and fucose oligosaccharides makes the MR a phagocytic receptor with broad pathogen specificity. Structurally, it consists of an extracellular region containing an amino terminal cysteine rich domain, a fibronectin type II repeat domain, eight CTLDs, a transmembrane region and a short cytoplasmic tail. The cytoplasmic tail is crucial to both the endocytic and phagocytic functions of the receptor, but little is known about the signals that lead to phagocytosis (East and Isacke, 2002; Stahl and Ezekowitz, 1998).Its expression was originally thought to be restricted to mammalian tissue macrophages but it is now known to be expressed on lymphatic and hepatic epithelium, kidney mesangial cells, tracheal smooth muscle cells and retinal pigment epithelium. Expression has also been observed on human monocyte-derived DCs (East and Isacke, 2002; Stahl and Ezekowitz, 1998) Several studies suggested that exclusive activation of the mannose receptor cannot induce phagocytosis and other co-receptors are usually needed (Kang et al., 2005; Taylor et al., 2005). In addition to this, depending on the recognised ligands, also proinflammatory signals can be also generated upon MR ligation (East and Isacke, 2002; Stahl and Ezekowitz, 1998).

Other than above the mentioned receptors there are many other receptors are reported to be involved in phagocytic process. Ligands binding to their cognate receptors trigger the cellular signalling which decides the fate and composition of the phagosome. Every receptors generate a unique signature on the phagosome (Hoffmann et al., 2010).

2.1.2. Phagocytic signalling

The signalling pathways elicited by a wide array of membrane receptors involve tyrosine phosphorylation cascades, followed by activation of many down-stream signalling molecules. Phagocytosis involves tyrosine kinases in many cases, although the need for tyrosine kinases may not be a requirement for all phagocytic systems.

Phagocytosis mediated by FcRs is largely mediated by kinases of the Src and Syk/Zap70 families. FcR ligand interaction induces the phosphorylation of specific tyrosine residues located within special amino acid motifs, named Immunoreceptor Tyrosine-based Activation Motifs (ITAMs) on the cytoplasmic portion of FcyRIIA and on accessory chains that associate with other FcRs (Garcia-Garcia and Rosales, 2002). ITAM phosphorylation by enzymes of the Src tyrosine-kinase family promotes Syk docking to ITAMs and Syk activation. There is abundant genetic and biochemical evidence supporting the role for Src and Syk family kinases in the regulation of FcγR-mediated phagocytosis (Garcia-Garcia and Rosales, 2002; Kwiatkowska and Sobota, 1999; Niedergang and Chavrier, 2004). Although some members of the Src kinase family have been found associated to specific FcRs, it is currently not clear whether this association is related to receptor-specific signalling pathways. It is also possible that all kinases of the Src family converge into a common signalling pathway that regulates phagocytosis (Groves et al., 2008).

Participation of tyrosine kinases in CR-mediated phagocytosis is controversial. Early reports demonstrated that phagocytosis of complement-opsonised zymosan (yeast cell wall) and of complement-opsonised erythrocytes is unaffected by tyrosine kinase inhibitors (Groves et al., 2008; Kwiatkowska and Sobota, 1999; Niedergang and Chavrier, 2004). This ruled out the participation of tyrosine kinases in this type of phagocytosis. This notion is further supported by the fact that macrophages from $Syk^{-/-}$ mice show normal levels of CR-mediated phagocytosis (Kiefer et al., 1998). However, β2 integrin stimulation by adhesive ligands, or by artificial integrin cross-linking with antibodies induces various cellular responses in a Src and/or Syk kinase-dependent manner (Mayadas and Cullere, 2005).

Additionally, it was reported that CR4-mediated phagocytosis of *Mycobacterium tuberculosis* induced tyrosine phosphorylation of several proteins. However, the direct involvement of tyrosine phosphorylation in CR4-mediated phagocytosis was not evaluated. Whether tyrosine kinases are indeed dispensable during CR-mediated phagocytosis remains unclear.

There are several proteins reported to be involved in signalling during the phagocytosis. Below I summarised the role of some important signalling molecules during Fc receptor (FcR), complement receptor (CR) and apoptotic cell receptor mediated phagocytosis.

Signalling Molecule	**FcR**	**CR**	**ACR**
Phosphatidylinositol 3 Kinase	+	+	+
Protein Kinase C	+	+	+
Phospholipase A2	+	+	N.D.
Phospholipase Cγ	+	-	+/-
Phospholipase D	+	-	N.D
Extracellular signal regulated Kinase	+	+/-	+/-

(+ = important, - = Not important, +/- Not clear, N.D. = not evaluated)

Much work remains to be done in describing the signalling pathways elicited by many phagocytic receptors. In particular a detailed understanding of the signalling pathways regulating CR-mediated phagocytosis, mannose receptor and phagocytosis of apoptotic cells is still lacking (Aderem and Underhill, 1999).

2.1.3. Phagosome maturation

Once internalised with help of actin dynamics (explained bellow), the phagosome matures via a series of fusion and fission events with endocytic pathway. The actin filaments that surround newly internalised phagosomes rapidly depolymerise, which leaves the phagosome membrane available to fuse with endosomes and lysosomes. The phagosomal membrane undergoes a progressive maturation, and its composition changes, first containing components of the plasma membrane, then early endosomes and subsequently acquiring markers found in the late endosome and lysosome compartments. In general, the earliest markers seen within the first few minutes after sealing of the phagosome include rab5, EEA1, PIP2 and other components of the early endosomes (Aderem and Underhill, 1999; Araki, 2006; Castellano et al., 2001; Hoffmann et al., 2010; May and Machesky, 2001).

Consistent with the acquisition of the proton pump, acidification of the phagosome rapidly occurs. Loss of the plasma membrane and endosomal proteins then coincides with the acquisition of late endosome/lysosome components. These include lysosome-associated membrane proteins (LAMPs), rab7, cathepsin D and other hydrolytic enzymes. During this period the pH of the phagosome continues to drop to levels consistent with the lysosome (pH 5) (Aderem and Underhill, 1999; Araki, 2006; Haas, 2007; Hoffmann et al., 2010; Vieira et al., 2002). The timing of these steps appears to depend on the type of particle being ingested and the nature of the receptors being engaged. Latex beads are particularly slow and this slow time-course has been useful in characterising the mechanisms of membrane delivery to the phagosome (Haas, 2007; Hoffmann et al., 2010; Underhill and Ozinsky, 2002; Vieira et al., 2002).

2.2. Actin cytoskeleton during phagocytosis

Much work remains to be done in describing the signalling pathways elicited by many phagocytic receptors. However, phagocytosis appears to be regulated by key signalling molecules that are shared by most phagocytic systems. In the end, however, all phagocytic systems must exploit the dynamic nature of the cytoskeleton to achieve particle internalisation. Phagocytic signalling pathways, in all systems, are designed to activate many cytoskeleton-remodelling molecules. The actin and microtubule cytoskeletons participate in the phagocytic process in different ways. The actin cytoskeleton is required for pseudopod extension, and as a structural framework for myosin-driven phagosome internalisation. On the other hand, the microtubule cytoskeleton appears to be necessary for local activation of Rho family GTPases at sites of phagosome formation. Different phagocytic systems show particular cytoskeleton requirements to achieve particle internalisation.

One of the earliest differences observed between different phagocytic systems were structural. These differences were found through microscopy studies. FcγR-mediated phagocytosis and apoptotic cell phagocytosis occur with extensive pseudopod extension surrounding the phagocytic targets. CR-mediated phagocytosis, in contrast, occurs in the absence of pseudopod extension, and complement-opsonised phagocytic targets appear to rather sink into the cell. These differences may reflect the cytoskeletal requirements for particle internalisation. The actin cytoskeleton is required for particle internalisation by FcγR,

and also by receptors for apoptotic cells, whereas CR-mediated phagocytosis depends on the actin and microtubule cytoskeletons.

2.2.1. Rho family GTPases and actin dynamics

Signalling elements critical to the control of actin reorganisation during a variety of phagocytic signalling processes are the Rho GTP-binding proteins. Rho family GTPases play a key role in the biochemical regulation of the actin and possibly microtubule cytoskeletons during phagocytosis (Chimini and Chavrier, 2000; Niedergang and Chavrier, 2005). The mechanism of activation of Rho family GTPases involves the transition from an inactive, GDP-bound, to an active GTP-bound state. This transition is catalysed by guanine nucleotide-exchange factors (GEFs) (Niedergang and Chavrier, 2005). When activated and bound to GTP, they interact with downstream effectors, for example to mediate Arp2/3 recruitment and actin polymerisation during phagocytosis. Inactive GDP-bound, Rho-family G proteins are thought to be cytosolic and bound to a guanine dissociation inhibitor (GDI)(Chimini and Chavrier, 2000; Niedergang and Chavrier, 2005).

Vav and p190RhoGEF are GEFs that are implicated in phagocytosis. Differential use of these GEFs has been observed among phagocytic systems (Groves et al., 2008; May and Machesky, 2001; Niedergang and Chavrier, 2005). Vav participates in FcγR-mediated phagocytosis, but not in CR-mediated phagocytosis (Groves et al., 2008; May and Machesky, 2001; Niedergang and Chavrier, 2005). During FcγR-mediated phagocytosis Vav is recruited to sites of phagosome formation where it specifically activates Rac. CR-mediated phagocytosis, on the other hand, appears to depend on p190RhoGEF (Groves et al., 2008; May and Machesky, 2001; Niedergang and Chavrier, 2005). Interestingly, pl90RhoGEF has been shown to interact with the microtubule cytoskeleton. Activation of Rho family GTPases during apoptotic cell phagocytosis, on the other hand, appears to be mediated by phosphorylation-dependent adapter molecules with associated GEF activity, such as $p130^{cas}$, CrkII, Dockl80, and ELMO-1 (Chimini and Chavrier, 2000). FcγR-mediated phagocytosis is regulated by the Rho family members Rac and Cdc42, but apparently not by Rho. In contrast, phagocytosis of complement-opsonised targets depends on Rho, but is independent of Rac and Cdc42 (Caron and Hall, 1998). However, when the lectin site on CR3 is engaged by microorganism-derived sugar ligands, phagocytosis proceeds in a Rac/Cdc42 dependent

manner and is accompanied of extensive pseudopod extension, structurally resembling FcγR-mediated phagocytosis (Chesarone and Goode, 2009).

2.2.2. Actin polymerisation and nucleation at sites of phagosome formation

A predominant feature of phagocytosis is the accumulation of actin and associated proteins at the base of the forming phagosome. It has long been recognised that remodelling of actin filaments is required for efficient particle internalisation and studies of the regulation of actin reorganisation have identified several proteins and lipids with direct roles in this process. Rho family GTPases have a fundamental role in the regulation of the formation of actin filaments that are necessary for pseudopod extension, and for myosin-driven particle internalisation. Rho family GTPases promote actin polymerisation at sites of phagocytosis by recruiting actin nucleation-promoting factors (NPFs), and the actin-nucleating complex Arp2/3 (Baum and Kunda, 2005; May and Machesky, 2001). While NPFs induce the activation of the Arp2/3 complex, the latter has a direct role in the formation and branching of new actin filaments. Although the recruitment of NPFs at sites of phagosome formation could be achieved through different ways among phagocytic systems, all of them require the activity of the Arp2/3 complex for particle internalisation. Arp2/3 recruitment to forming phagosomes can be achieved by its interaction with NPFs, with adapter molecules, or with some myosin isoforms (Castellano et al., 2001; Chesarone and Goode, 2009; May and Machesky, 2001)

In the FcγR phagocytic system, active Rac and Cdc42 at forming phagosomes induce the local recruitment of the hematopoietic-specific NPF WASP (Wiskott-Aldrich Syndrome Protein). WASP recruitment to forming phagosomes may be mediated through its direct interaction with active Rac/Cdc42. WASP recruitment then results in Arp2/3 activation at these sites. Active Arp2/3 in turn regulates the formation of actin fibres that are necessary for pseudopod extension (Castellano et al., 2001; Chesarone and Goode, 2009; Garcia-Garcia and Rosales, 2002; May and Machesky, 2001).

The participation of WASP in CR-mediated phagocytosis has not been evaluated. However, CR-mediated phagocytosis does depend on Arp2/3 recruitment to forming phagosomes. During CR-mediated phagocytosis the Arp2/3 complex is recruited in a Rho-dependent manner. In this system Arp2/3 recruitment to forming phagosomes is a down-stream event, occurring after activation of the Rho kinase-myosin II signalling pathway.

Additionally, Arp2/3 may be recruited to forming phagosomes by its interaction with myosin I, the only myosin isoform known to directly interact with Arp2/3. Because phagocytosis by CRs proceeds in the absence of pseudo-pod extension, the most likely role for actin filaments in this system, is to provide the structural framework for myosin-driven phagosome internalisation (Castellano et al., 2001; Chesarone and Goode, 2009; May and Machesky, 2001)

2.2.3. Actin driven phagosome internalisation

In addition to the role of actin polymerisation for pseudopod extension, actin filaments provide the structural framework for the myosin-driven contractile activity, necessary for particle internalisation (May and Machesky, 2001). This actin-dependent contractile activity is mediated by several myosin isoforms. Myosins are motor-proteins that couple their ATPase activity to movement along actin filaments (Castellano et al., 2001). By coupling its movement to adapter molecules, myosins can thus regulate the transport of vesicles, organelles and other particles along actin filaments. Several myosin isoforms have been found located around phagosomes, suggesting that some of them are required for phagosome internalisation (Chesarone and Goode, 2009).

Myosin II appears to be required for FcγR-mediated phagocytosis.[1] ' Pharmacological inhibition of myosin II, or of its upstream activator MLCK results in phagocytosis arrest. Other myosin isoforms, including myosin IC, myosin V and myosin IXb, have been found located around phagosomes during FcγR-mediated phagocytosis. It is thus possible that at least one of them participates in phagosome internalisation (Araki, 2006). CR-mediated phagocytosis also depends on myosin II activity. Myosin I has also been found located around phagosomes during CR-mediated phagocytosis. Additionally to the possible role for these myosin isoforms in phagosome internalisation, they may also participate in actin fibre formation by recruiting the Arp2/3 complex at forming phagosomes. The myosin isoforms required for phagosome internalisation during apoptotic cell phagocytosis have not yet been identified (Castellano et al., 2001; Chesarone and Goode, 2009; May and Machesky, 2001)

2.2.4. Actin severing and depolymerisation

During phagocytosis, as in many actin-dependent cellular processes, actin dynamics are not restricted to nucleation and polymerisation but are also regulated by

capping/uncapping, depolymerisation and severing (Wear et al., 2000). Disassembly of actin filaments occurs both during internalisation, albeit at very low levels, and after completion of uptake. In any case, every stage of actin disassembly requires a precise spatial and temporal coordination of an array of actin depolymerising proteins. Yet, it appears that it is not just the presence of specific functional proteins but also the absence and/or depletion of signalling molecules previously involved in earlier stages of phagocytosis, that contribute to the control of actin disassembly. Prompt disappearance of F-actin from phagosomes has been observed in *Dictyostelium* and in mammalian phagocytes; following closure of the phagocytic cup (Chesarone and Goode, 2009; Dominguez, 2009; Wear et al., 2000). The hydrolysis of phosphatidylinositol 4, 5 bis-phosphate (PIP2) from the phagosomal membrane that coincides with the dissociation of the actin network (Chesarone and Goode, 2009; Dominguez, 2009; Wear et al., 2000). This is consistent with the idea that optimal WASP/N-WASP-induced, Arp2/3-dependent actin polymerisation depends on two inputs on WASP: active Cdc42 and PIP2. Cdc42 activity need not be terminated; if WASP is no longer localised or activated by PIP2, it will not be able to bind and activate the Arp2/3 complex, halting actin nucleation and polymerisation (Chesarone and Goode, 2009; Dominguez, 2009).

2.2.5. The role of the cytoskeleton during phagosomal maturation

Compartments of the endocytic/exocytic pathway occupy characteristic locations within cells. The intracellular location of these compartments, as well as the traffic between them, is dependent upon the integrity of the microtubule network. In an analogous manner, the maturing phagosomal compartment is dependent upon the microtubule network for its transformation into a phagolysosomes. After a phagosome is formed at the cell periphery, it is transported toward the interior of the cell in a microtubule-dependent fashion. While phagosome motility has been observed in both directions along microtubules, dynein-mediated minus-end-directed movement seems to predominate over kinesin-mediated plus-end-directed movement, consistent with the centripetal movement of phagosomes observed in cells. The association of phagosomes with microtubules appears to be necessary for their maturation, as indicated by decreases in phagosomal acquisition of late-endosomal and lysosomal markers, including LAMP-2, (Desjardins et al., 1994b; Desjardins et al., 1994a) and by inhibition of phagosome-lysosome fusion in cells treated with microtubule depolymerising agents (Blocker et al., 1996). The mechanism by which phagosomes associate

with microtubules is yet to be discovered. One possibility is through members of the rab family of GTPases discussed above. Rab4a, rab5 and rab11 have been shown to associate with phagosomes and have demonstrated interactions with microtubules (Chimini and Chavrier, 2000).

Reorganisation of the actin-based cytoskeleton is important during phagosomal maturation as well as phagosome formation. As in the case of microtubules described above, actin microfilaments appear to play a role in the centripetal movement of phagosome after their formation. While small phagosomes (approximately 1 μm in diameter) can move along microtubules, a mechanism for phagosomal motility has been proposed that implicates myosin in the generation of force to move larger phagosomes along actin filaments (May and Machesky, 2001; Toyohara and Inaba, 1989). It has also been proposed that assembly of actin filaments on the surface of the phagosome could generate motility (Defacque et al., 2000). In this model, members of the ezrin, radixin, moesin (ERM) family of proteins are described as regulators of actin nucleation that may initiate the formation of actin structures on the surface of phagosomes. This model is supported by the demonstration that ezrin and moesin can nucleate F-actin assembly on the surface of phagosomes *in vitro* (Defacque et al., 2000). In addition to supporting phagosomal motility, F-actin filaments may contribute to the maturation of the fully formed phagosome by facilitating the delivery of other endosomal compartments to the phagosome. Studies in an *in vitro* system suggest that an appropriate level of actin filament assembly is required to allow phagosome-endosome fusion. Enough actin filaments are needed, emanating from the phagosome, for the efficient transport of endosomes to the phagosome (Jahraus et al., 2001a). An excess of F-actin around the phagosome, however, might impede the delivery of endosomes and retard biogenesis of the phagolysosomes. While much remains to be learned about this process *in vivo*, it is becoming clear that dynamic actin structures are prominent and functionally important features through the entire existence of a phagosome/phagolysosomes.

Till date significant amount of work has been done to understand role of actin (in both form: globular and filamentous) but still functions of many actin binding proteins yet to be discovered. For example, localisation five annexins (including known actin binder annexin A1 and annexin A2) was discovered almost a decade ago (Diakonova et al., 1997) but still we do not know their functional importance during phagocytosis.

2.3. Annexins

Annexins were discovered approximately 25 years ago. The first to be described as an isolated, purified protein was human annexin A7 (known as synexin) (Creutz et al., 1978). Annexins are a family of cytosolic Ca^{2+}-binding proteins characterised by non-EF hand or type II Ca^{2+} binding sites. Ca^{2+}-binding enables annexins to interact with membranes containing acidic phospholipids and Ca^{2+} dependent phospholipid binding is considered the unifying biochemical property in the annexin family. As Ca^{2+} dependent phospholipid binding proteins have emerged from multiple areas of investigation during the 1980s, they have been called by many different names (Table 1). In 1990, Crumpton and Dedman, with the agreement of most of the groups working in this field, developed a new nomenclature (Crumpton and Dedman, 1990). They are now called 'annexins'(Greek *annex* – to bind) since their main property is to bind to cellular membranes in a Ca^{2+} dependent manner. Till date 12 annexins common to vertebrates were recently classified in the annexin A family and named as annexins A1-A13 (Moss, 1992; Raynal and Pollard, 1994). Annexins outside vertebrates are classified into families B (in invertebrates), C (in fungi and some groups of unicellular eukaryotes), D (in plants), and E (in protists); at least 40 additional subfamilies await formal classification into these families.

2.3.1. Annexins structure

All annexins display similar properties regarding Ca^{2+} and phospholipid is due to a common primary structure. Each annexin is constituted of two different regions, the unique N-terminal domain, also called tail and the C-terminal domain named core domain. The core domain made up of four similar repeats, each approximately 70 amino acids long. Each repeat is made up of five α helices and usually contains a characteristic 'type 2' motif for binding calcium ions with the sequence 'GxGT-[38 residues]-D/E' (Figure 2A). Annexins bind to a wide variety of other proteins. Many annexins have posttranslational modifications, such as phosphorylation and myristoylation (Figure 2B); such modifications and surface remodelling of individual members presumably account for much of the subfamily specificity in annexin interactions (Gerke and Moss, 2002). The core domains of most vertebrate annexins have been analysed by X-ray crystallography, revealing conservation of their secondary and tertiary structures despite only 45-55% amino-acid identity among individual members. Each annexin repeat is folded into five α helices and

Table 1: Nomenclature of the annexins (Moss, 1992; Raynal and Pollard, 1994)

Annexin	Synonym	kDa
A1	lipocortin I (lipomodulin, macrocortin, renocortin)	38.6
	p35 (EGF receptor substrate)	
	calpactin II	
	chromobindin 9	
A2	calpactin 1 heavy chain	38.5
	p36 (pp60src substrate)	
	protein I	
	lipocortin II	
	chromobindin 8	
A3	lipocortin III	36.2
	placental anticoagulant protein (PAP)-lll	
	35-~-calcimedin	
	calphobindin III	
	inositol- 1,2-cyclic-phosphate 2-hydrolase	
A4	endonexin I	35.7
	chromobindin 4	
	placental anticoagulant protein (PAP)-II	
	placental protein PP4-X	
	lipocortin IV	
A5	placental anticoagulant protein (PAP)-I	35.8
	endonexin II	
	placental protein PP4	
	calphobindin 1	
	lipocortin V	
A6	p68	75.7
	67K-calelectrin	
	protein III	
	calphobindin II	
	Synhibin	
	lipocortin VI	
A7	synexin	50.2
A8	vascular anticoagulant (VAC)/3	36.7
A9	*Drosophila melanogaster* annexin	32.9
A10	*Drosophila melanogaster* annexin	35.6
A11	calcyclin-associated annexin (CAP)-50	53.9
A12	*Hydra vulgaris* annexin	35
A13	intestine-specific annexin (ISA)	35.3

these in turn are wound into a right handed super-helix. The four repeats pack into a structure that resembles a flattened disc, with a slightly convex surface. The more convex side contains novel types of Ca^{2+} binding sites, the so-called type II and type III sites, and faces the membrane when an annexin is associated peripherally with phospholipids. The more concave side points away from the membrane and thus appears accessible for interactions with the NH2-terminal domain and/or possibly cytoplasmic binding partners (Gerke and Moss, 2002; Moss, 1992; Moss and Morgan, 2004; Raynal and Pollard, 1994)

In contrast to the core domain, the sequence of the N-terminal domain is extremely variable, although with a few exceptions. The length N-terminal varies from a few amino acids, in annexin A4 and 5 to more than 160 in annexin A7 and 11. In these structures, the NH2-terminal sequences extend along the concave side of the molecule partially engaged in hydrophobic interactions with the protein core. Thus it appears that the short NH2-terminal domains of the smaller annexins, affect the Ca^{2+} dependent phospholipid binding executed by the convex, or opposite, side possibly through stabilising or destabilising slightly different conformations of the molecule. This underlines the regulatory importance of even the small NH2-terminal domains, which previously been postulated due to the presence of sites for posttranslational modifications (Gerke and Moss, 2002; Moss, 1992; Moss and Morgan, 2004; Raynal and Pollard, 1994). Variable N-terminal sequences resulted in significantly altered properties could functional diversity among highly conserved annexins. The N-terminus of annexins A1 and A2 also display some similarities; except for an intervening 11 residue sequence (Figure 2B). Annexin A2 binds an 11 kDa protein related to the S100A10 family of Ca^{2+} binding protein through residues located in its 'tail'. The resulting 90 kDa complex (2 subunits of annexin A2 and 2 of p11/S100A10) is much more sensitive to Ca^{2+} than monomeric annexin A2 for interaction with phospholipids (Gerke and Moss, 2002; Moss, 1992). In the case of annexin A1, covalent dimers described in placenta appeared to be produced by transglutaminase that cross-links residues localised within the proteinase sensitive N-terminal 29 amino acids of annexin A1. The functional implications of this modification are yet to be discovered. Post-translation modification on N-terminal sequence has a great impact on annexins activities (Moss and Morgan, 2004; Raynal and Pollard, 1994).

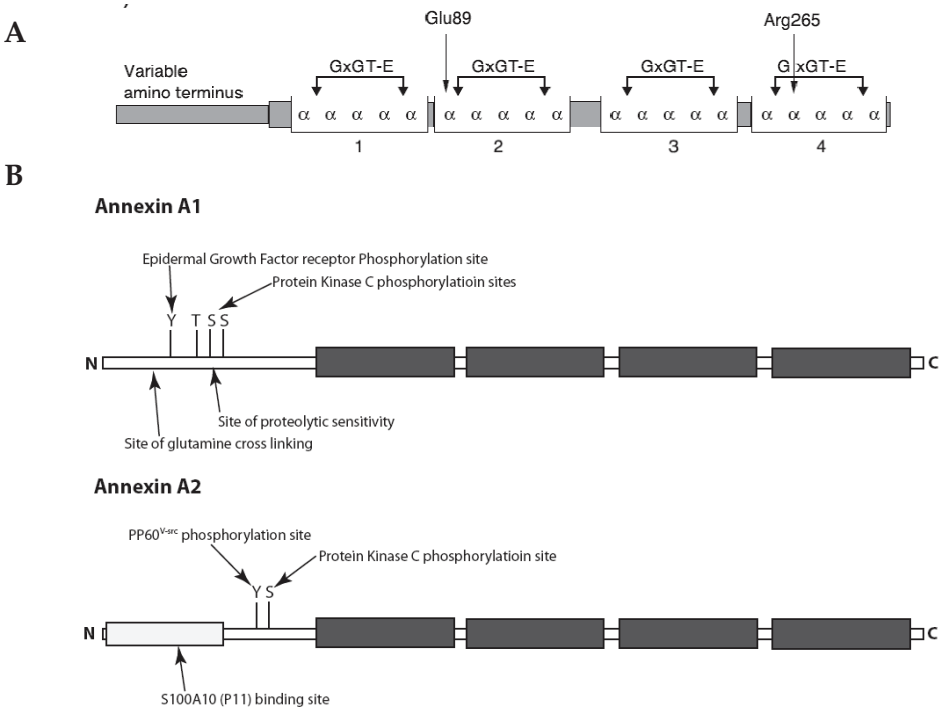

Figure 2: Structure of annexins: (A) Annexin proteins generally consist of a unique amino-terminal region (of 0-191 amino acids in vertebrates, for example) and a carboxy-terminal 'core region' of four homologous repeats, each 68-69 amino acids long and containing five α helices and a type-2 Ca^{2+} binding site with the sequence GxGT-[38 residues]-D/E. The indicated residues Glu89 and Arg265 are considered key components of the putative calcium channel function. Adapted from (Moss and Morgan, 2004).(B) The N terminal domains of annexin A1 and annexin A2 are similar in size and phosphorylation sites but differ in other ways. Adapted from (Moss, 1992)

2.3.2. Cellular distribution of annexins

Annexins are generally cytosolic proteins. Most annexins are abundant intracellular with pools of both a soluble form and a form stably or reversibly associated with components of the cytoskeleton or proteins that mediate interactions between the cell and the extracellular matrix proteins. In certain instances, annexins may be expressed at the cell surface, despite the absence of any secretory signal peptide. The expression level and tissue distribution of annexins span a broad range, from abundant and ubiquitous (annexins A1, A2, A4, A5, A6, A7, A11) to selective (annexin A3 and annexin A8 in neutrophils and placenta, respectively) or restrictive (annexin A9 annexin A10 and annexin A13 in the tongue, stomach and small intestine respectively)

2.4. Annexin A1

Annexin A1, formally known as lipocortin 1, initially identified as the anti-inflammatory protein and later its roles was also implemented in cancer (Cao et al., 2008), infection and apoptosis (Gan et al., 2008), vesicle transport (Futter and White, 2007), actin

dynamics (Hayes et al., 2004) and wound healing (Martin et al., 2008).Annexin A1, atypically secreted from cells (D'Acquisto et al., 2008). Intracellularly, annexin A1 is predominantly a cytosolic protein but it is also found on the plasma membrane and cellular organelles, like endosomes, phagosomes and multivesicular bodies, where the protein participates in inward vesiculation (Futter and White, 2007; Gerke et al., 2005; Lim and Pervaiz, 2007). The presence of annexin A1 on the phagosomal membrane seems to be functionally important in macrophages and neutrophils (Desjardins et al., 1994a).

Like any other annexins, annexin A1 goes through post-translation modifications. Annexin A1 gets phosphorylated on Tyr-21 by recombinant pp60c-src, recombinant pp50v-abl and Epidermal Growth Factor receptor/kinase (EGFR) *in vitro* (Varticovski et al., 1988). The tyrosine phosphorylation of annexin A1 greatly influences its lipid binding properties. Phosphorylation of annexin A1 by the EGFR reduced Ca^{2+} requirements of phospholipid vesicle binding and proteolytic degradation (Rothhut, 1997). Studies also suggested that tyr-21 phosphorylation is also important for EGF stimulated internal vesicle formation. The primary site of phosphorylation by protein kinase C was also near the amino terminus at Ser-27 where adenosine cyclic 3',5'-phosphate dependent protein kinase was phosphorylated annexin A1 on the carboxy-terminal half of the molecule at Thr-216 (Varticovski et al., 1988). Phosphorylation on ser-27 residue increases calcium requirement of annexin A1 to promote aggregation of chromaffin granules (Rothhut, 1997). In addition to promoting fusion of liposomes, annexin A1 and a truncated form of annexin A1 lacking nine residues from N-terminus were found to promote fusion of liposomes with plasma membrane vesicles isolated from neutrophils (Miele et al., 1988).

Annexin A1 has been found to interact with Filamentous actin (F-actin) *in vitro*; immunogold electron microscopy indicates that annexin A1 is associated with phagosome membrane. The actin binding observed for the annexin A1 *in vitro* could relate to the finding that protein co-localised with F-actin to EGF-induced membrane ruffles and to phagosomal membranes (Kusumawati et al., 2000). Annexin A1 may also influence actin polymerisation via a direct interaction with profiling. Although this has only been demonstrated *in vitro*, the interaction was reported to modulate both the ability of annexin A1 to bind phospholipids and the effect of profiling on actin polymerisation (Alvarez-Martinez et al., 1996; Alvarez-Martinez et al., 1997).

A translocation many annexins, including annexin A1, to the phagosome membrane of maturing phagosomes has been observed in a number of phagocytic cells and has been taken as an indication for the involvement of the proteins in phagocytosis (Diakonova et al., 1997; Gerke and Moss, 1997). In differentiated human monocytes, phagocytic uptake of *Brucella* bacteria (opsonised or non-opsonised) is accompanied by recruitment of annexin A1 structures to the site of entry (Kusumawati et al., 2000). Rapid translocation of annexin A1 was observed during the phagocytosis of non-pathogenic or killed bacteria (Harricane et al., 1996; Kaufman et al., 1996). Annexin A1 knockout also resulted in impaired phagocytosis of non-opsonised zymosan (Yona et al., 2005). Knockout of annexin A1 also altered the cytokines production and phagocytic receptor expression in mouse macrophages (Yang et al., 2006; Yang et al., 2009; Yona et al., 2004; Yona et al., 2006).

Annexin A1 makes up for 2-4% of the total cytosolic protein and is found in gelatinase granules in neutrophils. Annexin A1 is secreted on cellular adhesion to the endothelium when these gelatinase granules are released. On release, annexin A1 is thought to bind to its receptor, which brings about cell detachment and inhibits transmigration of leukocytes thereby blocking the inflammatory response (Lim et al., 1998). Formyl peptide receptor (FPR) or FPR like receptor 1 (FPRL1) have recently been shown to bind the N terminus of ANXA1.

2.5. Aim of the study

In last decade several proteomic studies have been set out to understand the protein composition of phagosomes (Desjardins et al., 1994a; Griffiths and Mayorga, 2007; Martinez-Solano et al., 2006; Morrissette et al., 1999; Slomianny et al., 2006) Most of these studies focused on the composition of the proteins rather than their individual functions. Like many other ABPs, annexins are also present on the phagosomes but their role in the phagosome biogenesis is still poorly understood.

Therefore the specific aims of the current study were:

1. To indentify the protein(s) important for phagosome and F-actin binding during late stages of phagocytosis using the conventional and advanced biochemical and proteomic techniques.
2. To check the importance of the identified protein during different stages of phagocytosis *in vivo*.
3. To evaluate the importance of the protein in different receptor mediated phagocytosis.

3. Materials and Methods

3.1. Cell Biology

3.1.1. Cultivation of cells

3.1.1.1. Reagents and instruments

- J774A.1 mouse macrophage-like cell line (German Resource Centre of Biological Material, DSMZ, Germany)
- Raw 264.7 mouse macrophage (ATCC: TIB-7, Manassas, VA, USA)
- Phosphate Buffered Saline (PBS): 137 mM NaCl + 2.7 mM KCl + 10 mM Na2HPO4 - 2H2O + 1.76 mM KH2PO4 , pH 7.4 (Sigma-Aldrich, Germany)
- Fetal Bovine Serum (FBS), (Biochrom KG, Germany)
- Complete cell culture medium: DMEM (4500 mg/l glucose) + 1% 10 000 U/10 000 μg/ml Penicillin/Streptomycin + 1% 200 mM L-Glutamine + 1% nonessential amino acids (all from Invitrogen, Germany)
- Trypsin-EDTA (Invitrogen, Germany)
- Dimethyl sulfoxide (DMSO) (Sigma-Aldrich, Germany)
- Sterile cell culture material, like pipettes, dishes and flasks, cell scraper, centrifuge tubes (TPP, Switzerland)
- Cryotubes, LabTek cell culture chambers (Nalge, USA); sterile filters (Sarstedt,Germany); syringes, cannula (Braun, Germany)
- Flow Hood (BDK, Germany); Centrifuge ZK 380 (Hermle, Germany); Incubator BB 16 (Heraeus, Germany) adjusted to 37 °C, 5% CO2

3.1.1.2. Procedure

J774.A1 and RAW 264.7 cells were maintained on 150 mm cell culture plates. Confluent cell layers were split using Trypsin-EDTA. For LBP isolation J774.A1 cells were grown on 245 × 245 mm plates. For phagocytic experiments cells were grown on 24 or 6 wells plates. To make liquid nitrogen stocks, cells were harvested using Trypsin-EDTA. Cells pellet was resuspended FBS containing 10% DMSO and kept at -20^{0}C for 2 hours followed by -80^{0}C over night. Next day cells were stored in liquid nitrogen. To avoid the influence of changes in the internalisation characteristics of this cell line, J774.A1 and RAW 264.7 macrophages were only used up to passage 25. New passages were obtained from that liquid nitrogen stocks.

3.1.2. Isolation of Latex Bead Phagosomes (LBP) and cytosol

3.1.2.1. Reagents and instruments

- Internalisation medium: DMEM (Invitrogen, Germany) + 10 mM HEPES-KOH, pH 7.5 (Sigma-Aldrich, USA)
- Different ligand coupled latex beads (refer 3.2)
- Protease inhibitor (PI) Cocktail Set III containing 100 mM AEBSF, 0.08 mM Aprotinin, 5 mM Bestatin, 1.5 mM E-64 protease inhibitor, 2 mM Leupeptin and 1 mM Pepstatin A (Calbiochem, Merck, Germany)
- Homogenisation buffer: 250 mM (= 8.6%) sucrose, 3 mM imidazole, 1 mM DTT, 1 mM PMSF, pH 7.4 (all from Sigma-Aldrich, USA), 1:1000 PI
- Solutions for discontinuous sucrose gradient centrifugation: Homogenisation buffer containing 62%, 55%, 37% and 25% sucrose, respectively
- Salt-stripping buffer: 2.6 M NaCl, 48% sucrose, 3 mM imidazole, pH 7.4, 1 mM DTT, 1 mM PMSF (all from Sigma-Aldrich, USA), 1:1000 PI
- Syringes, needles (Braun, Germany)
- Cell culture centrifuge ZK 380 (Hermle, Germany)
- Ultracentrifuge, UltraClear centrifuge tubes of different sizes, SW60Ti rotor, TLA 120.1 rotor (Beckman Coulter, USA)
- Centrifuge tubes, Sorvall TH-641 rotor (Thermo Fisher Scientific, USA)

3.1.2.2. Procedure

Isolation of LBP was carried out as described previously (Al Haddad et al., 2001; Desjardins et al., 1994a) with slight modifications. J774.A1 macrophages were grown in cell culture dishes until they reached around 80% confluency. Latex bead suspensions adjusted to 1% solids were vortexed, sonicated and washed three times in PBS to remove sodium azide. Stock solution of latex beads was added to pre-warmed internalisation medium at a ratio of 1:50. Cells were washed with PBS and internalisation medium was added. Uptake of latex beads ('pulse' time) was allowed for 1 hour at 37^0C under continuous wiping to increase internalisation efficiency. Non-internalised beads were removed by intensive washing of the cells with PBS followed by another hour of incubation in cell culture medium at 37^0C and 5% CO_2 ('chase' time). Subsequently, the medium was removed, cells were washed with PBS and harvested by detaching them from the dish with a cell scraper in ice-cold PBS. Cells were collected in 50 ml tubes and centrifuged with 800 rpm for 7 minutes at 4^0C. Pellets were resuspended in ice-cold PBS and centrifuged with 1500 rpm for 5 minutes

at 4^0C. Cell pellets were resuspended in ice-cold Homogenisation buffer and centrifuged with 2500 rpm for 5 minutes at 4^0C. The final volume of the cell pellet was mixed with the same amount of ice-cold Homogenisation buffer and lysed with a 1 ml syringe fitted to a 22-gauge needle on ice using 15-20 strokes. Homogenisation success and cell breakage was monitored by phase contrast microscopy after adding trypan blue. After centrifugation at 800×g for 15 minutes at 4^0C to remove nuclei and intact cells, the post-nuclear supernatant containing phagosomes was collected and gently mixed with the same amount of Homogenisation buffer containing 62% sucrose. Isolation of LBP was accomplished in a sucrose gradient, which was prepared by overlaying 3-4 ml of the PNS / 62% sucrose mix with 5 ml Homogenisation buffer containing 25% sucrose and 2 ml Homogenisation buffer containing 8.6% sucrose on top in ultracentrifugation tubes. Centrifugation was carried out in a Beckman ultracentrifuge and a Sorvall TH-641 rotor at 100.000×g for 60 minutes at 4^0C. Afterwards enriched and purified LBP formed a visible band between the 8.6% and the 25% sucrose interphase, which was collected by penetrating the tube wall with a 22-gauge needle. After determination of the concentration by measuring OD_{600nm}, isolated LBP were aliquoted, frozen in liquid nitrogen and stored at -80^0C.

For most preparations, additional salt-stripping was applied to isolated LBP to remove membrane-bound proteins. Isolated LBP were mixed with the same amount of salt-stripping buffer and incubated on a vertical tube rotator for 40 minutes at 4^0C. Salt-stripped LBP were adjusted to 40% sucrose including 1.3 M NaCl and purified by discontinuous sucrose gradient centrifugation. 1 ml of the 40% sucrose suspension was overlaid with 1.5 ml Homogenisation buffer containing 25% sucrose and 0.5 ml Homogenisation buffer containing 8.6% sucrose. Centrifugation was carried out in a Beckman ultracentrifuge and SW60Ti rotor at 45.000×g for 60 minutes at 4^0C. Afterwards, concentration of purified LBP was determined and suspension was aliquoted, snap-frozen in liquid nitrogen and stored at -80^0C.

3.1.3. Isolation of macrophage cytosol

3.1.3.1. Reagent and instruments

- HBKS buffer,: 25 mM HEPES, 0.1 mM EDTA, 2 mM EGTA, 2 mM $MgCl_2$, 50 mM KCl, 10% sucrose, 2 mM DTT, 1 mM PMSF (all from Sigma-Aldrich, USA), 1:1000 PI adjusted to pH 7.4
- Optima™ TL ultracentrifuge and TLA 120.1 rotor (Beckman Coulter, USA)

3.1.3.2. Procedure

J774.A1 macrophages were grown in cell culture dishes until they reached around 80% confluency. Culture medium was removed; cells were washed with PBS and harvested by detaching them from the dish with a cell scraper in ice-cold PBS. Cells were collected in 50 ml tubes and centrifuged with 800 rpm for 7 minutes at 4 °C. Pellets were resuspended in ice-cold PBS and centrifuged with 1500 rpm for 5 minutes at 4 °C. Cell pellets were resuspended in ice-cold HBKS and centrifuged with 2500 rpm for 5 minutes at 4 °C. The final volume of the cell pellet was mixed with ice-cold HBKS at a ratio of 2.5:1 and lysed on ice with a 5 ml syringe fitted to a 24-gauge needle using 15 strokes followed by a 25-gauge needle using around 10 strokes. Homogenisation success and cell breakage was monitored by phase contrast microscopy after adding trypan blue. After a centrifugation step at 9100×g for 15 minutes at 4^0C using a Beckman TLA 120.1 rotor, supernatant was collected, transferred to a new tube and centrifuged at 145000×g for 60 minutes at 4^0C. Protein concentration was determined according to (Bradford, 1976). Cytosol aliquots were snap-frozen in liquid nitrogen and stored at -80 °C. Macrophage cytosol also prepared with trypsinisation method

3.1.4. Radio labelling of total cell protein

3.1.4.1. Reagents and instruments

- Cysteine and methionine free DMEM
- ^{35}S (GE bioscience formally Amersham, Germany)
- Cysteine and methionine (both from sigma)

3.1.4.2. Procedure

J774.A1 cells were grown on 250mm culture plates overnight as mentioned before (refer3.1.1). On next day cells were washed with pre-warmed PBS and incubated with cysteine and methionine free DMEM for 1-2 hours to deplete any intracellular pool of cysteine and methionine. Thereafter cells were incubated with ^{35}S, 100 µg/ml cysteine and methionine, in cysteine and methionine free medium, containing 1% FCS, Penicillin/Streptomycin + nonessential amino acids for 12 hours. After incubation cells were washed with ice cold PBS to remove free ^{35}S. Cells were harvested and cytosol isolated as mentioned before (refer3.1.3).

3.1.5. Fixation and labelling of cells

3.1.5.1. Reagents and instruments

- 4% paraformaldehyde, 4% sucrose in PBS, pH 7.4 (Sigma-Aldrich, Germany)
- 50 mM NH_4Cl (Merck, Germany) in PBS
- 0.2% Triton X-100 (Roth, Germany) in PBS
- 0.1% Saponin (Cat. # 47036, Fluka, Germany) in PBS
- 1% Gelatin 'gold' (Sigma-Aldrich, USA) in PBS
- 0.2% Gelatin 'gold' in PBS
- ProLong gold mounting medium (Invitrogen, Germany)
- Glass slides and coverslips (Menzel GmbH, Germany)
- Rhodamine phalloidin and FITC phalloidin (Sigma-Aldrich, Germany)

3.1.5.2. Procedure

Cells were fixed in PBS containing 4% paraformaldehyde and 4% sucrose for 20 minutes at RT followed by quenching in PBS containing 50 mM NH4Cl for 10 minutes at RT. Permeabilisation, when required, was achieved by treatment with 0.2% Triton X-100 in PBS for 5 minutes at RT. For annexin A1 and annexin A2 staining cell permeabilisation was achieved with 0.1% saponin in PBS. After blocking of unspecific binding sites with PBS containing 1% white gelatin 'gold' for 60 minutes, samples were incubated with primary antibody (Table 2) diluted in blocking solution for 60 minutes at RT, followed by three washes with PBS containing 0.2% gelatin. Secondary antibodies (Table 2) were applied for 45 minutes at RT, again followed by three washes with PBS. Cells were stained with markers for F-actin with rhodamine phalloidin or FITC-phalloidin for 20 minutes at RT. Coverslips were washed in PBS containing 0.2% gelatin, PBS alone, in aqua dest and were mounted on glass slides using ProLong gold mounting medium (Invitrogen, Germany).

3.1.6. Macrophage transfection

3.1.6.1. Reagents and instruments

- Electroporation buffer: 140 mM Na_2PO_4, 5 mM KCl, 10 mM $MgCl_2$, pH 7.4, filter sterilised
- 0.2 cm electroporation cuvettes (Lonza/Switzerland)
- GenePulser II (BioRad, Germany):

3.1.6.2. Procedure

Electroporation

After trypsinisation cells were washed with pre-warmed PBS. 2 × 10^6 cells were resuspended in 100 µl Electroporation buffer. For nucleofection, between 0.1 - 1 nmol of siRNA/2-4 µg plasmid DNA were added and incubated for at least 5 minutes at RT. Subsequently macrophages were transferred to 0.2 cm electroporation cuvettes with subjected to two electric shocks using GenePulser II. The first electric shock was given with high voltage and low capacitance (1000 V, capacitance 10 µF), followed by second electric shock with low voltage and high capacitance (100 V, maximum capacitance). After electroporation 500 µl of complete growth medium was added quickly and the cells were directly seeded into 24-well plates. On next day gene expression and siRNA knockdown was check with appropriate methods.

Lipofection:

Annexin A1 siRNA (sc-29682) was transfected to RAW 264.7 macrophages (10-15,000 cells) using siRNA transfection reagent (sc-29528, Santa Cruz, USA) as per the manufacturer's instructions. After 72 hours of transfection cells were checked for the gene silencing and used for the experiments.

Lentivirus:

Annexin A1 shRNA lentiviral particles (sc-29682-V) was transfected to RAW 264.7 macrophages (10-15,000 cells) as per the manufacturer's instructions. After 72 hours of transfection cells were subjected to antibiotic selection. After 24 hours incubation in presence of antibiotic, cells were split and grown on 24 well plates for further experiment. For stably transfected cells selection, cells were maintained under constant antibiotic pressure at least for a week before freezing. During every experiment, annexin A1 knockdown was monitored by western blotting analysis.

3.2. Preparation of ligands coupled latex beads

Reagents and Instruments

Latex beads

- Blue-fluorescent carboxylate-modified microspheres containing 2% solids of diameter 1 µm (Cat. F8815; Invitrogen, Germany)

- Non-fluorescent Polybead® carboxylate-modified microspheres containing 2.68% solids of diameter 3 μm (Cat. #09850; Polysciences, Inc., USA)

Ligands

- Fish skin gelatin (FSG; Cat. G7765; Sigma-Aldrich, USA)
- Fc fragment of mouse IgG (Cat. 31205; Pierce Biotechnology, USA)
- Mannan from Saccharomyces cerevisiae (Man; Cat. M7504; Sigma-Aldrich, USA)

Reagents

- MES buffer (Cat. M8250; Sigma-Aldrich): 500 mM stock solution in Aqua dest.; diluted 100 mM and 50 mM solutions were adjusted to pH 6.7
- Stop buffer: 1% Triton X-100 in 10 mM Trizma base (Sigma-Aldrich, USA);adjusted to pH 9.4
- Modified Phosphate buffer : 50 mM $Na_3PO_4.12\ H_2O$ + 0.9% NaCl (both from Sigma-Aldrich, USA); adjusted to pH 7.4
- Activator of surface carboxyl groups: N-(3-Dimethylaminopropyl)-N′-ethylcarbodiimide hydrochloride (EDAC; Cat. E1769; Sigma-Aldrich, USA); 10 mg/ml stock solution in Aqua dest., prepared freshly
- Cross-linker: Concanavalin A from Canavalia ensiformis (ConA; Cat. C2010; Sigma-Aldrich, USA)
- Bovine serum albumin (BSA) and sodium azide (both from Sigma-Aldrich, USA)
- Sodium azide (Sigma-Aldrich, Germany)

3.2.1. Coupling of latex beads to fish skin gelatin (gelatin-beads)

Blue-fluorescent latex beads were vortexed and sonicated in an ultrasonic water bath for 2 minutes. 5 ml of beads suspension was mixed with 10 mg FSG diluted in 50 mM MES and filled to a final volume of 10 ml with 50 mM MES. The suspension was mixed on a vertical tube rotator for 15 minutes at room temperature (RT). Subsequently, 0.4 ml EDAC stock solution was added to bead suspension, mixed by vortexing and adjusted to pH 6.5 using about 10-15 μl 0.8 N NaOH (checked with pH indicator sticks). The suspension was mixed on a vertical tube rotator for 2 hours at RT. To quench the reaction, glycine powder was added to give a final concentration of 100 mM. The suspension was incubated for another 30 minutes on the vertical tube rotator at RT. Coupled latex beads were transferred to conical Eppis and centrifuged with 6.000×g for 5 minutes at 4^0C to separate particles from unbound protein. Pellets were resuspended in PBS and wash was repeated twice. Pellets

were resuspended and combined in PBS and suspension was adjusted to 1% solids by measuring OD_{600}nm using a spectrophotometer.

3.2.2. Coupling of latex beads to IgG (Fc fragment, Fc-beads)

Blue-fluorescent latex beads were vortexed and sonicated in an ultrasonic water bath for 2 minutes. 4 ml of beads suspension was mixed with 0.5 mg Fc fragment of mouse IgG. Suspension was filled to a final volume of 10 ml with 100 mM MES and mixed on a vertical tube rotator for 15 minutes at RT. Subsequently, 0.14 ml EDAC stock solution was added to bead suspension and mixed on a vertical tube rotator for 1 hour at RT. Another 0.14 ml EDAC was added and mixed for 1 hour. Subsequently, 2 ml stop buffer was added to the suspension, which was centrifuged in conical Eppis with 6.000 × g for 5 minutes at RT. Pellets were resuspended in stop buffer and centrifuged again followed by three washes in PBS. Coupled latex beads were resuspended and combined in PBS containing 0.03% FSG and suspension was adjusted to 1% solids by measuring OD_{600nm} using a spectrophotometer.

3.2.3. Coupling of latex beads to mannan (man-beads)

Blue-fluorescent latex beads were vortexed and sonicated in an ultrasonic water bath for 2 minutes 5 ml of bead suspension were mixed with 0.5 mg ConA and filled to a final volume of 10 ml with 100 mM MES. Suspension was mixed on a vertical tube rotator for 15 minutes at RT. Subsequently, 0.14 ml EDAC stock solution was added to bead suspension and mixed on a vertical tube rotator for 1 hour at RT. Another 0.14 ml EDAC were added and mixed for 1 hour. Subsequently, suspension was centrifuged in conical Eppis with 6.000×g for 5 minutes at 4^0C, pellets were resuspended in PBS and centrifuged again followed by another two washes in PBS. Pellets were resuspended in 7.5 ml PBS and 2 mg mannan was added. Suspension was mixed on a vertical tube rotator for 15 minutes at RT. Afterwards; 2 ml stop buffer was added to the suspension, which was centrifuged in conical Eppis again. Pellets were resuspended in stop buffer and centrifuged again followed by another spin down in stop buffer. Coupled latex beads were washed three times in PBS, resuspended in PBS containing 0.03% FSG and suspension was adjusted to 1% solids by measuring OD_{600nm} using a spectrophotometer. All coupled 1% latex bead suspensions were stored at 4^0C after adding 3 mM sodium azide.

3.3. Microscopy

Actin-binding assays were analysed by conventional epifluorescence microscopy as described previously (Al-Haddad et al. 2001). Fluorescence images were recorded by a chilled SenSys CCD camera system (Photometrics Inc., USA) and a Uniblitz D122 shutter (Vincent Associates, USA). For selective excitation and specific detection of emitted radiation of used fluorescent dyes, different filter sets were available (Nikon, Japan). Images were again transferred to a Macintosh computer and analysed by IPLab Spectrum software. Live cell imaging at 37 °C and analysis of fusion assays as well as uptake rates of fixed macrophages were performed by confocal fluorescence microscopy using a TCS SP2 laser-scanning microscope (Leica, Germany) equipped with a 405 nm diode laser, an argon-krypton laser with lines at 458, 476, 488, 514 nm and helium-neon lasers with 543, 594 and 633 nm lines. The system also contained acousto-optical tunable filters (AOTF), an acousto-optical beam splitter (AOBS) and four prism spectrophotometer detectors that permitted simultaneous excitation and detection of multiple fluorochromes. Three-dimensional scans of usually 0.2 or 0.3 um z-stacks were recorded and analysed by the help of the cross-sectioning option of Leica confocal software. Staining of cellular F-actin was used to differentiate between attached and fully internalised latex bead.

3.4. Protein Chemistry

3.4.1. Gel filtration

3.4.1.1. Reagent and Instruments

- HB: 25 mM HEPES, pH 7.4, 2 mM, $MgCl_2$, 0.1 mM EGTA, 0.1 mM EDTA, 2mM DTT
- Bio-silect SEC 400-5 column (Bio-Rad, Germany)
- Bio-Rad Biologic workstation
- Amino black reagent: 0.1% Amino Black in 50% methanol prepared in aqua dest
- Distaining Solution: 50% methanol and 10% Acetic Acid prepared in aqua dest.
- Protein Standard: 2mg/ml BSA solution (Thermo Scientific, Germany)

3.4.1.2. Procedure

The cytosol was fractionated by size exclusion chromatography with the use of Bio-Silect SEC 400-5 column on a Bio-Rad Biologic workstation. Usually 7-10 mg (~250 µl) cytosolic proteins (3.1.3) were loaded on column pre-equilibrated with HB and run at 0.5 ml/minute flow rate. Column was washed with 3 column volume of HB buffer and 250 µl

fractions were collected. To check the protein content in each collected fractions, 2 µl of fraction was blotted on nitrocellulose membrane and stained with amino black reagent for 2 minutes followed by the 2-3 times was with distaining solution. Stained nitrocellulose membrane was scanned and intensity of each spot was calculated. Spot intensity of each spot was compared with spot intensity of standards (at least 5 serial dilutions were prepared). Obtained fraction was flash frizzed in liquid nitrogen and stored at -80^{0}C for long term storage. Each protein containing fraction was checked for actin binding activity (3.5.1). Fractions showing the highest actin binding activity were pooled together active fraction, and used for the further fractionation. Pooled fraction referred as active fraction.

3.4.2. Ammonium precipitation

3.4.2.1. Reagent and Instruments

- Water saturated Ammonium Sulphate (nearly 4.5 M)
- HB (refer3.4.1)

3.4.2.2. Procedure

To further fractionation of proteins, 50 µl active fraction (refer 3.4.1) was transferred in 1.5 micro-centrifuge tubes. To achieve protein precipitation at 30% ammonium sulphate, saturated ammonium sulphate solution was added drop wise to active fraction. Mixture was kept at 4^{0}C with constant stirring for 45 minutes. Precipitated proteins were collected by centrifugation at 5000 × g for 15min at 4^{0}C. Supernatant was carefully transferred to another micro-centrifuge tube. To achieve protein precipitation at 50% ammonium sulphate, saturated ammonium sulphate solution was added to the supernatant of 30% ammonium sulphate as mentioned before. Amount to be added was calculated as mentioned in supplementary table 1. Similarly, protein was precipitated at 80% ammonium sulphate concentration. All pellets were resuspended in 50 µl in HB and were checked for actin binding activity (3.5.1).

3.4.3. Cation chromatography

3.4.3.1. Reagents and instruments

- Phospho-cellulose resin (P11, Millipore Germany)
- 4M NaCl
- HB (refer3.4.1)

3.4.3.2. Procedure

For protein fractionation, 50-100 µl of active fraction (refer 3.4.1) was incubated with 10 µl P11, pre-equilibrated with HB for 20 minutes at 40C. After two washes with HB to remove unbound proteins, bound proteins were eluted with 50-100 µl of 1M NaCl in HB. Eluted fractions were dialysed against HB before using in actin binding assay

3.4.4. Isolation of G-actin from rabbit muscle

3.4.4.1. Reagents and instruments

- Rabbit muscle acetone powder (M0637; Sigma-Aldrich, USA)
- Cheesecloth; Teflon-coated homogeniser; semi-permeable dialysis tubing, pore-size diameter: 5 nm, MW cut-off: 14 kDa (all from Roth, Germany)
- G-buffer, 5 mM Trizma base, 0.2 mM $CaCl_2$, 0.2 mM Na-ATP and 0.1% 2-mercaptoethanol pH 8.0 (all from Sigma-Aldrich, USA)
- Ultracentrifuge, Ti50 rotor (Beckman Coulter, USA)
- Sorvall T 647.5 rotor (Thermo Fisher Scientific, USA)

3.4.4.2. Procedure

G-actin was isolated by the method of Spudich & Watt (1971) with slight modifications. 5 g of rabbit muscle acetone powder was washed in aqua dest. twice for 5 minutes at 4^0C. Solutions were passed through several layers of sterile cheesecloth. Washed powder was incubated in 100 ml ice-cold G-buffer under continuous stirring (500 rpm) for 40 minutes at 4^0C. Solution was again passed through several layers of sterile cheesecloth. Filtrate was centrifuged in a T 647.5 rotor with 30.000 rpm for 15 minutes at 4^0C and supernatant was transferred to a beaker. While stirring slowly at 4^0C, solution was brought to 50 mM KCl, 2 mM $MgCl_2$ and 1 mM Na-ATP. The beaker was sealed with parafilm and incubated without stirring for 2 hours at 4^0C. The viscosity of the solution increased significantly during incubation. While gentle stirring, KCl concentration was increased to 0.6 M by adding crystalline KCl to remove tropomyosin complexes. Solution was gently stirred for 60 minutes at 4^0C followed by centrifugation using the T 647.5 rotor with 40.000 rpm for 2 hours at 4^0C. The supernatant was discarded and pellet was resuspended in 7.5 ml G-buffer. The solution was homogenised using a Teflon-coated rod homogeniser and transferred to dialysis tubing. While gentle stirring, the actin solution was dialysed against 1 l G-buffer for 36 hours at 4^0C. During dialysis, G-buffer was replaced completely after every 8 hours. After first dialysis cycle, solution was centrifuged again using the Ti50 rotor with 40.000 rpm for 2

hours at 4^0C. Supernatant containing G-actin was partly aliquoted and frozen in liquid N2 while pellet was discarded. 6 ml of supernatant were transferred to a new tube and salt concentrations were increased again (50 mM KCl, 2 mM MgCl2, 1 mM Na-ATP). The tube was sealed and incubated without stirring for 48 hours at 4^0C. The solution was centrifuged again using the Ti50 rotor with 40.000 rpm for 2 hours at 4^0C. The supernatant was discarded and pellet was resuspended in 4 ml G-buffer. The solution was homogenised again and transferred to dialysis tubing. While gentle stirring, the actin solution was dialysed against 1 l G-buffer for 36 hours at 4^0C. During dialysis, G-buffer was replaced completely after every 8 hours. After second dialysis cycle, solution was centrifuged again using the Ti50 rotor with 40.000 rpm for 2 hours at 4^0C. Pellet and supernatant containing purified G-actin were aliquoted, frozen in liquid nitrogen and stored at -80^0C.

3.4.5. Annexin A1 purification

3.4.5.1. Reagents and instruments

- **Buffer A**: 50mM Imidazole-HCl, pH 7.4, 300mM NaCl, 2mM $MgCl_2$, 2mM EGTA
- **Buffer B:** 10mM Imidazole-HCl, pH 7.4, 10mM NaCl, 1mM EGTA, and 1mM NaN_3
- **Buffer C:** 25mM Tris-HCl, pH 7.5, 150mM NaCl
- **Buffer D: (optional)** 10mM Tris-HCl, pH 7.5, 1mM DTT, 0.5mM EGTA, and 0.25mM PMSF
- *E. coli* BL21 (DE3) expression host
- 1 M IPTG
- 50 mg/ml Ampicillin
- DE52 column
- Chloroform-methanol extract of bovine brain (brain extract, type VII; Sigma B3635)

3.4.5.2. Procedure

Heat competent *E.coli* BL21 (DE3) was transformed with pKK AnxI (Seemann et al., 1996). Transformed bacteria were grown at 37^0C in LB medium containing 150 μg/ml ampicillin. Bacterial cells were induced with 0.4 mM IPTG at late log phase (0.8-1.0 OD_{600}). Cells were grown for another 4 hours and harvest the cells by centrifugation at 6000 × g for 20 minutes. Cell pellet from 200ml was re-suspended in 10ml Buffer A plus 1mM DTT, 1mM PMSF, 0.5mM Benzamidine and 1:500 protease inhibitors cocktail. Cells were lysed by

repeated freeze and thaw cycles followed by short sonication to shear DNA. Lysed cells were centrifuged at 100,000 × g for 30 min at 4^0C. Supernatant dialysed against Buffer B contain 1mM PMSF. Dialysed extract applied to a DE-52 column. The flow through was collected and 1:500 protease inhibitor cocktail, 1mM PMSF, 5mM $CaCl_2$ and 1mg/ml chloroform-methanol extract of bovine brain were added in flow through. Mixture was Incubate for 20 minutes at RT followed by centrifugation at 100,000 × g for 30 minutes. Pellet containing liposomes washed with buffer C containing 1mM DTT, and 0.25mM PMSF, 1:500 protease inhibitor cocktail and 2mM $CaCl_2$. Annexin A1 was eluted by incubating liposomes with buffer C containing 10mM EGTA, 1mM DTT, and 0.25mM PMSF. Finally eluted annexin A1 was dialysed against the HBS and flash freeze in small aliquots and stored at -80^0C.

3.4.6. SDS-PAGE

- SDS-PAGE reagents were prepared as mentioned in (Sambrook and Russell, 2006) all reagents were brought from Sigma-Aldrich, USA
- Molecular weight marker (BioRad, USA)
- Thermostat 5320 (Eppendorf, Germany), Mighty Small II electrophoresis device (Hoefer, Inc., USA), PowerPac 200 (BioRad, USA)
- MiniProtean tank blotting device (BioRad, USA)

3.4.6.1. Procedure

Cells were washed with PBS twice and 1x SDS sample buffer was added to lysed cells. Isolated phagosomes, cytosol and actin fractions were incubated with 1x SDS sample buffer directly. Subsequently, all SDS samples were boiled at 90^0C for 5 minutes to denature proteins. If necessary, DNA was destroyed by a short ultrasonic treatment on ice. The proteins were separated by vertical gel electrophoresis using 10% or 12% polyacrylamide gels. The samples were migrated in 1x running buffer in an electrophoresis device per gel set to constant 10 mA for around 15 minutes followed by a run at constant 20-30 mA for 70-100 minutes After separation, proteins were stained using Coomassie or silver staining or were transferred onto nitrocellulose membranes for further immunoblotting (3.4.7). For Coomassie staining, gels were incubated with Coomassie R250 staining solution for 45 minutes under vigorous shaking. Afterwards the stained gels were washed and distained with distaining solution for 45 minutes. Silver staining was carried out following the

manufacturer's instructions. Images of stained gels were taken with a conventional flat-bed scanner.

3.4.7. Immunoblotting

3.4.7.1. Reagents and instruments

- Blot buffer: 25 mM Trizma base, 200 mM glycine, 20% methanol
- 10X TBS: 10 mM Trizma base, 149 mM NaCl pH 7.4 (Merck, Germany)
- 1X TTBS: TBS containing 0.1% Tween-20 (Merck, Germany)
- Blocking buffer: TTBS containing 5% non-fat dry milk (Nestlé Food Co., USA)
- Ponceau S staining solution: 0.2% Ponceau S, 3% TCA (Serva, Germany)
- Stripping buffer: 1X TBS,
- Hybond nitrocellulose membranes, Hyperfilm and ECL western blot detection reagent (Amersham, GE Healthcare, UK)

3.4.7.2. Procedure

Following separation in acrylamide gels, protein mixtures were transferred to nitrocellulose (NC) membranes to analyse them for the presence of specific proteins applying antibodies, a method known as immuno- or western blotting. NC membranes, filter papers, sandwich pads and migrated acrylamide gels containing proteins were equilibrated in blot buffer for 20 minutes and assembled in cassettes following the manufacturer's instructions. The samples were transferred on to nitrocellulose membranes using a tank blotting device in blot buffer at constant 30 V overnight or 75 V for 90 minutes. Success of transfer was checked by protein staining using Ponceau S solution for 3 minutes Afterwards the membranes were rinsed with aqua dest. and images were taken using a conventional flat-bed scanner. Ponceau S staining was removed by washing with 1X TTBS before proceeding further. Before labelling, the membranes were incubated in blocking buffer containing 5% dry milk or, 5% BSA to block unspecific binding sites. For annexin A1, blocking was done using 5% dry milk + 1% FCS. There after dilutions of primary antibodies were prepared in blocking buffer and were applied for 1 hour at RT or overnight at 4^0C.

Membranes were washed three times with TTBS for 10 minutes followed by incubation with horseradish peroxidase (HRP)-conjugated secondary antibodies for 45-60 minutes. After another three washes in TTBS for 10 minutes and a final rinse in TBS, the NC membranes were exposed to ECL solution for 5 minutes at room temperature. Subsequently,

chemiluminescent signals were visualised onto films and scanned for quantification. If necessary, membrane was stripped using stripping buffer and used for immuno-blotting of second antibody.

Protein signals were quantified using ImageJ (NCBI freeware, USA) to determine quantity differences between the samples. For siRNA/shRNA knockdown, annexin A1 and tubulin ratio was used for analysis.

3.4.8. Liquid Chromatography and tandem Mass Spectroscopy (LC-MS/MS)

Protein eluted after cation chromatography was precipitated at 80% final ammonium sulphate concentration. The solutions were centrifuged with 14.000 rpm for 60 minutes at 4^0C. The pellet was dissolved, reduced with DTT and alkylated with iodoacetamide before being digested with 1 μg of Promega-modified trypsin for 24 hours at room temperature. A second 1 μg of trypsin was added and digestion was allowed to proceed for 24 more hours. The sample was acidified to 5% acetic acid and then desalted on a C18 column. Approximately 25% of the digest was introduced into the mass spectrometer for analysis using two run conditions. The complete procedure for LC-MS/MS was performed by the Biomolecular Research Facility at the Virginia University in Charlottesville, USA by the group of Dr. Nicholas Sherman. The LC-MS system consisted of a Finnigan LCQ ion trap mass spectrometer system (Thermo Fisher Scientific, Inc., USA) with a Protana nanospray ion source interfaced to a self-packed 8 cm × 75 μm id Phenomenex Jupiter 10 μm C18 reversed-phase capillary column. The extracts (0.5-10 μl volumes) were injected and the peptides were eluted from the column by an acetonitrile/0.1 M acetic acid gradient at a flow rate of 0.25 μl/minutes. The nanospray ion source was operated at 2.8 kV. The digest was analysed using the double play capability of the instrument acquiring full scan mass spectra to determine peptide molecular weights and product ion spectra to determine amino acid sequence in sequential scans. This mode of analysis produces approximately 3000 CAD spectra of ions ranging in abundance over several orders of magnitude. The data were analysed by database searching using the Sequest algorithm (developed by J. Eng and J. Yates, The Scripps Research Institute, La Jolla, USA) against mouse IPI accessions.This program converted the character-based representation of amino acid sequences in a protein database to fragmentation patterns, which were compared against the MS/MS spectrum generated on the target peptide. The algorithm initially identified amino acid sequences in

the database that match the measured mass of the peptide, compared fragment ions against the MS/MS spectrum and generated a preliminary score for each amino acid sequence. Then, a cross-correlation analysis was performed by correlating theoretical, reconstructed spectra against the experimental spectrum. Identified proteins were analysed using Scaffold software (Proteome Software, Inc., USA) applying different protein identification probability filter settings. We used stringent filtration criteria for protein selection which described in detail in results.

3.5. *In vitro* assays

3.5.1. Actin binding Assay (ABA)

3.5.1.1. Reagent and Instrument

- Purified G-actin (refer3.4.1)
- Rhodamin conjugated phalloidin (Sigma-Aldrich, USA)
- microscopy slides and 11 mm glass coverslips (Menzel GmbH, Germany)
- double-sided tape (3M Scotch, USA)
- poly-L-lysine (PLL; P1274; Sigma-Aldrich, Germany)
- G-buffer: 5 mM Trizma base, pH 8.0, 0.2 mM $CaCl_2$
- 3 mg/ml casein (Sigma-Aldrich; USA)
- HB: 25 mM HEPES, pH 7.4, 2 mM, $MgCl_2$, 0.1 mM EGTA, 0.1 mM EDTA, 2mM DTT
- HBS: HB containing 10% sucrose and 0.3 mg/ml casein
- VaLaP (Vaseline :Lanolin: Paraffin at 1:1:1)
- Nikon Diaphot 300 microscope (Nikon GmbH, Germany)

3.5.1.2. Procedure

Isolated G-actin from rabbit muscle (0.05 mM) was polymerised on ice in the presence of 2 mM $MgCl_2$ overnight. Subsequently F-actin was stabilised and labelled on ice with the same concentration (ratio: 1:1) of rhodamine-conjugated phalloidin for 2 hours. Prepared and stabilised F-actin fractions were kept on ice and were used for experiments within two weeks.

Coverslips were coated with 0.1 mg/ml poly-L-lysine diluted in aqua dest. for 15 minutes at RT to maintain homogenous F-actin network formation on the glass surface. Unbound PLL was removed by intensive rinsing with aqua dest. coversilps were air dried

and were used to build reaction chamber. Reaction chambers (~3 µl volume) were built from glass microscopy slides and coated coverslips using two pieces of double-sided tape (Figure 3).

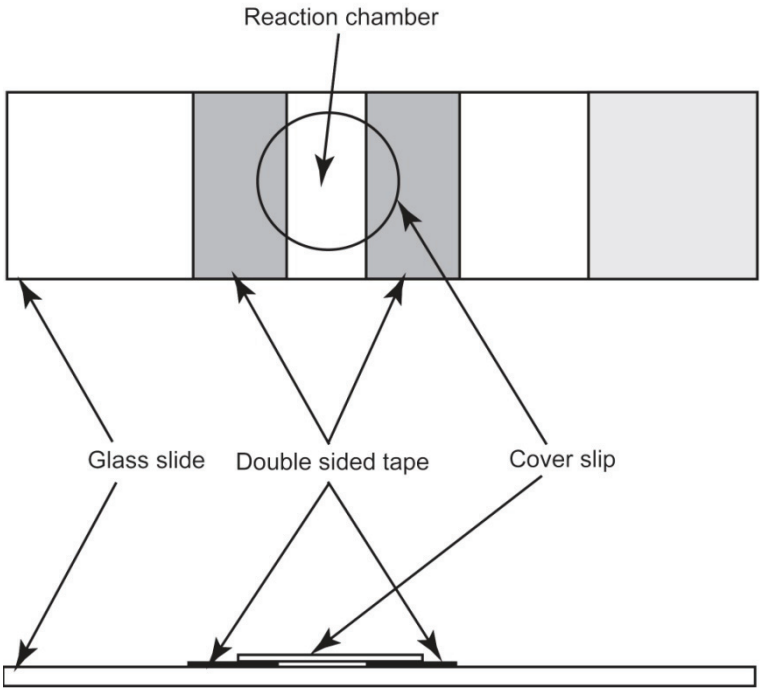

Figure 3: Schematic diagram of actin binding assay reaction chamber.

All experiment incubations were carried out in a moist chamber at RT. Stabilised and labelled F-actin was diluted in G-buffer containing 2mM $MgCl_2$ 0.2 mM Na-ATP and 2 mM DTT (always made fresh) at a ratio of 1:130. Diluted F-actin was perfused into the chamber and incubated for 3 minutes followed by a wash with 10 µl G-buffer with additives. Nonspecific binding was blocked by perfusion of the chamber with 10 µl casein diluted in HB for 5 minutes. Subsequently, excess F-actin and casein were washed out by 10 µl HBS. Binding reaction mixtures were prepared in HBS on ice with a final volume of 8-10 µl. Reaction mixtures were freshly prepared in the following order: 1.) HBS, 2.) cytosol/protein fraction 3.) additional factors (e.g. lipids, nucleotides, etc) and 4.) LBP. Isolated LBP were usually diluted to a working concentration of 0.006% [wt/vol]. Reaction mixtures were perfused into the chamber and incubated for 20 minutes. Thereafter, unbound LBP were washed out by perfusion of 10 µl HBS. Chambers were sealed using VaLaP. LBP binding was analysed by fluorescence microscopy with the use of a Nikon microscope. The bound phagosomes per field were counted (~field surface area of 22,000 μm^2) and values from at least 20 fields were averaged. The error bars reported are standard deviations of at least three independent experiments.

3.5.2. Actin nucleation assay

3.5.2.1. Reagent and Instrument

- 10x RB buffer: 100 mM HEPES-NaOH, 20 mM MgCl2, 1000 mM KCl, 5 mM EGTA, pH 8.0 (all from Sigma-Aldrich, Germany)
- 10x G buffer: 20 mM Tris-HCl, 2 mM $CaCl_2$, pH 8.0 (all from)
- 100 mM ATP-Mg^{2+} (Roche, Germany)
- 1 M DTT stock (Sigma-Aldrich, Germany)
- 0.2 mM Thymosin β4 stock (Sigma-Aldrich, Germany)
- 0.058 mM Alexa 594 labelled G-actin (corresponds to 2.5 mg/ml, refer 3.4.4)
- 0.25% fish skin gelatin
- Acetone
- Glass slide and cover slips

3.5.2.2. Procedure

Firstly glass slides were cleaned with acetone and were washed 2-3 times with aqua dest. followed by incubation for 5 minutes in 0.25% fish skin gelatin. Subsequently slides were dried and kept at 4^0C till further use. Gelatin coated slides can kept at 4^0C for 2 weeks.

Prepare 1X G Buffer containing 0.1 mM ATP and 0.1 mM DTT. Mix 10 µl 58 µM G-actin with 19 µl G buffer to bring it down to a final concentration of 20 µM. After 30 minutes on ice, mixture was centrifuge for 30 minutes at 10000 × g at 4 °C.

Actin/thymosin β4 (1:2.5 ratio) complexes were prepared by adding 10 µl 20 µM G-actin and 2.5 µl 200 µM thymosin-β4 in 7.5 µl aqua dest (20 µl final volume).

For actin nucleation reaction mixture was prepared by adding 1X RB buffer, 1X G buffer, 200 µM ATP, 2 µl G-actin/thymosin-β4 complexes, 1-5 µl of LBP (depending concentration), additive to be tested and x volume of aqua dest to bring final volume to 10 µl. Reaction mixture was incubated on ice for 5 minutes in dark. 2 µl reaction mixture was applied on gelatin coated glass slide and covered with 22×22 mm coverslip. Coverslip pressed carefully for even distribution of reaction mixture. Incubate the slide for 10-15 minutes in dark at RT. Percentage of actin nucleating LBP calculated from 50-100 analysed LBP.

3.6. Other methods

3.6.1. Fluorography

3.6.1.1. Reagent and Instrument

- 100% dimethylsufoxide DMSO
- 20% (w/w) solution of 2,5-diphenyloxazole (PPO) in DMSO
- Vacuum Gel Dryer

3.6.1.2. Procedure

The radio-labelled proteins were separated by electrophoresis using an aqueous polyacrylamide gel. Separation was followed by soaking the gel in about 20 times its volume of dimethylsufoxide (DMSO) for 30 minutes, and then immersed second time for 30 minutes in fresh DMSO to displace all the water from the gel. The gel was then soaked in a 20% (w/w) solution of PPO in DMSO to impregnate the gel with the scintillator PPO. Subsequently PPO was precipitated by immersing the gel in water and the gel was dried at high heat on vacuum drier. Dried gel was exposed to X-ray film directly in contact with each other at -70^{0}C. Next day, the X-Ray film was take out and developed.

Table 2 List of antibodies used in the study

Antibody against	Antigen	Produced in	Working concentration		Obtained from (reference)
			Western Blotting	IF	
Annexin A1	Human annexin A1	Rabbit	1:1500	1:150	Dr V. Gerke (Seemann et al., 1996)
Annexin A2	Human annexin A2	Mouse	1:1500	1:150	Dr V. Gerke (Thiel et al., 1991)
Moesin	Synthetic peptide	Rabbit	1:100 (actin binding assay)	-	Cell Signalling, Germany
α-tubulin	Synthetic peptide	Mouse	1:5000	-	Sigma-Aldrich, Germany
Filamin A	Synthetic peptide	Rabbit	1:1000	-	Cell signalling, Germany
Anti-rabbit Alexa-488	Rabbit IgG	Goat	1:300		Invitrogen, Germany
Anti-mouse Alexa-594	Mouse IgG	Goat	1:300		Invitrogen, Germany
Anti-rabbit-HRP conjugate	Rabbit IgG	Goat	1:5000		Sigma-Aldrich, Germany
Anti-mouse-HRP conjugate	Mouse IgG	Sheep	1:5000		Sigma-Aldrich, Germany

Table 3: List of used lipids and Nucleotide used in binding assay studies:

Component	Assay concentration	Solvent	Supplier
Arachidonic Acid	125 μM	EtOH	Sigma-Aldrich, USA
PtdIns (4,5)-bisphosphate (PIP2)	50 μM	EtOH	Sigma-Aldrich, USA
ATP	1 mM	Aqua dest	Sigma-Aldrich, USA
ADP	1 mM	Aqua dest	Sigma-Aldrich, USA
AMP-PNP	1 mM	Aqua dest	Sigma-Aldrich, USA
GTP	0.1 mM	Aqua dest	Sigma-Aldrich, USA
GDP	0.1 mM	Aqua dest	Sigma-Aldrich, USA
GMP-PNP	0.1 mM	Aqua dest	Sigma-Aldrich, USA

4. Results

4.1. Identification of novel ABP facilitate F-actin-LBP interaction *in vitro*

Phagosomes are membrane-bound organelles, which associate with many cytoskeleton components. Actin filaments and ABPs play an important role during particle internalisation. Studies also suggest that phagosomes rapidly lose their abundant actin coats soon after the internalisation which is an important phenomenon of phagosome maturation. The participation of actin and ABPs in later events of phagocytosis like acidification by fission and fusion events with different cell organelles is less clear. There are several insinuation like the capability of maturing phagosomes to nucleate actin (Defacque et al., 2000; Jahraus et al., 2001b) to interact with and recruit actin-associated proteins and the presence of actin and ABPs in mature phagosomes determined by proteomic analysis (Desjardins et al., 1994a) which supports an involvement of actin in these processes. Given the abundance of actin-binding proteins it seems inevitable that they must bind F-actin in cells, its precise role in phagosome biogenesis yet to be discovered.

To investigate the role of different proteins in F-actin-LBP interaction an *in vitro* actin binding assay (ABA) was developed in our lab, which allows analysis of these events step by step. The ABA relies on the step-wise perfusion of components in small reaction chambers on a glass slide. After the formation of stabilised actin networks on coverslips coated with PLL and blocked for unspecific binding sites, phagosomes and additional factors were perfused into the chamber to allow binding to these pre-formed actin networks. After incubation unbound components are washed out and samples are analysed by conventional fluorescence microscopy by determining numbers of bound phagosomes to actin filaments per microscopic field. This assay is not only highly reproducible, but gives highly quantitative results. Using this assay, one can test different reagents and proteins which can facilitate F-actin and gelatin-LBP interaction *in vitro*. With help of this assay, we already found myosin Va, a molecular motor protein, as a stimulatory factor which facilitate F-actin-ABP interaction as the ATP-dependent manner (Al Haddad et al., 2001).

4.1.1. J774.A1 macrophage cytosol stimulates F-actin-LBP interaction *in vitro*

Phagosomes containing non-degradable latex beads provide an elegant model system to study different aspects of phagocytosis and can be isolated with high purities. The analysis of these phagosomes and their binding to F-actin *in vitro* is important to understand the underlying molecular mechanisms. It was therefore important to investigate these

organelles in more detail. Study by (Al Haddad et al., 2001) were carried out using gelatin-LBP containing 1 μm latex beads coated with fish skin gelatin (gelatin-beads), which were isolated from J774.A1 macrophages by discontinuous sucrose gradient centrifugation after one hour pulse followed one hour chase. We selected gelatin-beads over other ligands because of low cost, easy to couple to carboxylated latex beads and most importantly non-specificity. To study the general mechanism of any protein gelatin-coated latex provide ideal platform because of its unbiased binding to the phagocytic receptors. Moreover, slow internalisation of gelatin-beads allowed me to characterise different stages of phagocytosis during *in vivo* studies.

Firstly, the basic prosperities of gelatin-LBP were checked. Isolated LBP containing gelatin-coupled latex beads (gelatin-LBP) were analysed without salt-stripping (Figure 4A). Interestingly, these gelatin-LBP were able to bind to F-actin *in vitro* ((Figure 4A). This demonstrates that gelatin-LBP carry the factor(s), which are involved in F-actin-LBP interaction. As expected, a salt-stripping of these gelatin-LBP strongly reduced its ability to F-actin in the ABA by removing membrane-bound proteins, whereas the addition of J774.A1 cytosol again restored the binding of salt-stripped gelatin-LBP (Figure 4B).

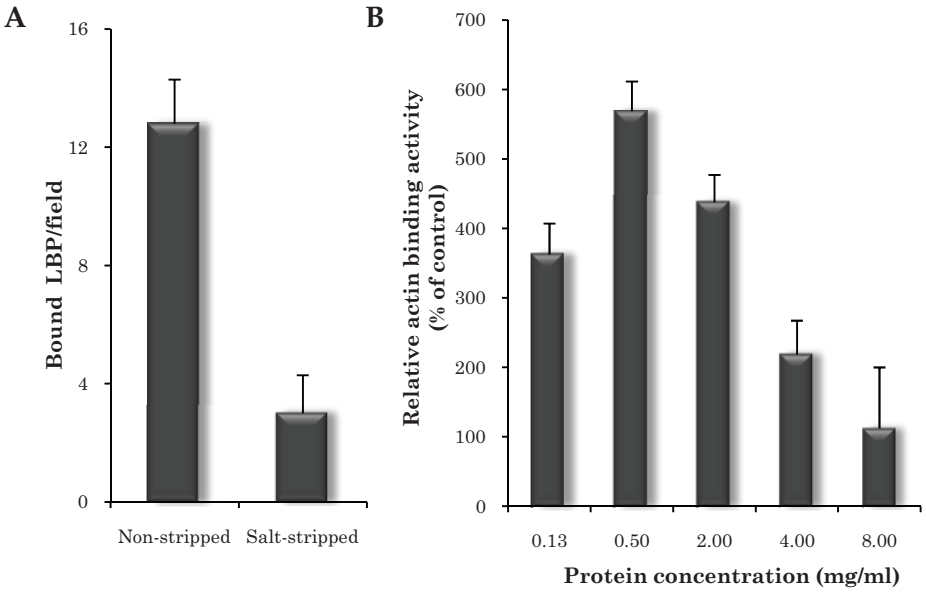

Figure 4: Actin biding activity of isolated gelatin-LBP. (A) Equal amount of non-stripped and salt-stripped was incubated on preformed actin network and average numbers of bound LBP per field were presented. (B) Different concentration of J774.A1 cytosol was incubated with gelatin-LBP for 20 minutes. Bound phagosome were counted and compared with the control (LBP incubated with HBS).

Required concentration and stimulation ability of the cytosol was greatly depended on individual cytosol. In general, lower concentrations of cytosol showed better stimulation of F-actin-LBP interaction. In current study I used 12 different cytosols which have show their

highest stimulatory activity between 0.05 and 2 mg/ml protein concentrations (see example in Figure 4B). Higher protein concentrations always caused reduction in F-actin-LBP interaction. Data suggested that the cytosol might contain both stimulatory and inhibitory activities which compete with each other for the binding site on LBP surface. Due to complexity of the cytosol for I decided to fractionate the cytosol.

4.1.2. Size exclusion chromatography of J774.A1 cytosol

To separate stimulatory factor(s) from the inhibitory factor(s), I firstly decided to use conventional protein separation techniques like size exclusion chromatography, ammonium sulphate precipitation, ion exchange chromatography. As the first step I used size exclusion chromatography or gel filtration for which I used small volume of highly concentrated (~35-40 mg/ml) J774.A1 cytosol. Cytosol was run on gel filtration column as mentioned in materials and methods. Each collected fraction was blotted on the nitro-cellulose membrane and stained with amino-black. Intensity of each blot was compared with standards to determine protein concentration of each fraction. The ensuing fractions containing proteins were checked for their ability to stimulate F-actin-LBP binding. The major part of the activity was found in initial fractions containing higher molecular weight proteins or protein complexes (Figure 5A). SDS-PAGE analysis showed that in these active fractions not only high molecular weight proteins, but also many low molecular proteins were present (Figure 5B). Fractions showing the highest activity were pooled together (here 29-31) and referred as active fraction. Active fraction gave nearly 1.7 times higher specific activity compared to cytosol (Table 4). Activity recovered after gel filtration was higher than the activity of the cytosol loaded on the column which indicated the presence of two proteins one stimulatory protein and another inhibitory protein. During the gel filtration both protein separated from each other which might be the reason for overall higher activity in the gel filtration fractions. Presence of Filamin A, annexin A1 and annexin A2 were checked with immunoblotting (Figure 5C). Although, all three proteins were found to be present in initial fractions (Figure 5D), annexin A2 and filamin A were not found in first protein containing filtration fraction. Since actin binding profile did not match with the filamin A profile in gel filtration fraction (Figure 5A and Figure 5D), I concluded that filamin A might not be the protein of our interest.

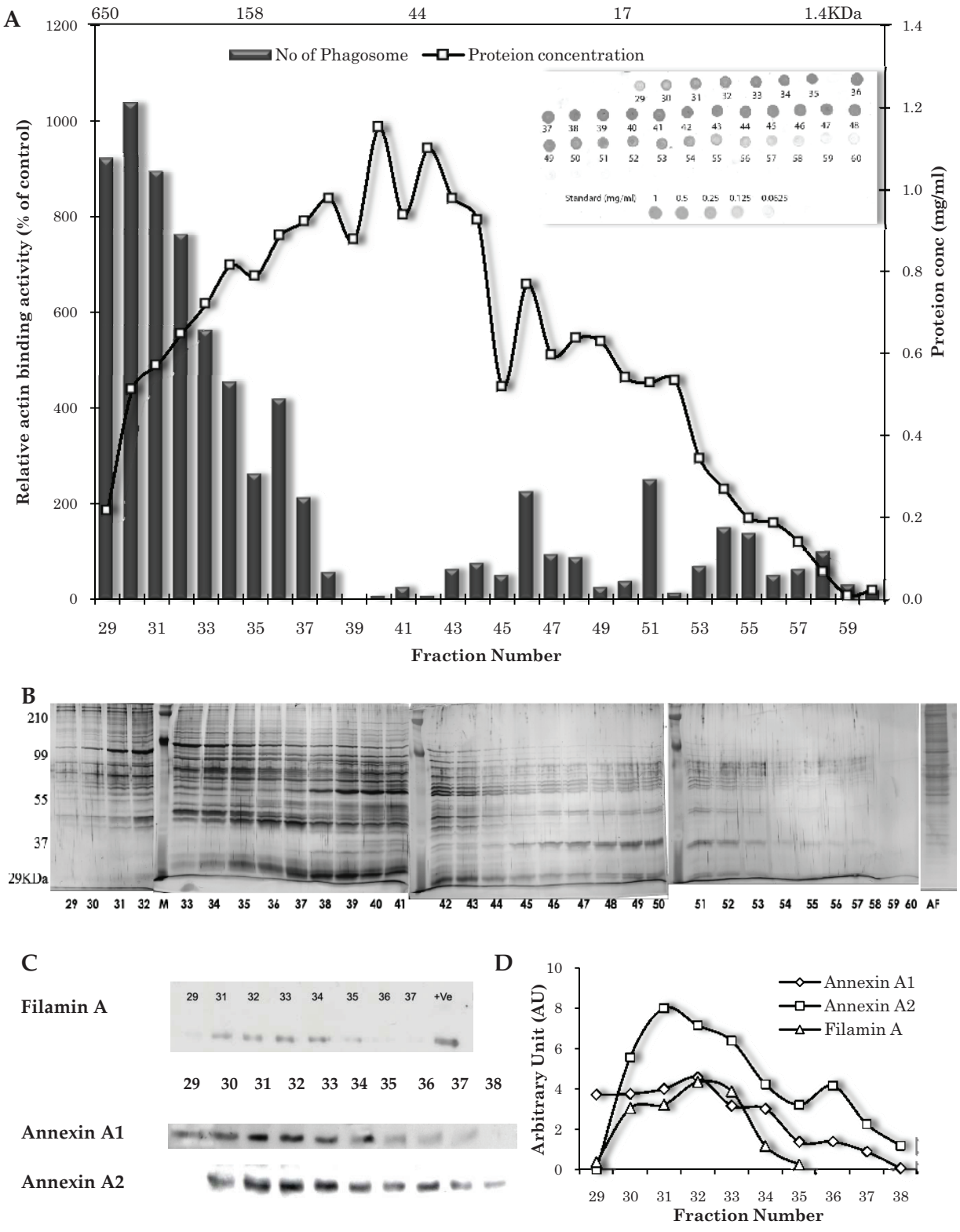

Figure 5: Fractionation of cytosol from J774A.1 macrophages by gel-filtration. Protein concentrations of gel filtration fractions were determined by amino black staining. Actin binding activity of protein containing fractions was checked. Molecular markers are shown on the top. Typical amino black staining is shown as insert in graph (A). To check the protein content initial protein containing fractions and active fraction (AF) were loaded on 12% SDS-PAGE and silver staining fractions were. Molecular markers sizes are shown on the left, Marker (*M*) (B). Immunoblotting of initial gel filtration fractions for filamin A, annexin A1 and annexin A2. +ve is total cell lysate (C), relative intensity of each proteins was calculated by Image J and presented as arbitrary unit (D).

4.1.3. Protein fractionation using ammonium sulphate precipitation method

For further purification, the active fraction was fractionated based on salt-out technique for protein precipitation. Here I preferred to use ammonium sulphate since in most cases protein precipitated by the ammonium sulphate can be renatured properly by dissolving in appropriate buffer and/or dialysis against low salt buffer. For the precipitation water saturated ammonium sulphate solution was added drop wise to 100 µl (~50-60 µg protein) active fraction and precipitated proteins were collected as mentioned in materials and methods. Most actin binding properties was found to be present in 30% ammonium sulphate cut fraction where 50% showed inhibition in actin binding activity (Figure **4A)**.

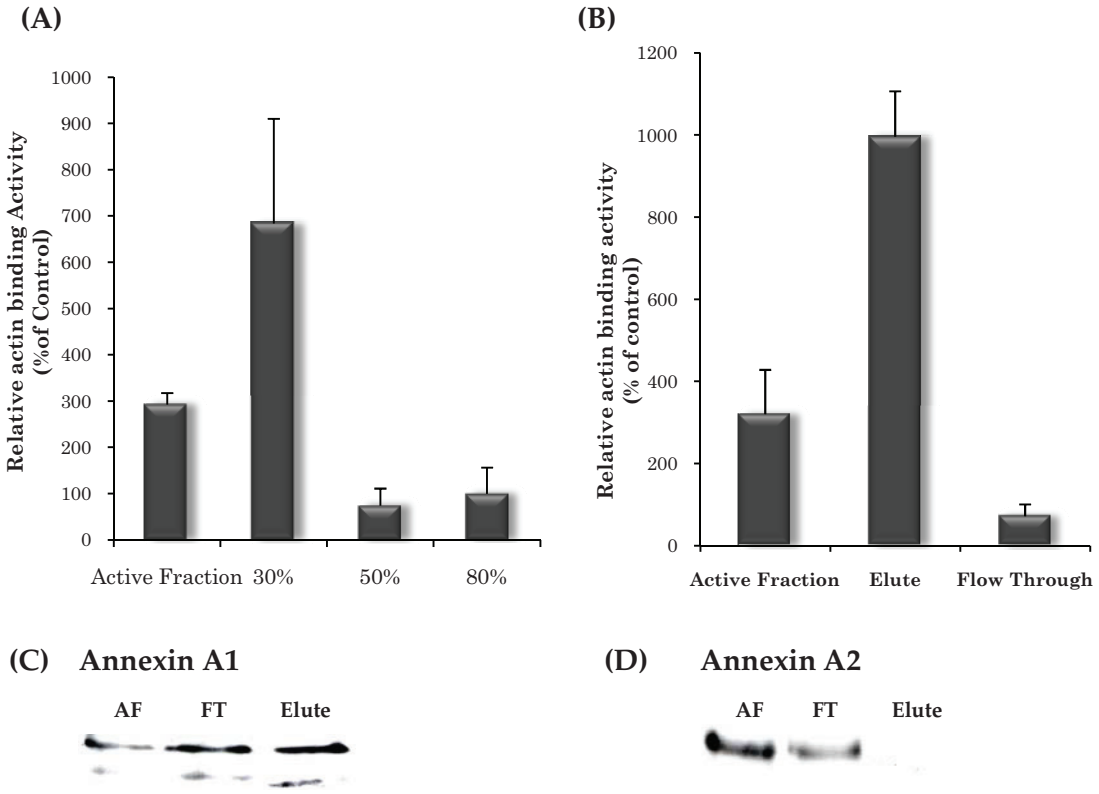

Figure 6: Purification of stimulatory factor from Active fraction. To isolate stimulatory protein from the active fraction, 50 µl active fraction was further fractionated by Ammonium Sulphate method (A) and cation chromatography (B). Active fraction was step by step precipitated at 30, 50 and 80% final ammonium sulphate concentration using water saturated ammonium sulphate solution as mentioned in material and method. Most of the stimulatory protein(s) found in protein precipitated at 30% ammonium sulphate concentration (A). Cation exchange chromatography was performed using phospho-cellulose resins. Proteins bound to resin and eluted with high-salts (Elute) contained all activity while proteins not bound to the resin (Flow Through) showed inhibition in F-actin-LBP binding activity. Presence of annexin A1 (C) and annexin A2 (D) in active fraction (AF) and phospho-cellulose unbound (FT) and eluted proteins (Elute) was analysed by immunoblotting.

Although ammonium sulphate gave us good separation, reproducibility of the method was a major drawback. Total 8 active fractions were precipitated with ammonium sulphate method in which only 75% active fractions gave clear separation of the activity. To get better

reproducibility, I decided to use more define methods like ion-exchange chromatography for protein fractionation.

4.1.4. Protein fractionation using cation chromatography

For precise protein fractionation, I decided to use cation chromatography using phospho-cellulose resign (P11). Similar to ammonium sulphate method 100 µl active fraction was subjected to cation chromatography. Proteins unbound to the resin were referred as flow through where proteins bound and proteins eluted with 1 M NaCl were referred as elute. Elute proteins contained most actin binding activity whereas unbound protein showed inhibitory activity (Figure 6B). Presence of inhibitory activity was more evident during cation chromatography as fraction gave nearly five times higher specific activity compared to active fraction and nearly 8 times higher activity compared to cytosol. Moreover the unbound proteins showed marked reduction in actin binding activity. I have also checked the presence of annexin A1 and annexin A2 during cation chromatography. Results showed that annexin A1 bound and eluted during cation chromatography but annexin A2 failed to bind to phospho-cellulose (Figure 6C and D) resin which indicated that annexin A1 might be the protein of our interest. As annexin A1 and annexin A2 show high structural similarity in their core and actin binding domain, before excluding annexin A2 we need further investigation.

Table 4: Purification of cytosolic fraction with enriched F-actin-LBP binding activity

Purification step	Protein concentration (mg/ml)	LBP/field	Specific activity (LBP/field/mg of protein)	Enrichment (%)
Control (buffer)	-	3.0	-	-
Cytosol	0.50	17.1	34	100
Active fraction	0.49	27.4	56	165
Cation chromatography	0.10	26.4	264	773

4.1.5. Proteomic analysis of phospho-cellulose eluted proteins

For further identification of proteins responsible for the F-actin-LBP interaction, the phospho-cellulose eluted fraction was analysed by mass spectrometry (LC-MS/MS). Mass spectrometry analysis identified 179 proteins. Considering the high sensitivity of the method and amount of the protein used for identification, I decided to use very stringent criteria for filtering the proteins. So as a first filter, proteins having less than 95% protein identification

probability and 2 unique peptides were removed, this resulted in 75 proteins of interest. Since the protein(s) of interest should also be a phagosome-binding protein, I compared our LC-MS/MS data with those previously obtained using mass spectrometry analysis of isolated LBP by Desjardins et al., 1994a and Hoffmann et al, 2010. This comparison resulted in 22 proteins which are known to be present on phagosomes (Table 5). In addition, the protein(s) of our interest has to be an ABP, which can link LBP and F-actin. According to a literature survey, only 11 of the 22 proteins have known actin binding property (Table 6). Out of 11 proteins only three, annexin A1, annexin A2 and moesin, have known lipid binding properties and thus were considered them for further investigation. Since moesin, a member of the ERM protein family, is known as nucleator of actin filament assembly on the phagosomes membrane and cannot bind to the lateral surface of preformed F-actin networks (Bretscher et al., 2000; Defacque et al., 2000), it could not be the protein of interest. Finally, I reduced the list to the two most probable candidates: annexin A1 and annexin A2.

Table 5: Phagosome-associating proteins present in phospho-cellulose eluted fraction.

No	Protein name	Accession numbers	Protein molecular weight (KDa)	Probability	Number of Unique Peptides
1	Ahnak AHNAK nucleoprotein isoform 1	IPI00553798	604.2	100%	92
2	Myh9 Myosin-9	IPI00123181	226.3	100%	66
3	Eef2 Elongation factor 2	IPI00466069	95.3	100%	10
4	Msn Moesin	IPI00110588	67.8	100%	8
5	Tkt Transketolase	IPI00137409	67.6	100%	7
6	Stip1 Stress-induced-phosphoprotein 1	IPI00121514	62.6	100%	5
7	Cct8 T-complex protein 1 subunit theta	IPI00469268	59.5	100%	2
8	Pkm2 Pyruvate kinase isozyme M2	IPI00407130	58.0	100%	20
9	Pdia3 protein disulfide isomerase associated 3	IPI00230108	56.7	100%	7
10	Eef1a1 Elongation factor 1-alpha 1	IPI00307837	50.7	100%	4
11	Eef1a2 Elongation factor 1-alpha 2	IPI00119667	50.4	100%	5
12	Eef1g Elongation factor 1-gamma	IPI00318841	50.0	100%	2
13	Pgk1;EG433594;EG668435 phosphoglycerate kinase 1	IPI00230002	44.5	100%	13
14	Aldoa Fructose-bisphosphate aldolase A	IPI00221402	39.3	100%	6
15	Anxa1 Annexin A1	IPI00230395	38.7	100%	3
16	Anxa2 Annexin A2	IPI00468203	38.7	100%	15
17	Mdh2 Malate dehydrogenase, mitochondrial precursor	IPI00323592	35.6	100%	3
18	Snx22;Ppib peptidylprolyl isomerase B	IPI00135686	23.7	100%	3
19	Prdx1 Peroxiredoxin-1	IPI00121788	22.2	100%	6
20	Hist1h1c Histone H1.2	IPI00223713	21.2	100%	3
21	2900073G15Rik myosin light chain, regulatory B-like	IPI00109044	19.9	100%	6
22	Arpc4;Ttll3 Actin-related protein 2/3 complex subunit 4	IPI00138691	19.6	100%	3

4.1.6. Recombinant annexin A1 stimulates F-actin-LBP interaction in a Ca^{2+}-dependent manner *in vitro*

Our initial results obtained during cation chromatography suggested that annexin A1 but not annexin A2 is responsible for the F-actin-LBP binding activity. To support our hypothesis that annexin A1, but not annexin A2, which is a close homologue in the annexin family, is responsible for the F-actin-LBP interactions I performed an *in vitro* actin binding assay in presence of bacterially expressed recombinant full-length annexin A1 and annexin A2. As expected, both the annexin A1 and annexin A2 failed to stimulate the F-actin-LBP interaction in the absence of Ca^{2+} (Figure 7). However, in the presence of Ca^{2+} annexin A1 strongly stimulate the gelatin-LBP-F-actin interaction, while annexin A2 failed to show a significant effect (Figure 7). Since the S100A10, light chain of annexin A2 is important for several of its biological activities (Miwa et al., 2008), an annexin A2 effect on the F-actin-LBP binding activity was also analysed using annexin A2/S100A10 hetero-tetramer complex purified from pig intestine (Gerke and Weber, 1984). Similar to bacterially expressed annexin A2, its hetero-tetramer complex was also failed to stimulate F-actin-LBP interaction both in presence and absence of Ca^{2+} (Figure 7). This supported our hypothesis that annexin A1, but not annexin A2, is a protein responsible for mediating the F-actin-LBP interaction *in vitro*. Results clearly indicate that annexin A1 is the protein which responsible for F-actin-LBP interaction, *in vitro*.

Table 6: Actin binging proteins present in phospho-cellulose eluted proteins.

No	Protein name	Accession numbers	Protein molecular weight (KDa)	Reference
1	Annexin A1 (Anxa1)	IPI00230395	38.7	(Blackwood and Ernst, 1990)
2	Annexin A2 (Anxa2)	IPI00468203	38.6	(Blackwood and Ernst, 1990)
3	Moesin (Msn)	IPI00110588	67.7	(Nakamura et al., 1999)
4	Elongation factor 2 (Eef2)	IPI00466069	95.3	(Bektas et al., 1994)
5	Elongation factor 1-alpha 1 (Eef1a1)	IPI00307837	50.7	(Ejiri, 2002)
6	Elongation factor 1-alpha 2 (Eef1a2)	IPI00119667	50.4	(Ejiri, 2002)
7	Myosin-9 (Myh9)	IPI00123181	226.3	(Knetsch et al., 1999)
8	Ttll3 Actin-related protein 2/3 complex subunit 4 (Arpc4)	IPI00138691	19.6	
9	2900073G15Rik myosin light chain, regulatory B-like	IPI00109044	19.9	(Fujita et al., 1999)
10	AHNAK nucleoprotein isoform 1 (Ahnak)	IPI00553798	604.2	(Benaud et al., 2004)
11	Pyruvate kinase isozyme M2 (Pkm2)	IPI00407130	58.0	(Arnold et al., 1971)

To confirm that inhibitory factor(s) can play also an important role in regulation of annexin F-actin-LBP binding activity. Bacterial purified annexin A1 was incubated either alone or with phospho-cellulose flows through fraction. Strong reduction in F-actin-LBP binding activity of annexin A1 was observed in presence of phospho-cellulose unbound proteins (Figure 7). Data clearly suggest the presence of inhibitory factors in phospho-cellulose flow through fraction.

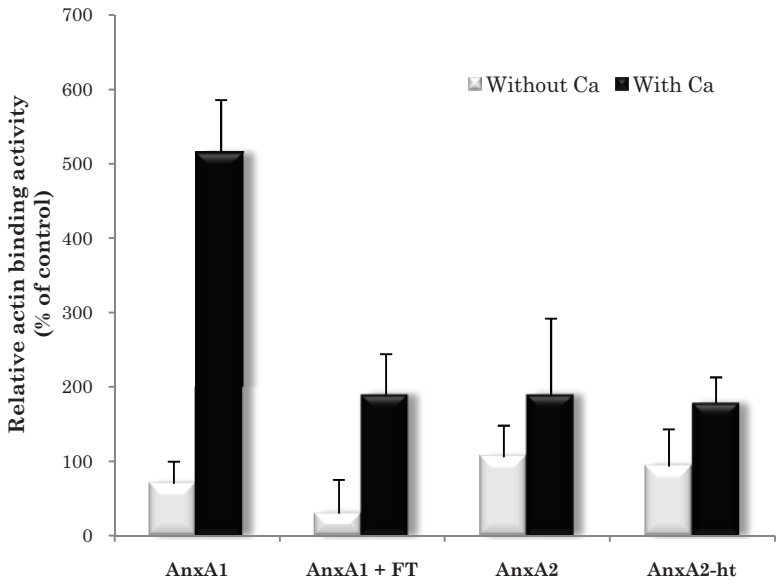

Figure 7: *In vitro* actin binding assay with purified exogenous annexin A1 and annexin A2. Bacterial expressed and purified annexin A1 (AnxA1) alone or with phospho-cellulose flow through (AnxA1 + FT), annexin A2 (AnxA2) and pig intestine annexin A2/S100A10 hetero-tetramer complex (AnxA2-ht) were incubated with the gelatin-LBP in presence of Ca^{2+} (With Ca) or absences of Ca^{2+} (Without Ca). Annexin A1 strongly stimulate F-actin-LBP binding in presence of Ca^{2+} where both annexin A2 and annexin A2/S100A10 hetero-tetramer complex failed to stimulate the binding.

4.1.7. Annexin A1 is present on isolated gelatin-LBP and binds to gelatin-LBP in Ca^{2+}-dependent manner

The results mentioned above showed that exogenous, bacterially expressed annexin A1 can facilitate F-actin-LBP interaction. In order to confirm the role of exogenous annexin A1, its presence on isolated gelatin-LBP was analysed. Using immunofluorescence staining I proved that annexin A1 was found on isolated gelatin-LBP (Figure 8 A, B, Non-stripped) that were not treated with high salt concentration (non-stripped). Isolated non-stripped LBP had many membrane associated proteins (Desjardins et al., 1994a; Hoffmann et al, 2010). When non-stripped gelatin-LBP were treated with 2M NaCl, they lost nearly all F-actin binding activity and a number of membrane associated proteins (Al Haddad et al., 2001; Defacque et al., 2000). In line with these data salt-stripping of gelatin-LBP also efficiently

removed pre-bound annexin A1 from gelatin-LBP membranes (Figure 8 A, B, salt-stripped). Interestingly, the addition of bacterially expressed full length annexin A1 or phospho-cellulose eluted proteins to salt-stripped gelatin-LBP restored both, the appearance of annexin A1 on gelatin-LBP and their F-actin binding activity (Figure 8 A, B and C). Furthermore, this effect was strongly Ca^{2+}-dependent (Figure 8 A and B). Fluorescence intensity on gelatin-LBP incubated with exogenous annexin A1 in the presence of Ca^{2+} was at least five times higher than gelatin-LBP incubated without Ca^{2+} (Figure 8 D).

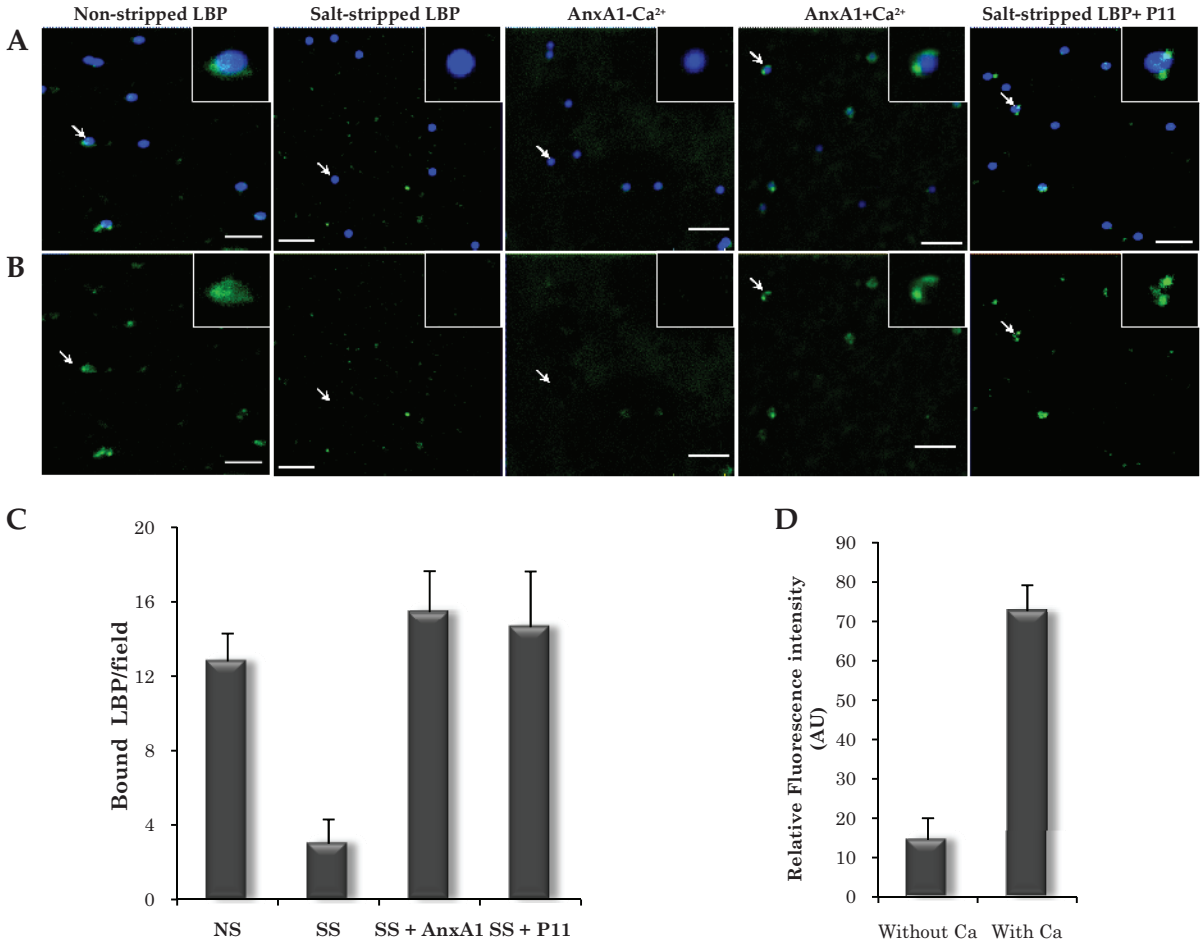

Figure 8: Presence of annexin A1 on gelatin-LBP. Gelatin-LBP (blue) were subjected to indirect immunofluorescence microscopy using antibody against annexin A1 (green). Inserts: LBP marked with arrow at 3x magnification. Bars = 5µm. Merged image of differently treated gelatin-LBP (A) and annexin A1 staining for differently treated gelatin-LBP (B). Actin binding activity of non-stripped (NS), salt-stripped (SS), salt-stripped gelatin-LBP incubated with annexin A1 in presence of Ca^{2+} (SS + AnxA1) and salt-stripped gelatin-LBP incubated with phospho-cellulose eluted proteins (SS + P11) (C). Quantification of annexin A1 fluorescence intensity on gelatin-LBP incubated with annexin A1 in presence or absence of Ca^{2+} (D). Immunofluorescence staining revealed that annexin A1 was present on non-stripped gelatin-LBP and removed by the salt-stripping. Annexin A1 reappeared on gelatin-LBP only after incubation with phospho-cellulose eluted protein or with annexin A1 in presence of Ca^{2+}.

4.1.8. Anti-annexin A1 antibodies inhibit F-actin-LBP interaction

Apart from being present on phagosomal membranes, annexin A1 was also found in cytosolic fractions that were enriched in F-actin-LBP binding activity (Figure 5C). Therefore I next analysed its involvement in the activity of this fraction by pre-incubating the annexin A1 containing, phospho-cellulose eluted fraction with rabbit polyclonal anti-annexin A1 antibodies. As a control, rabbit polyclonal anti-moesin antibodies were used. Blocking of annexin A1 with the anti-annexin A1 antibodies strongly reduced the F-actin-LBP interaction that was triggered by the phospho-cellulose eluted protein fraction (Figure 9). In contrast, the anti-moesin antibodies did not have any significant effect on the F-actin-LBP interaction (Figure 9). These data clearly argue that annexin A1 is the cytosolic protein of the phospho-cellulose eluted fraction that stimulates the gelatin-LBP-F-actin interaction *in vitro.*

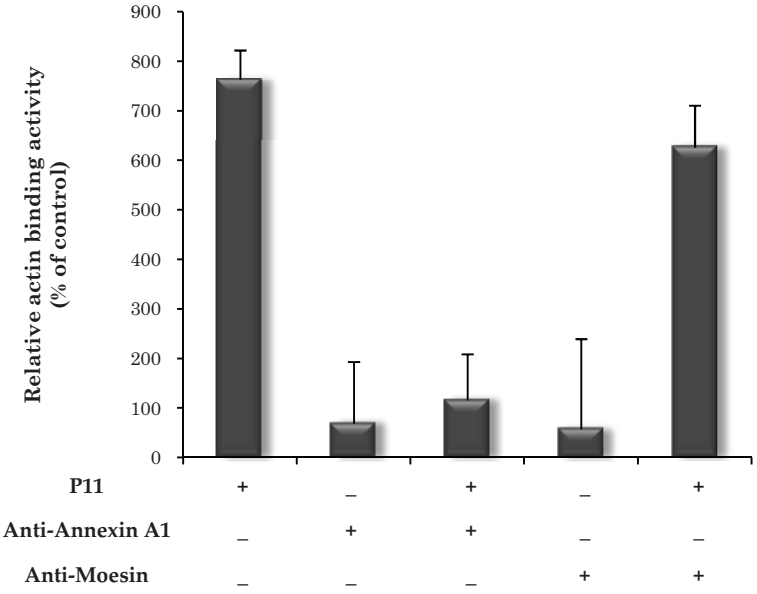

Figure 9: Inhibition of actin binding activity using specific antibodies. Relative F-actin-LBP binding activity of phospho-cellulose eluted proteins (P11) alone or with phospho-cellulose eluted proteins pre-incubated with anti-annexin A1 (Anti-annexin A1) or anti- moesin antibodies (Anti-moesin). Incubation of phospho-cellulose eluted protein with anti-annexin A1 strongly reduced its F-actin-LBP binding activity, while anti-moesin antibody did not have any effect.

4.1.9. Effect of nucleotides and phospholipids on Annexin A1 F-actin-LBP binding activity

Previous study by (Al Haddad et al., 2001) suggested that F-actin-LBP binding can be affected by the nucleotide. Therefore, I analysed the effect of different nucleotides and phospholipids on annexin A1 F-actin-LBP stimulatory activity. Annexin A1, Ca^{2+}, and gelatin-LBP was incubated for 20 minutes before perfusing in the reaction chamber. Previous study by (Blackwood and Ernst, 1990) suggested that annexin A1 does not bind to

phosphatidylcholine (PC), so I used it as a negative control in current study. The F-actin-LBP binding activity of annexin A1 in presence of Ca^{2+} was considered as 100%. Incubation of annexin A1 with ATP and ADP showed more than 50% reduction in its F-actin-LBP binding activity (Figure 10). On the other hand, presence of GTP had no effect on annexin A1 F-actin-LBP stimulatory activity. Surprisingly AMP-PNP dramatically increased annexin A1 F-actin-LBP binding activity. Incubation of annexin A1 with PIP2 strongly reduces it stimulatory effect (Figure 10). Similar to PC, cholesterol did not show any effect on F-actin-LBP binding activity of annexin A1 while PS and AA stimulated annexin A1 F-actin-LBP binding activity (Figure 10).

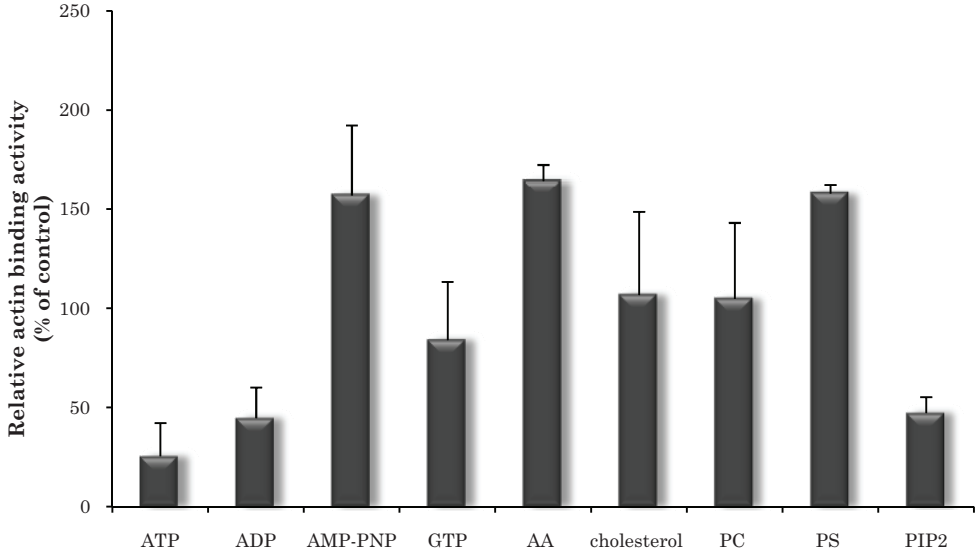

Figure 10: Effect of different nucleotides and phospholipids on annexin A1's F-actin-LBP binding activity. Annexin A1 was preincubated with ATP, ADP, AMP-PNP, GTP, arachidonic acid (AA), Cholesterol, phosphatidylcholine (PC), phosphatidylserine (PS) and phosphatidylinositol (4, 5) bis-phosphate (PIP2) in presence of Ca^{2+}. Actin binding activity of annexin A1 in presence of Ca^{2+} was considered as 100%.

4.1.10. Annexin A1 knockdown cells show impaired phagocytosis of gelatin beads

Previous studies have shown that phagocytosis was impaired in macrophages isolated from annexin A1-knockout mice (Hannon et al., 2003). In order to analyse in more detail the role of annexin A1 in phagocytosis, annexin A1 was down-regulated using siRNA in cultured RAW 264.7 macrophages. The control and mock transfected cells did not show any reduction in annexin A1 expression while siRNA-transfected cells showed a nearly 50% reduction in total annexin A1 levels (Figure 11A and B). Phagocytic activity (number of latex beads per cell) of mock-transfected cells was comparable with control non-transfected cells

(Figure 11C). However, siRNA transfected cells showed a nearly 50% reduction in their phagocytic activity (Figure 11C).

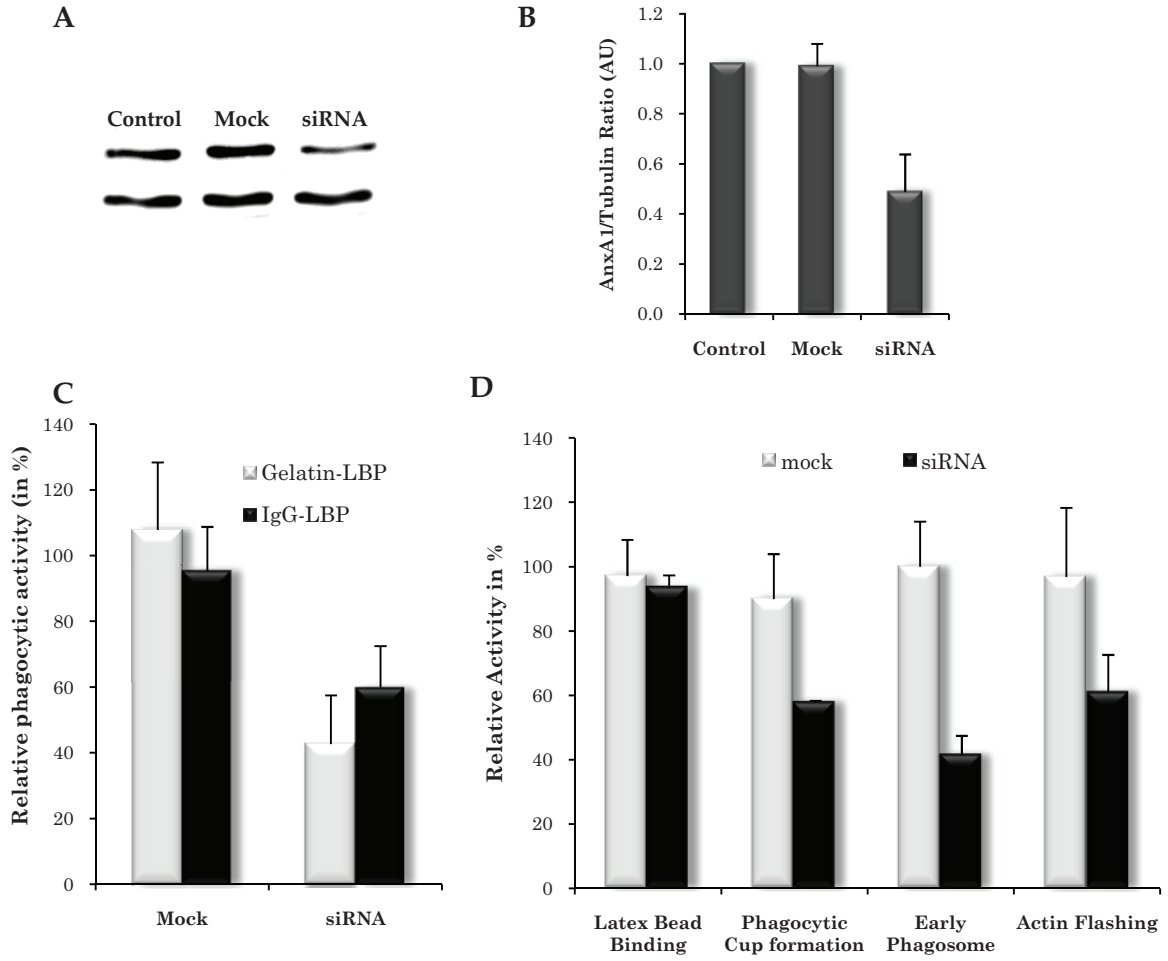

Figure 11: Annexin A1 knockdown cells showed impaired phagocytosis. Immunoblotting of the cell lysates prepared from control cells *(Control)*, mock cells *(Mock)* and siRNA cells *(siRNA)* with anti-annexin A1 *(Annexin A1)* and anti-α-tubulin *(α Tubulin)* antibodies (A). Quantification of annexin A1 expression data obtained by immunoblotting, 3 independent experiments (B). Relative phagocytic activity for gelatin or Fc coated latex beads (latex beads/cell) of transfected cells. Average of 3 independent experiments (C). Mock transfected and siRNA transfected RAW 264.7 macrophages were incubated with 3 μm latex beads for different times (see materials and methods) to analyse latex beads binding, phagocytic cup formation, early phagosome formation, and actin flashing. Annexin A1 knockdown does not affect latex beads binding but significantly reduced other phagocytic activities (D).

Several studies indicated that annexin A1 knockout reduced the expression of some phagocytic receptors in mouse macrophages (Hannon et al., 2003; Yona et al., 2004). Therefore I checked whether the reduction of phagocytic activity in annexin A1 depleted cells was a primary consequence of the reduced annexin A1 levels or a secondary effect resulting from a potential decrease in cell surface receptors. First, I addressed this by choosing a well defined Fcγ receptor (FcγR) mediated phagocytic pathway, because the expression of FcγRs is not affected in annexin A1 knockout macrophages (Hannon et al.,

2003; Yona et al., 2004). The experiments were performed using 1 μm latex beads coated with mouse IgG Fc fragments (Fc-beads), which, as shown previously, internalised specifically through FcγRs (Ahmad et al., 2010; Hoffmann et al., 2010). Although phagocytic efficiency of Fc-beads was nearly 2.5 times higher than that of gelatin-beads, siRNA transfected RAW 264.7 macrophages also showed a significant reduction (~40%) in phagocytic activity (Figure 11C). These results indicated that annexin A1 is involved in the phagocytic uptake of beads and that the reduced phagocytosis in annexin A1 depleted cells is not due to a possible effect on receptor expression.

Next, I investigated the role of annexin A1 in four major events of phagocytosis: ligand-receptor binding, phagocytic cup formation, early gelatin-LBP formation and actin flashing of late gelatin-LBP. SiRNA transfected RAW 264.7 macrophages were incubated with 3 μm latex gelatin-beads for different times and the binding and uptake of gelatin-beads was analysed as described in material and methods. Annexin A1 knockdown did not affect beads binding to RAW 264.7 macrophages (Figure 11D), but resulted in impaired phagocytic cup formation (Figure 11D). The reduction in annexin A1 expression also resulted in nearly 60% decrease in early phagosome formation (Figure 11D). Furthermore, siRNA knockdown experiments revealed that the reduction in annexin A1 expression reduced the transient F-actin assembly on late gelatin-LBP, which is also referred as "actin-flashing" phenomena (Liebl and Griffiths, 2009; Yam and Theriot, 2004). Following 1 hour pulse and 2 hours chase regime, siRNA mediated reduction of annexin A1 expression caused a nearly 40% decrease of actin flashing events at the gelatin-LBP (Figure 11D).

Since annexin A1 knockdown had a strong inhibitory effect in phagocytic events where F-actin dynamics plays a key role, I studied spatial and temporal dynamics of annexin A1 association with gelatin-LBP during phagocytic events mentioned above.

4.1.11. Spatial and temporal co-localisation of annexin A1 and F-actin during phagocytosis

Since actin polymerisation is a major and indispensible step of phagocytic cup formation (Castellano et al., 2001) and since annexin A1 is an F-actin binding protein possible involved in linking actin filaments to nascent phagosomes, I analysed a potential co-localisation of annexin A1 and F-actin at phagocytic cups. Therefore, macrophages were

triple stained with rhodamine-phalloidin for F-actin, anti-annexin A1 antibodies and the cytosolic marker Celltracker™.

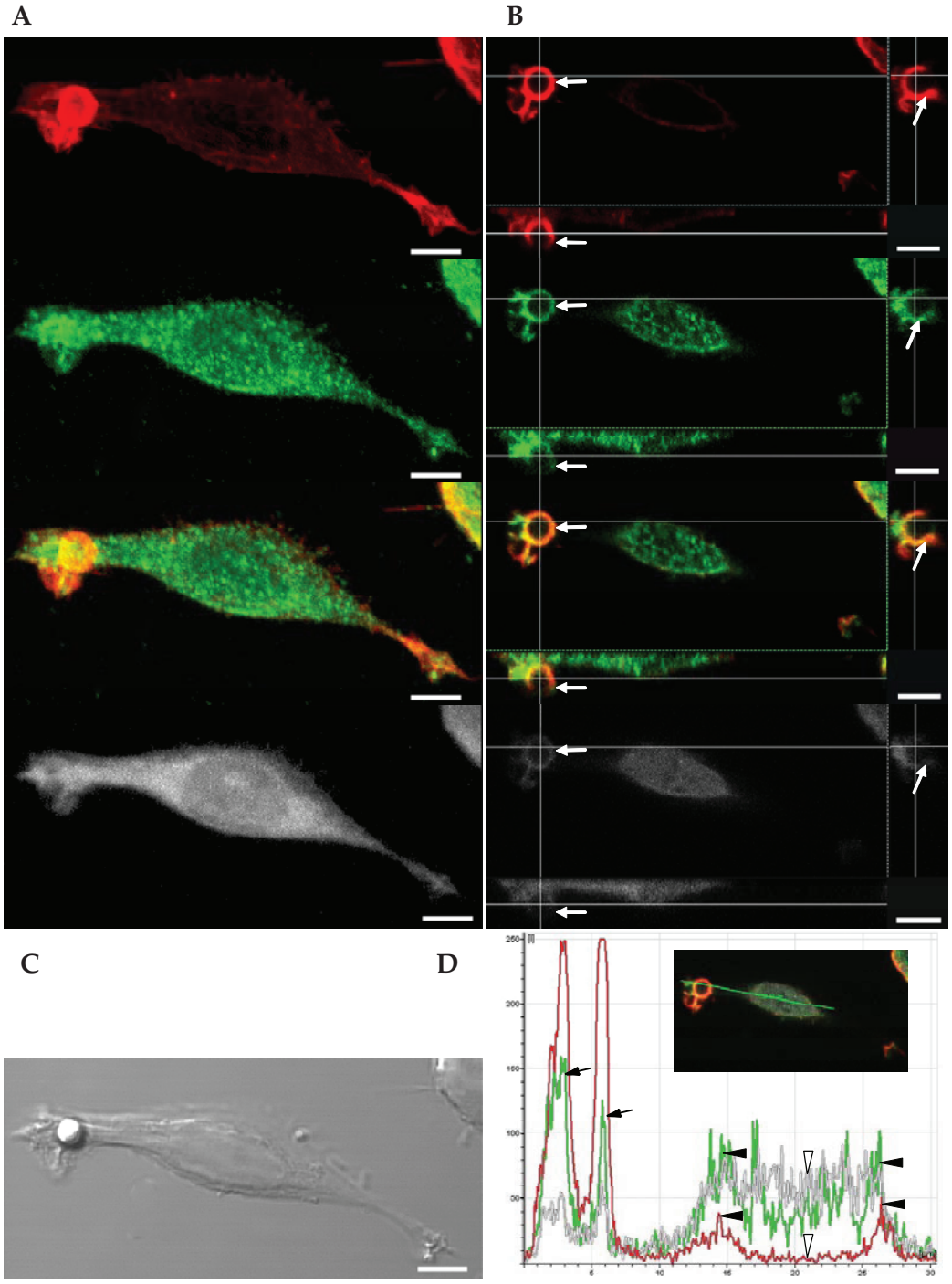

Figure 12: Co-localisation of LBP and annexin A1 during early stages of phagocytosis. RAW 264.7 cells were incubated with latex beads in internalisation medium for 5 minutes followed by fixing and staining. Cells were stained for annexin A1 (green), F-actin (Red) and a cytosolic marker (Celltracker™ in grey). (A) Maximum intensity projection of confocal images. (B) 3D cross section images of phagocytic cup formation. Annexin A1 co-localised with F-actin on extended filopodia of phagocytic cups (arrows). (C) DIC image shows position of latex bead. (D) Section of confocal images analysed for fluorescence profile. Histogram shows fluorescence intensities of F-actin (red line), annexin A1 (green line) and Celltracker™ (grey line). Higher annexin A1 concentration can be seen at phagocytic cups (arrows) compared to the cytosol (arrow heads) and the cell membrane (filled arrow heads). Bars = 5µm.

As expected, strong fluorescent staining of F-actin was observed at sites of latex bead uptake (Figure 12A and C) and at the cell periphery (Figure 12A). On the other hand, both annexin A1 and Celltracker™ appeared to be more or less evenly distributed in the cytosol (Figure 12A). Therefore, a 3D cross-section analysis of confocal images was carried out (Figure 12B). This analysis clearly showed that annexin A1 co-localised with F-actin on phagocytic cup (Figure 12B, arrows). To obtain further insight, I analysed confocal images for fluorescence intensity of the individual dyes (Figure 12D). Along with F-actin, the intensity of annexin A1 staining was found to be higher on phagocytic cups (Figure 12D, arrows) compared to the staining intensity of the cytosol (Figure 12D, arrow heads) and plasma membrane marker (Figure 12D, filled arrow heads). These data indicated that annexin A1 indeed accumulated at phagocytic cups.

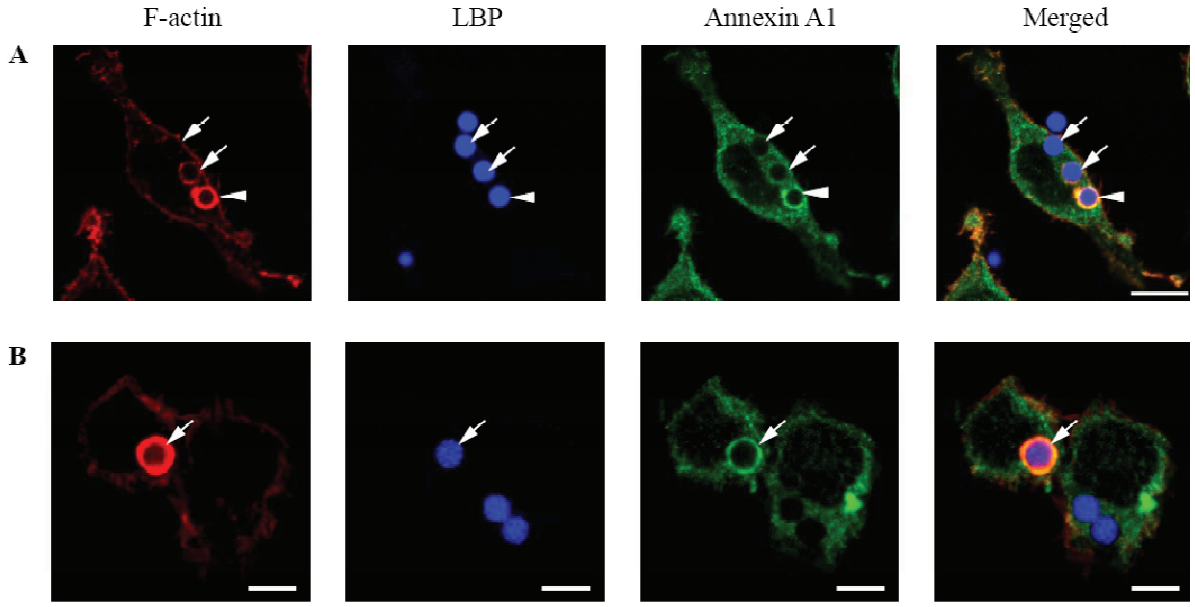

Figure 13: Annexin A1 co-localised with F-actin at early and late stages of phagocytosis. RAW 264.7 cells were incubated with gelatin-beads in internalisation medium for 30 minutes (A) or a 60 minutes pulse plus 120 minutes chase (B). Annexin A1 (green) co-localised with F-actin (red) on early gelatin-LBP (blue) (arrow head) and transiently actin flashing gelatin-LBP. The accumulation of annexin A1 on gelatin-LBP eventually decreased as phagosome matures (B, arrows). Bars = 5µm.

Naive LBP acquire a dense F-actin network on the membrane, which gradually decrease as LBP become more mature (Castellano et al., 2001). Indeed, after uptake I observed an F-actin accumulation on gelatin-LBP (Figure 13A, arrow head) and then F-actin dissociation from gelatin-LBP (Figure 13A, arrows). Notably, both events were accompanied by an increase and then decrease of gelatin-LBP-associated annexin A1 (Figure 13A). At late stages of phagocytosis some gelatin-LBP showed actin flashing. This also correlated with an annexin A1 accumulation near actin-flashing gelatin-LBP (Figure 13B).

4.1.12. Annexin A1 knockdown does not alter gelatin-LBP maturation

The complete molecular mechanism and physiological importance of actin flashing is far from understood (Liebl and Griffiths, 2009). In our current study we observed that in control only less than 10% of LBP undergo actin flashing. However, we checked the possible involvement of annexin A1 in LBP maturation process. We incubated non-transfected, mock transfected and annexin A1 siRNA transfected cells with 3 μm gelatin-beads for 30 minutes, followed by fixing and immune-fluorescence staining with the late phagosome marker LAMP2. The number of LAMP2 positive LBP per internalised gelatin-beads was counted and presented in percentage. Obtained data are presented in the figure below. These data indicate that there is no marked difference in phagosome maturation process. This finding is mentioned in our revised manuscript in the discussion (page no 16) (if necessary we can include these data as supplementary material).

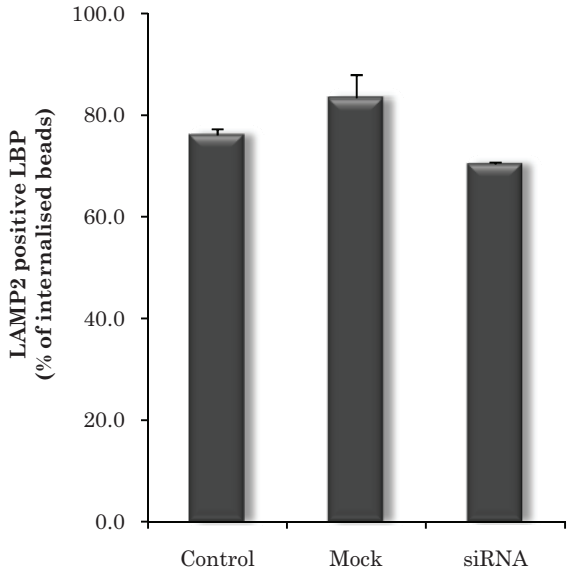

Figure 14: Effect of Annexin A1 knockdown on phagosome maturation. Gelatin-beads were incubated with RAW 264.7 macrophage for 30 minutes and cells were stained with the late phagosome marker LAMP2 as an indicator of phagosome maturation. Knockdown of annexin A1 does not have any effect on gelatin-LBP maturation process.

4.1.13. Annexin A1 could not support actin nucleation on gelatin-LBP

Recently annexin A2 showed to be involved in actin polymerisation on endosomes membrane (Morel et al., 2009). To investigate the possible involvement of annexin A1 in actin polymerisation, I performed actin nucleation assay using purified and alexa-594 labelled G-actin. Since annexin A2 was reported to nucleate actin, it was used as the positive control. Obtained data suggested that salt-stripped gelatin-LBP alone or in the presence of

1mM Ca^{2+} failed to stimulate actin polymerisation (Figure 15). As expected annexin A2 strongly stimulate actin nucleation on gelatin-LBP surface in presence of Ca^{2+}. Data also suggest that annexin A1 alone can stimulate actin polymerisation on gelatin-LBP surface which further increases by addition on 1 mM Ca^{2+} (Figure 15).

Since in presence of 1 mM Ca^{2+} and ATP actin can polymerise (Tellam, 1985) and annexin A1 can bundle the polymerised actin filaments (Glenney, Jr. et al., 1987), it was important to confirm that observed actin nucleation was not a false positive results. To confirm the obtained data, gelatin-LBP were incubated with annexin A1 in the presence or absence of Ca^{2+}, followed by LBP purification by discontinuous sucrose gradient. Purified LBP were subjected to actin nucleation assay as mentioned before in presence or absence Ca^{2+}. Neither annexin A1 incubated with Ca^{2+} nor without Ca^{2+} were able to nucleate actin on LBP surface both in presence or absence of Ca^{2+}. Local F-actin accumulation was observed only on the LBP which were incubated with annexin A1 in presence of Ca^{2+} (Figure 15C). Observed data suggest that annexin A1 is important for the actin binding to the LBP but it does not play any role in actin polymerisation.

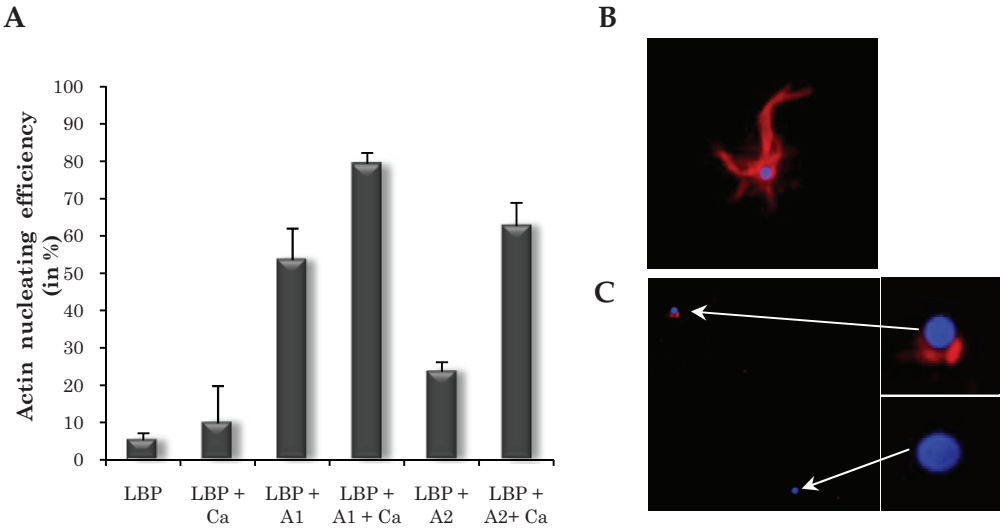

Figure 15: *In vitro* actin nucleation assay. (A) gelatin-LBP (*LBP*) were incubated at RT for 10-15 minutes with purified Alexa 594 labelled G-actin, ATP, β-thymosin, and DTT on gelatin coated slides. Effect of annexin A1 (*A1*) and annexin A2 (*A2*) on actin nucleation on gelatin-LBP were checked in the presence and absence of Ca^{2+} (*Ca*). (B) Typical actin nucleating gelatin-LBP in presence of annexin A1 and Ca^{2+}. (C) Actin accumulation on LBP purified following incubation with bacterial expressed annexin A1 in presence of Ca^{2+}. Inserts are 5 times magnification of actin accumulating and non-accumulating LBP.

Taken together our results indicate that annexin A1 is spatially and temporally co-localised with F-actin on phagosome membrane during early and late stages of phagocytosis and act as functional linker between F-actin and LBP. Moreover our data also suggest that

annexin A1 provides the structural support and might not have any direct role in polymerisation.

4.2. Ligand-receptor interaction decide the involvement of annexin A1 during macrophage phagocytosis

Previous study by (Hoffmann et al., 2010) suggested that different receptor mediated phagocytosis leave unique signatures on different LBP which includes proteins composition of the LBP. In their study they also showed that annexin A1 is present on Fc receptor mediated LBP (Fc-LBP) but not on the mannose receptor mediated LBP (man-LBP). Study in knockout mice by (Yona et al., 2004) also suggested stimulus dependent defect in mouse macrophages. These studies inspired us to look more insight into the role of annexin in different receptor mediated phagocytosis. Due to several limitations inclusion of all characterised phagocytic receptors was not possible. To cover two major groups of phagocytic receptors, I used Fc fragment of mouse IgG and mannan coated latex beads which internalised through non-opsonic mannose receptor and opsonic FcγRs, respectively (Ahmad et al., 2010; Hoffmann et al., 2010).

4.2.1. Different receptor derived non-stripped LBP show different F-actin binding affinity.

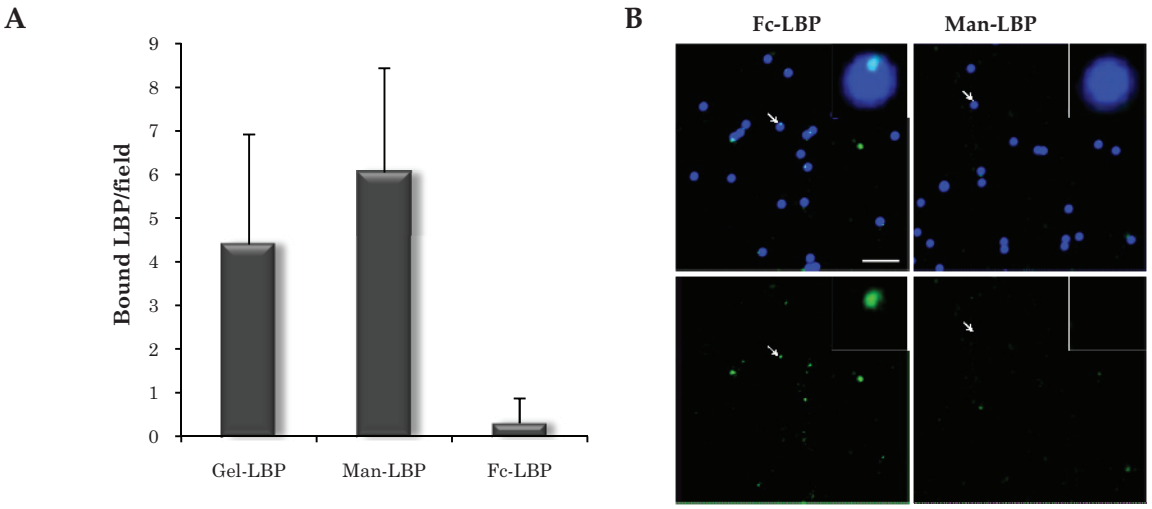

Figure 16: F-actin binding activity of different LBP. (A) Differently receptors derived LBP showed different F-actin binding activity. (B) Fc-LBP and Man-LBP (blue) were subjected to indirect immunofluorescence microscopy using antibody against annexin A1 (green). Inserts shows LBP marked with arrow at 3x magnification. Bars = 5µm. Upper panel shows merged image of differently LBP and lower panel shows annexin A1 staining for differently LBP

To study the effect of annexin A1 on different LBP, first I characterise F-actin binding activity of purified non-stripped LBP. I performed actin binding activity using the same concentration of purified LBP. Obtained data showed in (Figure 16A), which clearly suggest

that different receptors derived LBP had different F-actin binding affinity. Non-stripped man-LBP showed highest F-actin-LBP binding activity followed by geltain-LBP. Fc-LBP showed the least F-actin-LBP binding activity which was nearly 10-12 times lower than that of gelatin-LBP and man-LBP.

Next I checked the presence of annexin A1 on purified non-stripped LBP. In agreement with previous study by (Hoffmann et al., 2010), annexin A1 was not found on man-LBP but was present on Fc-LBP (Figure 16B).

4.2.2. Recombinant annexin A1 stimulates F-actin-LBP interaction of non-stripped and salt-stripped LBP

Since not all LBP harbour annexin A1 on their membrane, I checked the effect of bacterial expressed recombinant annexin A1 on different LBP in presence or absence of Ca^{2+}. Moreover, I also checked the effect on only Ca^{2+} on purified LBP. As expected I could see the increase in F-actin-LBP binding for the gelatin and Fc LBP, where no effect was observed on man-LBP (Table 7). On other hand annexin A1 alone strongly reduces all LBP F-actin binding activity. Interestingly, stimulatory effect of annexin A1 was different in different LBP F-actin binding activity but in all cases the maximum bound LBP per field was restricted nearly to 13 LBP per field. These data clearly argue at given annexin A1 and LBP concentration, number of binding sites for annexin A1 on LBP membrane was a limiting factor. Although annexin a1 was not present on man-LBP, incubation with recombinant annexin A1 resulted in nearly 3 fold increase in F-actin-LBP binding activity. Results indicate that in intracellular condition annexin A1 binding was regulated by an unknown factor or a competition for same binding site restrict annexin A1 biding to man-LBP.

Table 7: Effect of annexin A1 on different LBP F-actin binding activity (bound LBP/field)

	LBP	LBP + Ca^{2+}	LBP + AnxA1	LBP + AnxA1 + Ca^{2+}
Gelatin-LBP	4.8 ± 0.5	7.9 ± 0.5	1.1 ± 0.6	10.9 ± 2.0
Fc-LBP	1.1 ± 0.7	4.3 ± 0.5	0.4 ± 0.1	10.2 ± 3.8
Man-LBP	4.4 ± 0.1	4.0 ± 0.3	0.4 ± 0.1	12.8 ± 0.6

Non-stripped LBP contain more than 1000 proteins on their surfaces (Hoffmann et al., 2010) so there could be an obvious competition for the binding sites so to study the effect of annexin A1 on different LBP, salt-stripped LBP was incubated with bacterial purified recombinant annexin A1 in presence or absence of Ca^{2+}. Similar to non-stripped LBP, presence of annexin A1 resulted in increase in F-actin-LBP binding activity (Figure 17 A).

Stimulation in Fc-LBP and man-activity was nearly 2 times higher than gelatin-LBP. To confirm the presence of annexin A1 on Fc and man-LBP were subjected to indirect immunofluorescence. Immunofluorescence confirms the Ca^{2+} dependent annexin A1 binding to both Fc and man-LBP (Figure 17B). Since receptors signalling affect protein composition of LBP including the lipid metabolic enzymes (Hoffmann et al., 2010), I hypothesise that amount of various phospholipids might be altered on different receptor mediated LBP which ultimately leads to different annexin A1 dependent stimulatory effect.

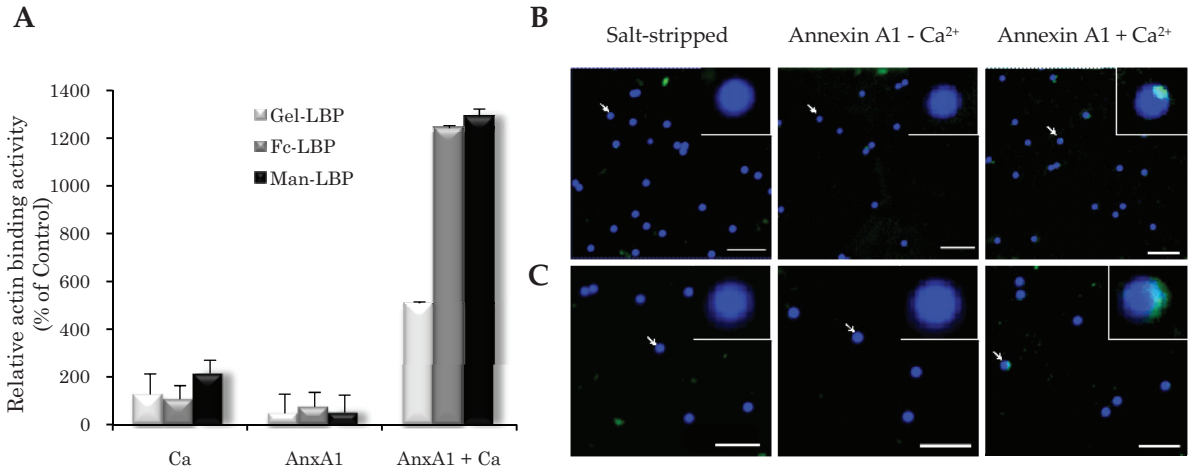

Figure 17: Annexin A1 stimulates F-actin-LBP binding activity of different LBP in Ca^{2+} dependent manner. (A) Bacterial expressed recombinant annexin A1 was incubated with different salt-stripped LBP together with Ca^{2+} alone (Ca), annexin A1 alone (AnxA1) or annexin A1 and Ca^{2+} (AnxA1 + Ca). (B) Fc-LBP and (C) Man-LBP (blue) were subjected to indirect immunofluorescence microscopy using antibody against annexin A1 (green). Inserts shows LBP marked with arrow at 3x magnification. Bars = 5μm.

4.2.3. Annexin A1 knockdown macrophages show reduced Fc-beads phagocytosis but does not affect man-beads phagocytosis

To confirm the role of annexin A1 in FcγR mediated phagocytosis and annexin independent phagocytosis in mannose receptor mediated phagocytosis, annexin A1 expression was knockdown using lentivirus carrying shRNA against annexin A1. Lentivirus transfection resulted in stably transfected RAW 264.7 cell line which showed more than 90% reduction in annexin A1 expression (Figure 18). Annexin A1 shRNA expression was also stable for at least 2 freeze and throw cycles. Stably transfected macrophages showed more than 40% reduction in their phagocytic activity while no effect had been observed on man-beads phagocytosis. Obtained data confirmed previous observation that annexin A1 is important for Fc-beads phagocytosis but not in man-beads phagocytosis.

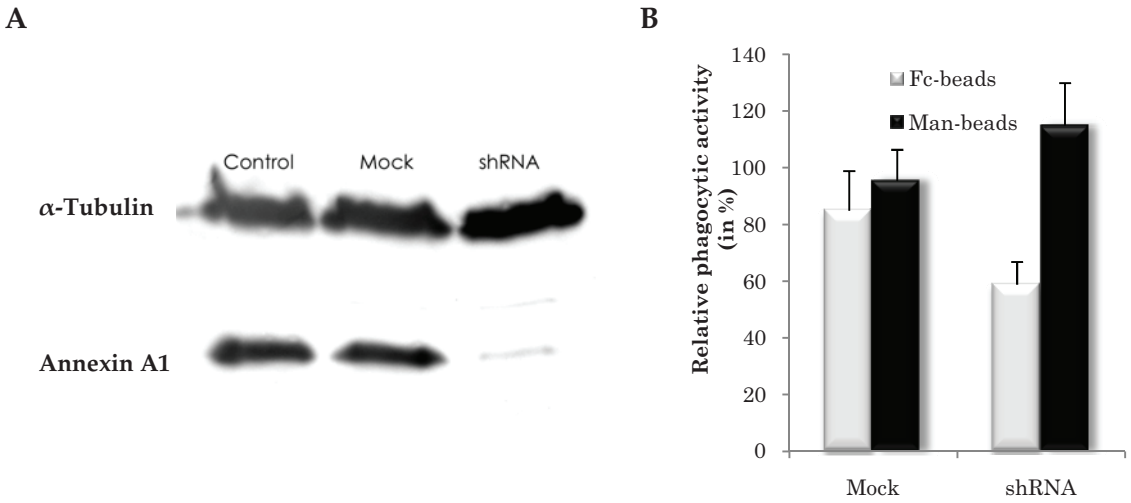

Figure 18: Relative phagocytic activity for Fc or Man-beads in transfected RAW 264.7 macrophages. (A) Annexin A1 expression in non-transfected cells (Control), control shRNA (Mock) and annexin A1 shRNA (shRNA) transfected cells. (B) Reduction in annexin A1 expression resulted in reduced phagocytic activity for the Fc-beads, where no effect was observed in man-beads phagocytosis.

4.2.4. Annexin A1 does not co-localise with F-actin on naive man-LBP but strongly co-localise on Fc-LBP.

To analyse a potential co-localisation of annexin A1 and F-actin on Fc and Mannose LBP, 3 μm latex Fc or man-beads were incubated with RAW 264.7 macrophages for 10 minutes followed by fixation and staining as mentioned in materials and methods. Careful evaluation of naive actin positive LBP revelled that annexin A1 co-localised with F-actin on Fc-LBP (Figure 19A) but not on man-LBP (Figure 15B). Obtained data collaborate previous that annexin A1 is not involved in mannose receptor mediated phagocytosis but an important component of Fc receptor mediated phagocytosis. RAW 264.7

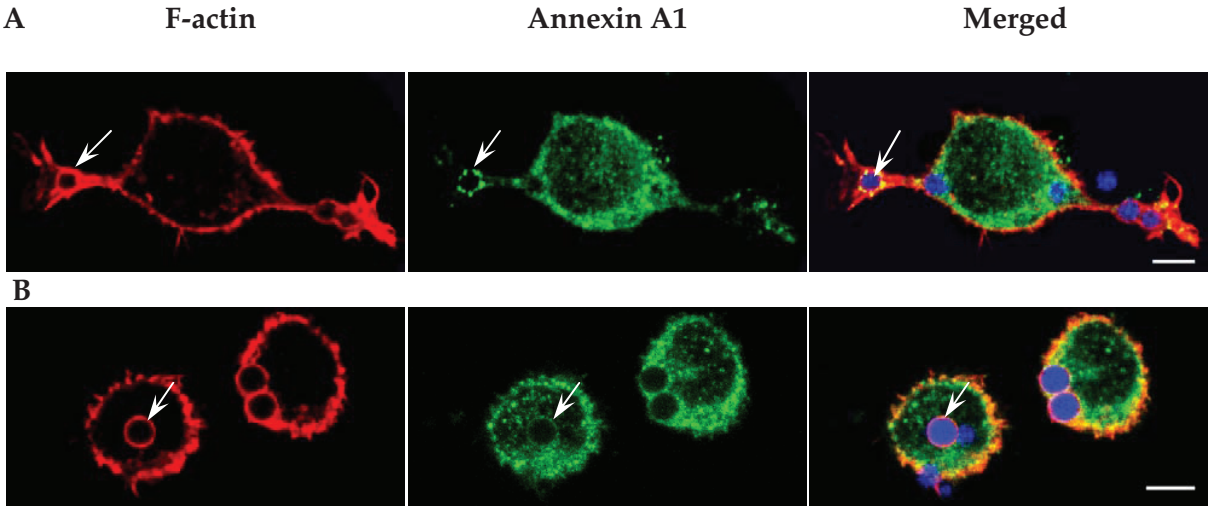

Figure 19: Annexin A1 co-localise with F-actin on Fc-LBP but not on man-LBP. Fc-beads (A) and man-beads (B) were incubated with RAW 264.7 macrophages for 10 minutes followed by the immunofluorescence staining for annexin A1 and rhodamine-phalloidin staining for F-actin.

Taken together, my observations suggest that annexin A1 recruitment on LBP is receptor specific. Annexin A1 found to be important in nonspecific and FcγR mediated phagocytosis where it provide structural support during different stages of phagocytosis. It will be interesting to investigate that in absence of annexin A1 which protein provide structural support during man-beads internalisation

4.3. Exogenous annexin A1 alter macrophage phagocytic activity.

ANXA1 is released from pituitary cells in response to a glucocorticoid challenge (Chapman et al., 2003), so first I decided to check the secretion of annexin A1 during the different receptor mediated phagocytosis but I did not succeed to get enough amount of annexin A1 which could be detected by western blotting. Annexin A1 was reported in anti-inflammatory cytokine expression (Yang et al., 2006; Yang et al., 2009) which believed to be regulated by the annexin A1 binding to its extracellular receptor FPRL2 (Formyl Peptide Like Receptor 2).

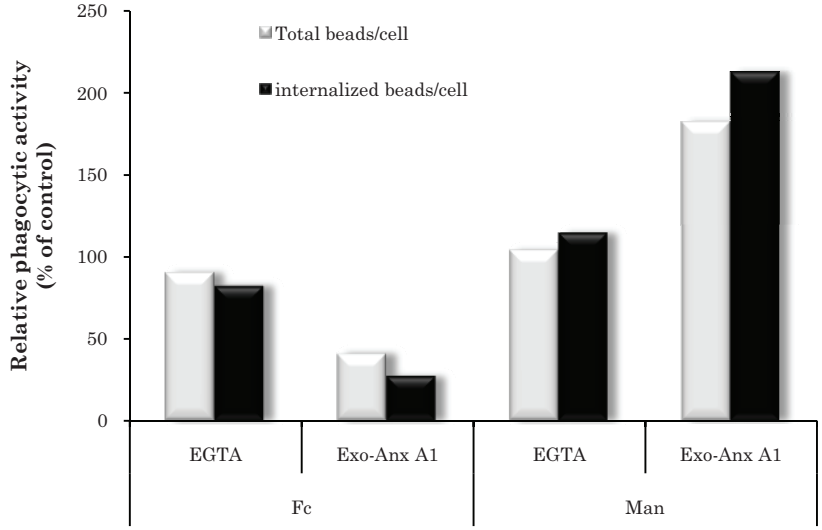

Figure 20: Exogenous annexin A1 altered macrophage phagocytosis. J774.A1 macrophages were incubated with extracellular annexin A1 for 30 minutes before adding Fc or man-coated latex beads. Extracellular annexin A1 strongly stimulated man-beads phagocytosis but reduced Fc-beads phagocytosis.

To study the possible role of annexin A1 in regulation of RAW 264.7 macrophage phagocytosis, I incubated bacterial expressed recombinant annexin A1 for 30 before adding Fc or man-beads. Cells were also incubated with 2mM EGTA to study the extracellular membrane bound annexin A1. The removal of extracellular membrane bound annexin A1 did not affect the macrophage phagocytosis and was similar to the control Figure 20. Extracellular annexin A1 strongly reduced the Fc-beads phagocytosis while extracellular

annexin A1 strongly stimulate the annexin A1 phagocytosis (Figure 16). The extracellular annexin A1 not only affect latex bead binding to macrophages but also decrease and increase Fc and Man-beads internalisation, respectively (Figure 20).

Obtained data seek further investigation evaluation. Further investigation did not pursue in current study but data provide further insight into the different role of annexin A1 in different receptor mediated phagocytosis.

4.4. Stimulus dependent involvement of annexin A2 as a functional linker between F-actin and LBP

Since different receptor mediated phagocytosis had different protein composition. Since the annexin A1 had different effect on different receptor mediated phagocytosis, we checked that what effect of annexin A2 had on different LBP F-actin-LBP binding activity.

4.4.1. Annexin A2 can stimulate Fc-LBP and man-LBP binding to F-actin but failed to stimulate gelatin-LBP

To analyse the possible role of annexin A2 in F-actin-LBP binding activity, different salt-stripped LBP were incubated with bacterial purified recombinant annexin A2 in presence or absence of Ca^{2+}. As mentioned before annexin A2 failed to stimulate gelatin-LBP binding to F-actin but it strongly stimulate Fc-LBP and man-LBP. Moreover, stimulation in man-LBP was nearly 2 times higher than Fc-LBP. Obtained data suggest not only annexin A1 but annexin A2 also have different effect on different LBP.

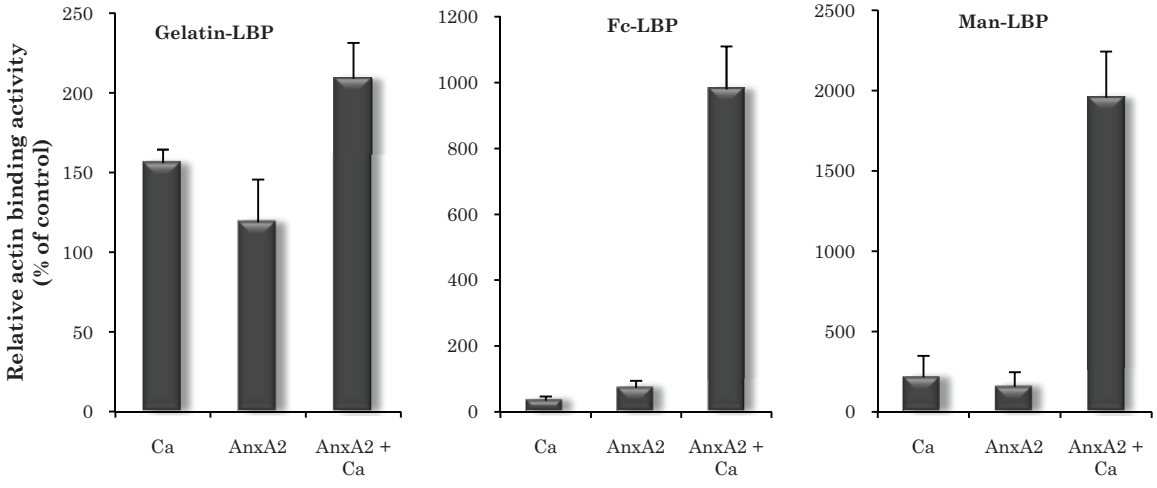

Figure 21: Effect of annexin A2 on different salt-stripped LBP. Different salt-stripped LBP were incubated with Ca^{2+} alone (Ca), bacterial expressed recombinant annexin A2 in absence (AnxA2) or in presence of Ca^{2+} (AnxA2 + Ca).

4.4.2. Annexin A1 and annexin A2 competes for the same binding site on different LBP.

Since lipid properties are very common for annexin A1 and annexin A2, I asked whether annexin A1 and annexin A2 compete for the same binding site or they have co-operative effect on F-actin-LBP binding. To study the effect, LBP were incubated with equal amount of annexin A1 and annexin A2 in presence of Ca^{2+}. Co-incubation did not further increase LBP binding to F-actin, which suggested that in the case of Fc and Man-LBP, annexin A1 and annexin A2 compete to bind, probably for the same binding site, on LBP surface. Surprisingly, co-incubation of annexin A1 and annexin A2 reduce the gelatin-LBP binding to F-actin.

4.4.3.

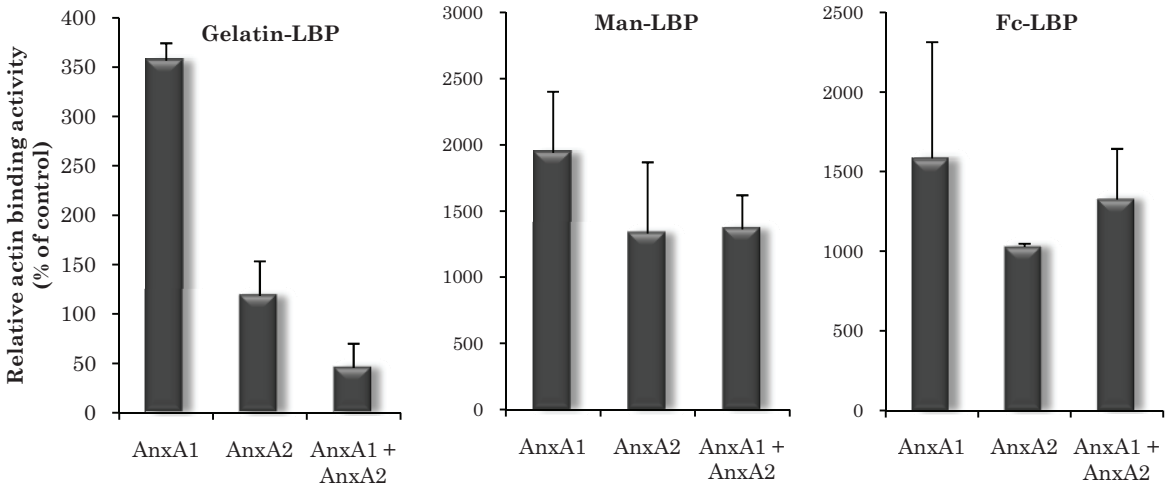

Figure 22: Annexin A1 and annexin A2 compete for the same binding site on LBP. Annexin A1 and annexin A2 were co-incubated individually or together with different LBP in presence of Ca^{2+} before applying to F-actin network.

Taken together, my results also suggest that annexin A2 recruitment on LBP surface is driven by the receptor signalling. Although obtained data need to be confirmed by *in vivo* studies.

5. Discussion

5.1. Annexin A1 stimulates F-actin and gelatin-LBP interaction, *in vitro*.

Once recognised by the cell surface receptors, internalisation and subsequent intracellular transport of phagocytic particles require a highly regulated and dynamic interaction of the phagosome membrane with cytoskeletal elements. Particle engulfment requires extensive remodelling of membrane and actin cytoskeleton (May and Machesky, 2001). The newly formed phagosome possesses a dense coat of actin and ABPs that subsequently decrease with time and are eventually lost (Castellano et al., 2001; Greenberg et al., 1990; May and Machesky, 2001). Although signalling pathways for F-actin polymerisation during phagocytosis have been extensively studied (Allen and Aderem, 1996; Castellano et al., 2001; Diakonova et al., 2002), the mechanics of actin dynamics during phagosome formation and particularly the role of ABPs remain poorly understood. Since several years our group focuses on the identification of the ABPs involved in phagosome-F-actin interaction. In a previous study, I had shown that the unconventional myosin Va is important for proper phagosome inward transport at post internalisation stages of phagocytosis (Al Haddad et al., 2001). In the current study I identified annexin A1 as a new ABP responsible for mediating phagosome interactions with the actin cytoskeleton.

To search for new players in phagosome biogenesis I used the latex beads system and developed an *in vitro* light microscopy assay to study phagosome-F-actin interactions (Al Haddad et al., 2001). LBP loaded with non-degradable fluorescence latex beads provide several unique advantages to study molecular interactions between a defined membranous organelle and the cytoskeleton (Al Haddad et al., 2001; Desjardins and Griffiths, 2003). Latex bead system allowed to isolated organelle which is functionally active for a wide spectrum of functions (Desjardins and Griffiths, 2003). Moreover the possibility to couple latex beads to single ligands and study their selective receptor-mediated uptake allows us to follow maturation processes in more detail. In addition, one of the most important advantage is that LBP can be isolated (>95% of purity) in single step procedure by flotation using a discontinuous sucrose gradient (Desjardins et al., 1994b; Desjardins et al., 1994a; Desjardins and Griffiths, 2003; Stuart et al., 2007). Our F-actin-LBP binding assay has also several important advantages. It is simple, easy to manipulate, robust and requires minimum actin, LBP and tested probes (Al Haddad et al., 2001).

In this assay, the macrophage cytosol stimulated the F-actin-LBP interaction *in vitro* at low protein concentrations (~0.5 mg/ml). However, an isolation of biochemically pure

individual factors was not possible due to limitation of macrophages cytosol as a starting material. Therefore, as a first step I decided to fractionate macrophage cytosol and isolate a fraction enriched in F-actin-LBP binding activity and then identified potential candidates by LC-MS/MS. After cytosol fractionation with gel-filtration and subsequent phospho-cellulose chromatography, I obtained a fraction that had about 8 times higher F-actin-LBP binding activity than the starting cytosol (Table 4). Proteomic analysis of this active fraction and systematic filtration of obtained data resulted in 12 ABPs; among these annexin A1 was found as the most promising protein, which can be involved in F-actin-LBP interaction.

Several previous studies already reported the presence of annexins on phagosome membrane (Desjardins et al., 1994a; Diakonova et al., 1997). The annexin super family consists of 13 calcium binding proteins with a significant degree of biological and structural homology. Annexin A1 is one of the first characterised members of this family, which bind to phospholipids and actin in presence of calcium (Glenney, Jr. et al., 1987). Furthermore, Diakonova et al.1997 found the presence of five different annexins (1 to 5) on LBP. I confirmed the presence of annexin A1 on gelatin-LBP by immunofluorescence microscopy (Figure 8) and showed that annexin A1 can produce the interaction between F-actin and gelatin-LBP *in vitro* (Figure 7).

Annexin 1 binds and bundles F-actin in a Ca^{2+}-dependent manner, although high Ca^{2+} concentrations are essential to establish this interaction *in vitro* (Glenney, Jr. et al., 1987; Schlaepfer and Haigler, 1987). Bacterially expressed recombinant annexin A1 requires 1mM Ca^{2+} for actin binding in an *in vitro* assay (Figure 7), which is consistent with previous finding (Glenney, Jr. et al., 1987). However, the regulatory role of Ca^{2+} in mediating an annexin A1 and F-actin interaction inside the cell is not clear. Since it was already reported that presence of phospholipids or accessory molecules strikingly reduced the affinity of annexins towards Ca^{2+} (Powell and Glenney, 1987; Schlaepfer and Haigler, 1987), I suggest the presence of different mechanisms for F-actin and annexin A1 interaction *in vivo*. A stimulation of F-actin-LBP interaction in absence of Ca^{2+} by gel-filtration fractions and phospho-cellulose eluted proteins supports my hypothesis (Figure 6). However, an addition of Ca^{2+} to these fractions further increased their F-actin-LBP binding activity. Therefore, the role of Ca^{2+} in regulating the interaction between F-actin, annexin A1 and LBP during phagocytosis requires further investigations.

Interestingly, my fractionation studies revealed that the cytosol contains most probably not only factors stimulating F-actin-LBP linkage like annexin A1 and myosin Va (Al-Haddad et al., 2001), but also unknown inhibitory factor(s). Due to the presence of these inhibitory factors, annexin A1 present in the phospho-cellulose unbound protein fraction (Figure 6C) could not stimulate F-actin-LBP binding (Figure 6B). The presence of these inhibitory factor(s) was confirmed by F-actin-LBP binding experiments, carried out with recombinant annexin A1 in the absence or presence of aliquots of the phospho-cellulose unbound protein fraction. These revealed a nearly 2.5 times decrease in the annexin A1 stimulatory activity in the presence of the unbound protein fraction (Figure 7). The identification of this inhibitory factor(s), which could play an important role in the regulation of the annexin A1-LBP-F-actin interaction, will be a specific aim of future studies.

5.2. Annexin A1 acts as a functional linker between F-actin and gelatin-LBP, *in vivo*.

Most annexins are abundant intracellular proteins (Raynal and Pollard, 1994) and in polymorphonuclear leukocytes (PMN) annexin A1 comprises nearly 2% of total cellular protein which is almost half of the amount of actin (Lim and Pervaiz, 2007; Perretti and Flower, 1996; Raynal and Pollard, 1994). In PMNs and monocytes approximately 17% and 33%, respectively, of total annexin A1 is associated with the plasma membrane (Perretti and Flower, 1996). In my immunofluorescence analysis I could also clearly see the high amount of annexin A1 both in the cytoplasm and in ruffles of the plasma membrane (Figure 12 and 13). The fact that annexin A1 co-localised with F-actin at plasma membrane filopodia and ruffles indicated that annexin A1 could play a role during phagocytic cup formation and particle uptake.

My siRNA data and previous knockout studies also demonstrated the importance of annexin A1 for phagocytic activity (Hannon et al., 2003). siRNA transfected RAW 264.7 macrophages showed at least 50% reduction in annexin A1 expression and similar reduction in the phagocytic activity (Figure 11). Also peritoneal macrophages from annexin A1 knockout mice showed impaired phagocytosis (Yona et al., 2004; Yona et al., 2006) and lower zymosan internalisation correlating with a higher number of zymosan particles that remained bound to the cells surface (Yona et al., 2004). Interestingly, neither knockout nor

knockdown of annexin A1 completely abolish the phagocytic activity of macrophages indicating the existence of alternative but less effective mechanism for phagocytosis.

The molecular mechanism by which membrane bound annexin A1 modulates actin cytoskeleton reorganisation is yet to be discovered. However some reports already established an association of annexin A1 with F-actin (Diakonova et al., 1997; Glenney, Jr. et al., 1987; Kusumawati et al., 2001; Schlaepfer and Haigler, 1987). Based on these and my findings, I propose a mechanism, in which phospholipids play a key role in spatial-temporal recruitment of annexin A1 to cell membranes from cytoplasm. Phosphatidylinositol 4, 5-bisphosphate (PIP2) is well known for its role in actin remodelling and as an annexin A1 binding partner (Blackwood and Ernst, 1990). PIP2 influences F-actin formation and extension by binding to a variety of actin capping and monomer binding proteins (Mao and Yin, 2007; Takenawa and Itoh, 2001; Yeung and Grinstein, 2007). In addition during phagocytosis a transient accumulation of PIP2 at phagocytic site was observed due to phosphatidylinositol-4-phosphate-5-kinase (PI4P5K) activity (Coppolino et al., 2002; Scott et al., 2005). Therefore, local PIP2 production at the phagocytic site can provide additional binding sites for cytosolic annexin A1. I suggest that this increase in local PIP2 concentration leads to annexin A1 recruitment and accumulation at phagocytic sites (Figure 12B). Membrane-bound annexin A1 then links the growing F-actin to the plasma membrane in order to keep them near the membrane in proper directionality and finally generate enough support and strength for membrane protrusions and phagocytic cup formation.

Following particle internalisation cell signalling events lead to actin de-polymerisation which is believed to be an important process for phagosome maturation (Liebl and Griffiths, 2009; May and Machesky, 2001). Hydrolysis of PIP2 from phagocytic sites was observed shortly after the initial phase of accumulation and elimination of PIP2 at the time of sealing appears to be required for successful completion of phagocytosis (Scott et al., 2005; Yeung and Grinstein, 2007). Before the cup closes the PIP2 is degraded by the phospholipase Cγ (PLCγ) but this is the time where phosphatidic acid (PA) is produced by phospholipase D from phosphatidylcholine (Yeung and Grinstein, 2007). Annexin A1 has higher affinity towards PA compared to other phospholipids (Blackwood and Ernst, 1990). Availability of other binding sites, possibly those rich in PA, helps retention of annexin A1 at this point. Soon after the cup closes, the PA concentration also decreases on the phagosome membrane (Yeung and Grinstein, 2007), which might lead to loss of annexin A1 from the phagosome

surface (Figure 12B). Here I suggest that decreasing annexin A1 concentrations result in a reduction of F-actin on the phagosome due to absence of a membrane linker protein. Taking together I suggest that annexin A1 is not directly involved in the actin dynamics but provides structural support for a membrane-F-actin connection during the particle internalisation.

Even at late stages of phagocytosis annexin A1 found to be associated with gelatin-LBP *in vitro* (Figure 8A), which is consistent with previous findings (Diakonova et al., 1997). I observed that annexin A1 was not evenly distributed on gelatin-LBP surface rather it found as patches on isolated gelatin-LBP (Figure 8A). This kind of annexin A1 patch distribution can be explain by its different affinity towards phospholipids (Blackwood and Ernst, 1990). Moreover, Annexin A1 does not bind to the phosphatidylcholine and phosphatidylethanolamine (Blackwood and Ernst, 1990) which covers nearly 43% and 15% of total phospholipids present in 60 minutes pulse and 60 minutes chase LBP, respectively (Desjardins et al., 1994a). Since nearly 60% of total surface of LBP is not available for annexin A1 binding, it is not surprising that the annexin A1 present as isolated patches on LBP membrane.

Recently a transient actin flashing on phagosomes, which took place at late phagocytosis, was reported (Liebl and Griffiths, 2009). I found that annexin A1 was also present on the actin flashing LBP (Figure 13B). An accumulation of annexin A1 on flashing LBP strongly correlated with that of F-actin, and a functional involvement of annexin A1 in actin flashing was confirmed by annexin A1 knockdown, which dramatically reduced actin flashing on LBP. Reduction in actin flashing was proportional to reduction in annexin A1 expression with 50% reduction of annexin A1 resulting in nearly 40% reduction in actin flashing events (Figure 11D). The data once again indicate that annexin A1 is a functional linker between LBP and F-actin during the both early and late stages of phagocytosis.

5.3. N-terminal domain might not be important for F-actin and LBP binding activity.

Annexins differ in their N-terminal domains, which believed to define their function and binding to specific protein ligands (Moss, 1992; Raynal and Pollard, 1994)Annexins A1 harbour phosphorylation sites for EGF receptor kinase at Tyr-20 and Protein Kinase C at Ser-27. However, the functional importance of the annexin A1 phosphorylation is not very clear.

Annexin A1 tyrosine phosphorylation at Tyr-20 residue promote its proteolytic degradation (Chuah and Pallen, 1989) and N-terminal-truncated protein requiring less Ca^{2+} for phospholipid binding (Ando et al., 1989). Interaction of annexin A1 with membrane (Wang and Creutz, 1994) and liposome (Porte et al., 1996) has been found to be regulated by phosphorylation of N-terminal domain. However, binding to liposomes and the liposome-aggregating ability of annexin A1 are differently regulated. Annexin A1 S27E mutation, which mimicked phosphorylated state of N-terminal domain does not modify binding to liposomes while the ability of annexin A1 to aggregate liposomes is abolished (Porte et al., 1996). I observed that the presence of serine/threonin and tyrosine kinases inhibitors in macrophage cytosol do not alter its stimulatory effect in F-actin-LBP interaction. Moreover the core domain which contain actin binding site of different annexins shares high homology and the removal of N terminal domain does not alter annexin A1 association with phagosomes in J774A.1 cell line (Kusumawati et al., 2001), it is tempting to speculate that one of the annexin protein family members, probably annexin A2, takes over its role in phagocytosis. Although the data suggest that annexin A1 phosphorylation might not be important for its interaction with F-actin, further *in vivo* investigation has to be carried out.

5.4. Ligand-receptor interaction regulates the involvement of annexin A1 in phagocytosis

It is well accepted that different receptor mediated phagocytosis takes different maturation pathways and also harbour different protein and lipid composition. A significant number of the proteins that are synthesised in response to a phagocytic signal can be expected to play a general role in phagosome maturation and functions. The most obvious class of proteins that can influence these processes are those that are inserted into the membrane or delivered within the lumen of the phagosome. Given that each receptor induced a significant fraction of its own specific set of genes (Hoffmann et al., 2010) and so the protein composition, it was interesting to compare the actin binding properties of the different LBP. As expected different receptor mediated phagosome had different F-actin binding properties (Figure 16). Though man-beads internalised and mature much faster than the Fc-beads, after 60 minutes pulse time both have equal percentage of LAMP-2 positive phagosomes (Hoffmann et al., 2010). Considering this fact I suggest that obtained differences in F-actin binding of different not-stripped is not due the different stage of phagosome

maturation rather due to the different protein composition of LBP. Study by (Hoffmann et al., 2010) proved that annexin A1 is present on Fc-LBP but not on man-LBP. In agreement with his study we found that annexin A1 was not present on the man-LBP (Figure 16B). Here, I hypothesis that reduced Fc-LBP binding was due the presence of unidentified inhibitory factor which block the annexin A1 F-actin binding activity. In absence of annexin A1, man-LBP F-actin binding activity might be supported by other F-actin-LBP linker protein like myosin Va. Annexin A1 independent F-actin binding of man-LBP was further supported by the fact that presence of Ca^{2+} increased the other (Fc and Gelatin-LBP) F-actin-LBP binding activity but failed to stimulate man-LBP F-actin binding activity (Table 4). In *in vitro* condition purified annexin A1 was able to stimulate all studied non-stripped LBP indicates that under *in vivo* conditions proteins competes for the same binding sites on LBP membrane. Similar to the gelatin-LBP, salt-stripping greatly reduce the F-actin binding activity of different LBP. After the salt-stripping, annexin A1 showed similar stimulatory effect on Fc and man-LBP (Figure 17). This observation further supports my theory of competitive binding of different proteins on LBP surface under *in vivo* condition. *In vitro* data was further corroborated by the *in vivo* study where I showed co-localisation of annexin A1 with F-actin only on early Fc-LBP (Figure 19).

It is tempting to speculate that the association of annexin A1 with phagosomes is simply mediated through their ability to bind to membranes in a Ca^{2+} dependent fashion, but that this is not so straight forward. Some intracellular pathogens have evolved structures and mechanisms, which allow them to leave the usual pathway, thus avoiding an encounter with much or all of the macrophage killing and degradation machinery, including the exposition to reactive oxygen metabolites. Usage of hospitable receptor, recruitment friendly protein or prevention of hostile protein recruitment is some of the many survival strategies employed by intracellular microorganism to evade host immune system (Haas, 2007). Cargo specific recruitment of Annexin A1 was first reported by (Harricane et al., 1996). In their study they first time reported that annexin A1 is recruited only on non-pathogenic *E. coli* or dead *Brucella suis* phagosome where live pathogenic *B. suis* prevent the recruitment of annexin A1 periphagosomal region. Intracellular stimuli dependent annexin A1 recruitment on phagosome membrane subserve a more subtle role, perhaps as regulators of the initial signalling process that follows the interaction of the organism with the phagocytic cell itself.

The study by (Yona et al., 2004) proposed the stimulus specific defect in the phagocytic activity of peritoneal macrophages obtained from annexin A1 knockout mouse (Yona et al., 2004). With help of flow-cytometry analysis they suggested that peritoneal macrophages showed impaired phagocytosis of non-opsonised zymosan particles where no defect was observed when opsonised zymosan where used. Moreover they showed that annexin A1 knockout resulted in altered expression of several cell membrane receptors and altered macrophage activation. In contradictory to their finding, I observed that reduced annexin A1 in RAW 264.7 macrophages resulted in impaired phagocytosis of Fc-beads but no effect was seen on man-beads phagocytosis (Figure 18). Obtained data need careful interpretation since cell line specific difference in the protein activity is frequently observed. Moreover cells from knockout animals known to behave differently compared to transient protein knockdown.

5.5. Extracellular annexin A1 modulates macrophage phagocytic activity.

Researchers interested in the mechanisms and control of phagocytosis has frequently speculated on the possible role of the annexin family. In these processes some groups focussing upon an external and others on an internal role for the protein. My previous studies provide insight in to the intracellular role of the annexin A1 in phagosome biogenesis. Next, I decide to evaluate role extracellular annexin A1 in phagocytosis. (Becker and Grasso, 1988) first time reported that dexamethasone induced the release of a protein suppressed phagocytosis of yeast particles from elicited murine macrophages. Later this protein is identified as annexin A1. Later studies by (McKanna, 1995) proposed that that annexin A1 had multiple roles in regulating the apoptotic event and the ensuing removal of cells by macrophages and suggested that the presence of this protein might be responsible for the lack of inflammatory changes characteristically observed during this response.

Extracellular annexin A1 signals through a seven-membrane-spanning G-protein-coupled receptor (GPCR) known as formyl peptide receptor 2 (FPR2; also known as ALXR in humans), which is also the receptor for the anti-inflammatory molecule lipoxin A4 (Perretti, 2003). Human ALXR belongs to a small family of receptors consisting of three members (FPR1, ALXR and FPR3) that are coupled to G-proteins and are expressed by several cell types, including human neutrophils, monocytes, macrophages, endothelial cells and epithelial cells (Perretti and D'Acquisto, 2009). Annexin A1 and peptides derived from its N-terminal region compete with lipoxin A4 and also with another ALXR ligand, serum

amyloid protein A, for binding to ALXR (Perretti, 2003; Perretti and D'Acquisto, 2009). Intriguingly, peptides derived from the annexin A1 N-terminal region have been shown to activate all three receptors of the FPR family *in vitro* (Dahlgren et al., 2000).

In agreement with previous studies I suggest that the observed reduced Fc-beads internalisation was due to the anti-inflammatory action of annexin A1 (Figure 20). FcγR receptor mediated phagocytosis usually accompanied by the macrophage activation and inflammatory response (Garcia-Garcia and Rosales, 2002). Extracellular annexin A1 generate the anti-inflammatory signalling and reduced the activation of macrophage which might result in reduced Fc-beads internalisation. Surprisingly, extracellular annexin A1 stimulated mannose receptor mediated man-beads internalisation (Figure 20) which also believed to generate also pro-inflammatory signals (East and Isacke, 2002; Stahl and Ezekowitz, 1998). Stimulation in apoptotic neutrophils internalisation by annexin A1 and N-terminal peptide have been reported previously (Scannell et al., 2007) but molecular mechanism behind this effect is yet to be discovered.

Downstream signalling following annexin A1-induced ALXR activation involves transient phosphorylation of extracellular-regulated kinase 1 and 2 (Chatterjee et al., 2005; Hayhoe et al., 2006). Blocking of ALXR with a monoclonal antibody prevented annexin A1-induced inhibition of human neutrophils transmigration and adhesion to endothelial-cell monolayer under flow (Perretti and D'Acquisto, 2009).Interestingly, when these cells are activated, cytokine release is exacerbated by the absence of this protein. The exact mechanism by which the lack of annexin A1 results in this enhanced cytokine production is not completely understood but a likely explanation emerging from recent studies is the absence of an important negative feedback loop, autocrine stimulation by annexin A1 of the FPR receptor family in these cells. Although the intracellular signalling pathways have yet to be completely elucidated, recent experimental evidence now supports the involvement of this receptor family in the transduction of signals from extracellular annexin A1 (Ernst et al., 2004; Gavins et al., 2003; Hayhoe et al., 2006; Perretti et al., 2001). Although substantial progress has been made in understanding of signalling transduction by extracellular annexin A1, it still far from understood. My primary results with extracellular annexin A1 provided promising direction but considerable amount of work need to be done before, I make any conclusion. Time and situation permits, I would like to pursue this study to provide more insight in to role of extracellular annexin A1 in phagosome biogenesis.

6. References

Aderem, A. and Underhill, D. M. (1999). Mechanisms of phagocytosis in macrophages. *Annu. Rev. Immunol.* 17, 593-623.

Ahmad, S. F., Chtcheglova, L. A., Mayer, B., Kuznetsov, S. A. and Hinterdorfer, P. (2010). Nanosensing of Fcgamma receptors on macrophages. *Anal. Bioanal. Chem.*

Al Haddad, A., Shonn, M. A., Redlich, B., Blocker, A., Burkhardt, J. K., Yu, H., Hammer, J. A., III, Weiss, D. G., Steffen, W., Griffiths, G. et al. (2001). Myosin Va bound to phagosomes binds to F-actin and delays microtubule-dependent motility. *Mol. Biol. Cell* 12, 2742-2755.

Allen, L. A. and Aderem, A. (1996). Molecular definition of distinct cytoskeletal structures involved in complement- and Fc receptor-mediated phagocytosis in macrophages. *J. Exp. Med.* 184, 627-637.

Alvarez-Martinez, M. T., Mani, J. C., Porte, F., Faivre-Sarrailh, C., Liautard, J. P. and Sri, W. J. (1996). Characterization of the interaction between annexin I and profilin. *Eur. J. Biochem.* 238, 777-784.

Alvarez-Martinez, M. T., Porte, F., Liautard, J. P. and Sri, W. J. (1997). Effects of profilin-annexin I association on some properties of both profilin and annexin I: modification of the inhibitory activity of profilin on actin polymerization and inhibition of the self-association of annexin I and its interactions with liposomes. *Biochim. Biophys. Acta* 1339, 331-340.

Ando, Y., Imamura, S., Hong, Y. M., Owada, M. K., Kakunaga, T. and Kannagi, R. (1989). Enhancement of calcium sensitivity of lipocortin I in phospholipid binding induced by limited proteolysis and phosphorylation at the amino terminus as analyzed by phospholipid affinity column chromatography. *J. Biol. Chem.* 264, 6948-6955.

Araki, N. (2006). Role of microtubules and myosins in Fc gamma receptor-mediated phagocytosis. *Front Biosci.* 11, 1479-1490.

Arnold, H., Henning, R. and Pette, D. (1971). Quantitative comparison of the binding of various glycolytic enzymes to F-actin and the interaction of aldolase with G-actin. *Eur. J. Biochem.* 22, 121-126.

Baum, B. and Kunda, P. (2005). Actin nucleation: spire - actin nucleator in a class of its own. *Curr. Biol.* 15, R305-R308.

Becker, J. and Grasso, R. J. (1988). Suppression of yeast ingestion by dexamethasone in macrophage cultures: evidence for a steroid-induced phagocytosis inhibitory protein. *Int. J. Immunopharmacol.* 10, 325-338.

Bektas, M., Nurten, R., Gurel, Z., Sayers, Z. and Bermek, E. (1994). Interactions of eukaryotic elongation factor 2 with actin: a possible link between protein synthetic machinery and cytoskeleton. *FEBS Lett.* 356, 89-93.

Benaud, C., Gentil, B. J., Assard, N., Court, M., Garin, J., Delphin, C. and Baudier, J. (2004). AHNAK interaction with the annexin 2/S100A10 complex regulates cell membrane cytoarchitecture. *J. Cell Biol.* 164, 133-144.

Blackwood, R. A. and Ernst, J. D. (1990). Characterization of Ca2(+)-dependent phospholipid binding, vesicle aggregation and membrane fusion by annexins. *Biochem. J.* 266, 195-200.

Blocker, A., Severin, F. F., Habermann, A., Hyman, A. A., Griffiths, G. and Burkhardt, J. K. (1996). Microtubule-associated protein-dependent binding of phagosomes to microtubules. *J. Biol. Chem.* 271, 3803-3811.

Bradford, M. M. (1976). A rapid and sensitive method for the quantitation of microgram quantities of protein utilizing the principle of protein-dye binding. *Anal. Biochem.* 72, 248-254.

Bretscher, A., Chambers, D., Nguyen, R. and Reczek, D. (2000). ERM-Merlin and EBP50 protein families in plasma membrane organization and function. *Annu. Rev. Cell Dev. Biol.* 16, 113-143.

Cao, Y., Li, Y., Edelweiss, M., Arun, B., Rosen, D., Resetkova, E., Wu, Y., Liu, J., Sahin, A. and Albarracin, C. T. (2008). Loss of Annexin A1 Expression in Breast Cancer Progression. *Appl. Immunohistochem. Mol. Morphol.*

Caron, E. and Hall, A. (1998). Identification of two distinct mechanisms of phagocytosis controlled by different Rho GTPases. *Science* 282, 1717-1721.

Castellano, F., Chavrier, P. and Caron, E. (2001). Actin dynamics during phagocytosis. *Semin. Immunol.* 13, 347-355.

Chapman, L. P., Epton, M. J., Buckingham, J. C., Morris, J. F. and Christian, H. C. (2003). Evidence for a role of the adenosine 5'-triphosphate-binding cassette transporter A1 in the externalization of annexin I from pituitary folliculo-stellate cells. *Endocrinology* 144, 1062-1073.

Chatterjee, B. E., Yona, S., Rosignoli, G., Young, R. E., Nourshargh, S., Flower, R. J. and Perretti, M. (2005). Annexin 1-deficient neutrophils exhibit enhanced transmigration in vivo and increased responsiveness in vitro. *J. Leukoc. Biol.* 78, 639-646.

Chesarone, M. A. and Goode, B. L. (2009). Actin nucleation and elongation factors: mechanisms and interplay. *Curr. Opin. Cell Biol.* 21, 28-37.

Chimini, G. and Chavrier, P. (2000). Function of Rho family proteins in actin dynamics during phagocytosis and engulfment. *Nat. Cell Biol.* 2, E191-E196.

Chuah, S. Y. and Pallen, C. J. (1989). Calcium-dependent and phosphorylation-stimulated proteolysis of lipocortin I by an endogenous A431 cell membrane protease. *J. Biol. Chem.* 264, 21160-21166.

Coppolino, M. G., Dierckman, R., Loijens, J., Collins, R. F., Pouladi, M., Jongstra-Bilen, J., Schreiber, A. D., Trimble, W. S., Anderson, R. and Grinstein, S. (2002). Inhibition of phosphatidylinositol-4-phosphate 5-kinase Ialpha impairs localized actin remodeling and suppresses phagocytosis. *J. Biol. Chem.* 277, 43849-43857.

Creutz, C. E., Pazoles, C. J. and Pollard, H. B. (1978). Identification and purification of an adrenal medullary protein (synexin) that causes calcium-dependent aggregation of isolated chromaffin granules. *J. Biol. Chem.* 253, 2858-2866.

Crumpton, M. J. and Dedman, J. R. (1990). Protein terminology tangle. *Nature* 345, 212.

D'Acquisto, F., Perretti, M. and Flower, R. J. (2008). Annexin-A1: a pivotal regulator of the innate and adaptive immune systems. *Br. J. Pharmacol.* 155, 152-169.

Dahlgren, C., Christophe, T., Boulay, F., Madianos, P. N., Rabiet, M. J. and Karlsson, A. (2000). The synthetic chemoattractant Trp-Lys-Tyr-Met-Val-DMet activates neutrophils preferentially through the lipoxin A(4) receptor. *Blood* 95, 1810-1818.

Defacque, H., Egeberg, M., Habermann, A., Diakonova, M., Roy, C., Mangeat, P., Voelter, W., Marriott, G., Pfannstiel, J., Faulstich, H. et al. (2000). Involvement of ezrin/moesin in de novo actin assembly on phagosomal membranes. *EMBO J.* 19, 199-212.

Desjardins, M., Celis, J. E., van Meer, G., Dieplinger, H., Jahraus, A., Griffiths, G. and Huber, L. A. (1994a). Molecular characterization of phagosomes. *J. Biol. Chem.* 269, 32194-32200.

Desjardins, M. and Griffiths, G. (2003). Phagocytosis: latex leads the way. *Curr. Opin. Cell Biol.* 15, 498-503.

Desjardins, M., Huber, L. A., Parton, R. G. and Griffiths, G. (1994b). Biogenesis of phagolysosomes proceeds through a sequential series of interactions with the endocytic apparatus. *J. Cell Biol.* 124, 677-688.

Diakonova, M., Bokoch, G. and Swanson, J. A. (2002). Dynamics of cytoskeletal proteins during Fcgamma receptor-mediated phagocytosis in macrophages. *Mol. Biol. Cell* 13, 402-411.

Diakonova, M., Gerke, V., Ernst, J., Liautard, J. P., van, d., V and Griffiths, G. (1997). Localization of five annexins in J774 macrophages and on isolated phagosomes. *J. Cell Sci.* 110 (Pt 10), 1199-1213.

Dominguez, R. (2009). Actin filament nucleation and elongation factors--structure-function relationships. *Crit Rev. Biochem. Mol. Biol.* 44, 351-366.

East, L. and Isacke, C. M. (2002). The mannose receptor family. *Biochim. Biophys. Acta* 1572, 364-386.

Ejiri, S. (2002). Moonlighting functions of polypeptide elongation factor 1: from actin bundling to zinc finger protein R1-associated nuclear localization. *Biosci. Biotechnol. Biochem.* 66, 1-21.

Ernst, S., Lange, C., Wilbers, A., Goebeler, V., Gerke, V. and Rescher, U. (2004). An annexin 1 N-terminal peptide activates leukocytes by triggering different members of the formyl peptide receptor family. *J. Immunol.* 172, 7669-7676.

Fujita, K., Ye, L. H., Sato, M., Okagaki, T., Nagamachi, Y. and Kohama, K. (1999). Myosin light chain kinase from skeletal muscle regulates an ATP-dependent interaction between actin and myosin by binding to actin. *Mol. Cell Biochem.* 190, 85-90.

Futter, C. E. and White, I. J. (2007). Annexins and endocytosis. *Traffic.* 8, 951-958.

Gan, H., Lee, J., Ren, F., Chen, M., Kornfeld, H. and Remold, H. G. (2008). Mycobacterium tuberculosis blocks crosslinking of annexin-1 and apoptotic envelope formation on infected macrophages to maintain virulence. *Nat. Immunol.* 9, 1189-1197.

Garcia-Garcia, E. and Rosales, C. (2002). Signal transduction during Fc receptor-mediated phagocytosis. *J. Leukoc. Biol.* 72, 1092-1108.

Gavins, F. N., Yona, S., Kamal, A. M., Flower, R. J. and Perretti, M. (2003). Leukocyte antiadhesive actions of annexin 1. *Blood* 101, 4140-4147.

Gerke, V., Creutz, C. E. and Moss, S. E. (2005). Annexins: linking Ca2+ signalling to membrane dynamics. *Nat. Rev. Mol. Cell Biol.* 6, 449-461.

Gerke, V. and Moss, S. E. (1997). Annexins and membrane dynamics. *Biochim. Biophys. Acta* 1357, 129-154.

Gerke, V. and Moss, S. E. (2002). Annexins: from structure to function. *Physiol Rev.* 82, 331-371.

Gerke, V. and Weber, K. (1984). Identity of p36K phosphorylated upon Rous sarcoma virus transformation with a protein purified from brush borders; calcium-dependent binding to non-erythroid spectrin and F-actin. *EMBO J.* 3, 227-233.

Glenney, J. R., Jr., Tack, B. and Powell, M. A. (1987). Calpactins: two distinct Ca++-regulated phospholipid- and actin-binding proteins isolated from lung and placenta. *J. Cell Biol.* 104, 503-511.

Greenberg, S., Burridge, K. and Silverstein, S. C. (1990). Colocalization of F-actin and talin during Fc receptor-mediated phagocytosis in mouse macrophages. *J. Exp. Med.* 172, 1853-1856.

Griffiths, G. and Mayorga, L. (2007). Phagosome proteomes open the way to a better understanding of phagosome function. *Genome Biol.* 8, 207.

Groves, E., Dart, A. E., Covarelli, V. and Caron, E. (2008). Molecular mechanisms of phagocytic uptake in mammalian cells. *Cell Mol. Life Sci.* 65, 1957-1976.

Haas, A. (2007). The phagosome: compartment with a license to kill. *Traffic.* 8, 311-330.

Hannon, R., Croxtall, J. D., Getting, S. J., Roviezzo, F., Yona, S., Paul-Clark, M. J., Gavins, F. N., Perretti, M., Morris, J. F., Buckingham, J. C. et al. (2003). Aberrant inflammation and resistance to glucocorticoids in annexin 1-/- mouse. *FASEB J.* 17, 253-255.

Harricane, M. C., Caron, E., Porte, F. and Liautard, J. P. (1996). Distribution of annexin I during non-pathogen or pathogen phagocytosis by confocal imaging and immunogold electron microscopy. *Cell Biol. Int.* 20, 193-203.

Hayes, M. J., Rescher, U., Gerke, V. and Moss, S. E. (2004). Annexin-actin interactions. *Traffic.* 5, 571-576.

Hayhoe, R. P., Kamal, A. M., Solito, E., Flower, R. J., Cooper, D. and Perretti, M. (2006). Annexin 1 and its bioactive peptide inhibit neutrophil-endothelium interactions under flow: indication of distinct receptor involvement. *Blood* 107, 2123-2130.

Hoffmann, E., Marion, S., Mishra, B. B., John, M., Kratzke, R., Ahmad, S. F., Holzer, D., Anand, P. K., Weiss, D. G., Griffiths, G. et al. (2010). Initial receptor-ligand interactions modulate gene expression and phagosomal properties during both early and late stages of phagocytosis. *Eur. J. Cell Biol.* 89, 693-704.

Jahraus, A., Egeberg, M., Hinner, B., Habermann, A., Sackman, E., Pralle, A., Faulstich, H., Rybin, V., Defacque, H. and Griffiths, G. (2001a). ATP-dependent membrane assembly of F-actin facilitates membrane fusion. *Mol. Biol. Cell* 12, 155-170.

Jahraus, A., Egeberg, M., Hinner, B., Habermann, A., Sackman, E., Pralle, A., Faulstich, H., Rybin, V., Defacque, H. and Griffiths, G. (2001b). ATP-dependent membrane assembly of F-actin facilitates membrane fusion. *Mol. Biol. Cell* 12, 155-170.

Kang, P. B., Azad, A. K., Torrelles, J. B., Kaufman, T. M., Beharka, A., Tibesar, E., DesJardin, L. E. and Schlesinger, L. S. (2005). The human macrophage mannose receptor directs Mycobacterium tuberculosis lipoarabinomannan-mediated phagosome biogenesis. *J. Exp. Med.* 202, 987-999.

Kaufman, M., Leto, T. and Levy, R. (1996). Translocation of annexin I to plasma membranes and phagosomes in human neutrophils upon stimulation with opsonized zymosan: possible role in phagosome function. *Biochem. J.* 316 (Pt 1), 35-42.

Kiefer, F., Brumell, J., Al Alawi, N., Latour, S., Cheng, A., Veillette, A., Grinstein, S. and Pawson, T. (1998). The Syk protein tyrosine kinase is essential for Fcgamma receptor signaling in macrophages and neutrophils. *Mol. Cell Biol.* 18, 4209-4220.

Knetsch, M. L., Uyeda, T. Q. and Manstein, D. J. (1999). Disturbed communication between actin- and nucleotide-binding sites in a myosin II with truncated 50/20-kDa junction. *J. Biol. Chem.* 274, 20133-20138.

Kusumawati, A., Cazevieille, C., Porte, F., Bettache, S., Liautard, J. P. and Sri, W. J. (2000). Early events and implication of F-actin and annexin I associated structures in the phagocytic uptake of Brucella suis by the J-774A.1 murine cell line and human monocytes. *Microb. Pathog.* 28, 343-352.

Kusumawati, A., Liautard, J. P. and Sri, W. J. (2001). Implication of annexin 1 in phagocytosis: effects of n-terminal domain deletions and point mutations of the phosphorylation site Ser-27. *Cell Biol. Int.* 25, 809-813.

Kwiatkowska, K. and Sobota, A. (1999). Signaling pathways in phagocytosis. *Bioessays* 21, 422-431.

Liebl, D. and Griffiths, G. (2009). Transient assembly of F-actin by phagosomes delays phagosome fusion with lysosomes in cargo-overloaded macrophages. *J. Cell Sci.* 122, 2935-2945.

Lim, L. H. and Pervaiz, S. (2007). Annexin 1: the new face of an old molecule. *FASEB J.* 21, 968-975.

Lim, L. H., Solito, E., Russo-Marie, F., Flower, R. J. and Perretti, M. (1998). Promoting detachment of neutrophils adherent to murine postcapillary venules to control inflammation: effect of lipocortin 1. *Proc. Natl. Acad. Sci. U. S. A* 95, 14535-14539.

Mao, Y. S. and Yin, H. L. (2007). Regulation of the actin cytoskeleton by phosphatidylinositol 4-phosphate 5 kinases. *Pflugers Arch.* 455, 5-18.

Martin, G. R., Perretti, M., Flower, R. J. and Wallace, J. L. (2008). Annexin-1 modulates repair of gastric mucosal injury. *Am. J. Physiol Gastrointest. Liver Physiol* 294, G764-G769.

Martinez-Solano, L., Nombela, C., Molero, G. and Gil, C. (2006). Differential protein expression of murine macrophages upon interaction with Candida albicans. *Proteomics.* 6 Suppl 1, S133-S144.

May, R. C. and Machesky, L. M. (2001). Phagocytosis and the actin cytoskeleton. *J. Cell Sci.* 114, 1061-1077.

Mayadas, T. N. and Cullere, X. (2005). Neutrophil beta2 integrins: moderators of life or death decisions. *Trends Immunol.* 26, 388-395.

McKanna, J. A. (1995). Lipocortin 1 in apoptosis: mammary regression. *Anat. Rec.* 242, 1-10.

Miele, L., Cordella-Miele, E., Facchiano, A. and Mukherjee, A. B. (1988). Novel anti-inflammatory peptides from the region of highest similarity between uteroglobin and lipocortin I. *Nature* 335, 726-730.

Miwa, N., Uebi, T. and Kawamura, S. (2008). S100-annexin complexes--biology of conditional association. *FEBS J.* 275, 4945-4955.

Morel, E., Parton, R. G. and Gruenberg, J. (2009). Annexin A2-dependent polymerization of actin mediates endosome biogenesis. *Dev. Cell* 16, 445-457.

Morrissette, N. S., Gold, E. S., Guo, J., Hamerman, J. A., Ozinsky, A., Bedian, V. and Aderem, A. A. (1999). Isolation and characterization of monoclonal antibodies directed against novel components of macrophage phagosomes. *J. Cell Sci.* 112 (Pt 24), 4705-4713.

Moss, S. E. (1992). *The Annexins*. London: protland press limited.

Moss, S. E. and Morgan, R. O. (2004). The annexins. *Genome Biol.* 5, 219.

Nakamura, F., Huang, L., Pestonjamasp, K., Luna, E. J. and Furthmayr, H. (1999). Regulation of F-actin binding to platelet moesin in vitro by both phosphorylation of threonine 558 and polyphosphatidylinositides. *Mol. Biol. Cell* 10, 2669-2685.

Niedergang, F. and Chavrier, P. (2004). Signaling and membrane dynamics during phagocytosis: many roads lead to the phagos(R)ome. *Curr. Opin. Cell Biol.* 16, 422-428.

Niedergang, F. and Chavrier, P. (2005). Regulation of phagocytosis by Rho GTPases. *Curr. Top. Microbiol. Immunol.* 291, 43-60.

Ofek, I., Goldhar, J., Keisari, Y. and Sharon, N. (1995). Nonopsonic phagocytosis of microorganisms. *Annu. Rev. Microbiol.* 49, 239-276.

Perretti, M. (2003). The annexin 1 receptor(s): is the plot unravelling? *Trends Pharmacol. Sci.* 24, 574-579.

Perretti, M. and D'Acquisto, F. (2009). Annexin A1 and glucocorticoids as effectors of the resolution of inflammation. *Nat. Rev. Immunol.* 9, 62-70.

Perretti, M. and Flower, R. J. (1996). Measurement of lipocortin 1 levels in murine peripheral blood leukocytes by flow cytometry: modulation by glucocorticoids and inflammation. *Br. J. Pharmacol.* 118, 605-610.

Perretti, M., Getting, S. J., Solito, E., Murphy, P. M. and Gao, J. L. (2001). Involvement of the receptor for formylated peptides in the in vivo anti-migratory actions of annexin 1 and its mimetics. *Am. J. Pathol.* 158, 1969-1973.

Porte, F., de Santa, B. P., Phalipou, S., Liautard, J. P. and Widada, J. S. (1996). Change in the N-terminal domain conformation of annexin I that correlates with liposome aggregation is impaired by Ser-27 to Glu mutation that mimics phosphorylation. *Biochim. Biophys. Acta* 1293, 177-184.

Powell, M. A. and Glenney, J. R. (1987). Regulation of calpactin I phospholipid binding by calpactin I light-chain binding and phosphorylation by p60v-src. *Biochem. J.* 247, 321-328.

Rabinovitch, M. (1995). Professional and non-professional phagocytes: an introduction. *Trends Cell Biol.* 5, 85-87.

Ravetch, J. V. and Bolland, S. (2001). IgG Fc receptors. *Annu. Rev. Immunol.* 19, 275-290.

Raynal, P. and Pollard, H. B. (1994). Annexins: the problem of assessing the biological role for a gene family of multifunctional calcium- and phospholipid-binding proteins. *Biochim. Biophys. Acta* 1197, 63-93.

Rothhut, B. (1997). Participation of annexins in protein phosphorylation. *Cell Mol. Life Sci.* 53, 522-526.

Sambrook, J. and Russell, D. W. (2006). *The condensed protocols from Molecular cloning : a laboratory manual*. New York: Cold Spring Harbor Laboratory Press.

Scannell, M., Flanagan, M. B., deStefani, A., Wynne, K. J., Cagney, G., Godson, C. and Maderna, P. (2007). Annexin-1 and peptide derivatives are released by apoptotic cells and stimulate phagocytosis of apoptotic neutrophils by macrophages. *J. Immunol.* 178, 4595-4605.

Schlaepfer, D. D. and Haigler, H. T. (1987). Characterization of Ca2+-dependent phospholipid binding and phosphorylation of lipocortin I. *J. Biol. Chem.* 262, 6931-6937.

Schutt, C. (1999). Fighting infection: the role of lipopolysaccharide binding proteins CD14 and LBP. *Pathobiology* 67, 227-229.

Scott, C. C., Dobson, W., Botelho, R. J., Coady-Osberg, N., Chavrier, P., Knecht, D. A., Heath, C., Stahl, P. and Grinstein, S. (2005). Phosphatidylinositol-4,5-bisphosphate hydrolysis directs actin remodeling during phagocytosis. *J. Cell Biol.* 169, 139-149.

Seemann, J., Weber, K., Osborn, M., Parton, R. G. and Gerke, V. (1996). The association of annexin I with early endosomes is regulated by Ca2+ and requires an intact N-terminal domain. *Mol. Biol. Cell* 7, 1359-1374.

Slomianny, M. C., Dupont, A., Bouanou, F., Beseme, O., Guihot, A. L., Amouyel, P., Michalski, J. C. and Pinet, F. (2006). Profiling of membrane proteins from human macrophages: comparison of two approaches. *Proteomics.* 6, 2365-2375.

Smith, L. C., Azumi, K. and Nonaka, M. (1999). Complement systems in invertebrates. The ancient alternative and lectin pathways. *Immunopharmacology* 42, 107-120.

Stahl, P. D. and Ezekowitz, R. A. (1998). The mannose receptor is a pattern recognition receptor involved in host defense. *Curr. Opin. Immunol.* 10, 50-55.

Stuart, L. M., Boulais, J., Charriere, G. M., Hennessy, E. J., Brunet, S., Jutras, I., Goyette, G., Rondeau, C., Letarte, S., Huang, H. et al. (2007). A systems biology analysis of the Drosophila phagosome. *Nature* 445, 95-101.

Swanson, J. A. and Hoppe, A. D. (2004). The coordination of signaling during Fc receptor-mediated phagocytosis. *J. Leukoc. Biol.* 76, 1093-1103.

Takenawa, T. and Itoh, T. (2001). Phosphoinositides, key molecules for regulation of actin cytoskeletal organization and membrane traffic from the plasma membrane. *Biochim. Biophys. Acta* 1533, 190-206.

Taylor, P. R., Gordon, S. and Martinez-Pomares, L. (2005). The mannose receptor: linking homeostasis and immunity through sugar recognition. *Trends Immunol.* 26, 104-110.

Tellam, R. (1985). Mechanism of CaCl2-induced actin polymerization. *Biochemistry* 24, 4455-4460.

Thiel, C., Weber, K. and Gerke, V. (1991). Characterization of a Ca(2+)-binding site in human annexin II by site-directed mutagenesis. *J. Biol. Chem.* 266, 14732-14739.

Toyohara, A. and Inaba, K. (1989). Transport of phagosomes in mouse peritoneal macrophages. *J. Cell Sci.* 94 (Pt 1), 143-153.

Underhill, D. M. and Ozinsky, A. (2002). Phagocytosis of microbes: complexity in action. *Annu. Rev. Immunol.* 20, 825-852.

Varticovski, L., Chahwala, S. B., Whitman, M., Cantley, L., Schindler, D., Chow, E. P., Sinclair, L. K. and Pepinsky, R. B. (1988). Location of sites in human lipocortin I that are phosphorylated by protein tyrosine kinases and protein kinases A and C. *Biochemistry* 27, 3682-3690.

Vieira, O. V., Botelho, R. J. and Grinstein, S. (2002). Phagosome maturation: aging gracefully. *Biochem. J.* 366, 689-704.

Wang, W. and Creutz, C. E. (1994). Role of the amino-terminal domain in regulating interactions of annexin I with membranes: effects of amino-terminal truncation and mutagenesis of the phosphorylation sites. *Biochemistry* 33, 275-282.

Wear, M. A., Schafer, D. A. and Cooper, J. A. (2000). Actin dynamics: assembly and disassembly of actin networks. *Curr. Biol.* 10, R891-R895.

Yam, P. T. and Theriot, J. A. (2004). Repeated cycles of rapid actin assembly and disassembly on epithelial cell phagosomes. *Mol. Biol. Cell* 15, 5647-5658.

Yang, Y. H., Aeberli, D., Dacumos, A., Xue, J. R. and Morand, E. F. (2009). Annexin-1 regulates macrophage IL-6 and TNF via glucocorticoid-induced leucine zipper. *J. Immunol.* 183, 1435-1445.

Yang, Y. H., Toh, M. L., Clyne, C. D., Leech, M., Aeberli, D., Xue, J., Dacumos, A., Sharma, L. and Morand, E. F. (2006). Annexin 1 negatively regulates IL-6 expression via effects on p38 MAPK and MAPK phosphatase-1. *J. Immunol.* 177, 8148-8153.

Yeung, T. and Grinstein, S. (2007). Lipid signaling and the modulation of surface charge during phagocytosis. *Immunol. Rev.* 219, 17-36.

Yona, S., Buckingham, J. C., Perretti, M. and Flower, R. J. (2004). Stimulus-specific defect in the phagocytic pathways of annexin 1 null macrophages. *Br. J. Pharmacol.* 142, 890-898.

Yona, S., Heinsbroek, S. E., Peiser, L., Gordon, S., Perretti, M. and Flower, R. J. (2006). Impaired phagocytic mechanism in annexin 1 null macrophages. *Br. J. Pharmacol.* 148, 469-477.

Yona, S., Ward, B., Buckingham, J. C., Perretti, M. and Flower, R. J. (2005). Macrophage biology in the Anx-A1-/- mouse. *Prostaglandins Leukot. Essent. Fatty Acids* 72, 95-103.

Acknowledgment

First and foremost, I would like express my gratitude to PD Dr Sergei Kuznetsov for accepting me as a PhD student and allowing me to get introduced with the fascinating science of the cytoskeleton and phagocytosis. I am grateful to him for an experience that I will carry with me throughout my life. I thank Prof. Dieter Weiss for all those short but yet informative conversations and discussions during my whole stay. I am equally thankful to DFZ (DFG; KU1528/3; SFB629) and European Commission for Marie Curie research fellowship (MRTN-CT-2006-035946) for providing much needed financial support.

I am very much grateful to Dr Volker Gerke for providing purified proteins, plasmid constructs and valuable guidance for my manuscript preparation. I am also very grateful to Prof. Jean Gruenberg and Dr E. Morel for providing purified annexin A2 protein and pGEX AnxA2 expression vector (Department of Biochemistry, University of Geneva, Switzerland). I would also like to acknowledge my previous supervisor Dr Achyut Sinha and Dr Santanu Datta, who inspired me to undertake my graduate study. I am also thankful to Prof. Gareth Griffiths to be a referee of my PhD thesis.

Furthermore, I would like to thank all previous and recent members of the microscopy centre for all their practical help, the nice atmosphere and numerous fruitful talks about life and science. I am afraid of missing many but Furquan, Ramona, Eik, Ben, Tareck, Heiko deserve special mention. Ms Birgit Wobith deserves special thanks not only for her technical supports but also for outside laboratory helps.

I would like to thank my friends who have supported me during this journey. The years I spent in Rostock would not have been as wonderful without my friends Furquan & Sana, Rahul, Lata & Bhaskar, Ankits, Jay, Sachin, Naveen, Raymond, Marie and Ben. I am especially thankful to Dr Savvas for helping me in initial stage of my life in Rostock. Life would not have been the same without these during my stay in Rostock. I also thank other countless people I met in Rostock for the wonderful friendship they offered me

I owe deepest gratitude to my parents without their basic lessons of life; I would not be the person I am today. I obliged much more than I could ever return to them in whole my life.

My beloved wife and daughter procure special place in my acknowledgement. I cannot express my gratitude in words but I am very much grateful to them for providing much needed emotional and moral support. In their company everyday was so cheerful that I never felt ups and down. Dear, thanks a lot for standing next to me and providing me strength to fight against odds in our life.

Curriculum Vitae

Personal Information

Name:	Devang Patel
Date of Birth and Place:	26th June, 1981, Unjha, India
Current Address:	Karl Str. 15, 18055-Rostock, Germany
Permanent Address:	A-13 Samruddhi Tenament, Vatva Road, Isanpur, Ahmedabad 382443, Gujarat, India

Education

Since April 2007	PhD student at University of Rostock, Germany
March 2002 - March 2003	Masters of Applied Science (Biotechnology), University of Western Sydney, Australia
June 1998 –June 2001	Bachelor of Science (Biochemistry with vocational Biotechnology), Gujarat University, India

Research Experience

Since March 2008	Marie Curie Early Stage Researcher, Project "Role of annexin A1 in phagocytosis" University of Rostock, Germany
April 2007 – March 2008	Project Assistant, University of Rostock, DFG Project "New protein involved in phagosome F-actin interaction"
December 2003 - March 2007	Associate Research Scientist, AstraZeneca India Private Limited, Bangalore, India
March 2002 – December 2002	Masters Thesis, "Cellulolytic enzyme production in submerged fermentation"

Publications

Patel, D. M.; Ahmad S. F.; Weiss D. G.; Gerke V.; Kuznetsov S. A. (2010) Annexin A1 as a functional linker between the actin filaments and phagosomes during the phagocytosis, J. Cell. Sci. (Returned with minor revision)

Patel, D. M.; Ahmad S. F.; Weiss D. G.; Gerke V.; Kuznetsov S. A. (2010) Influence of receptor signalling on annexin A1 recruitment during Fc and Mannose receptor mediated phagocytosis. (Under preparation for FEBS Letters)

Ahmad S. F., **Patel D**. **M.**, Weiss D. G., Kuznetsov S. A.; Influence of Fcγ receptor distribution on mannose receptor mediated phagocytosis in mouse macrophages (manuscript under preparation for *J. Cell Sci.*)

Presentations and Talks

Patel, D. M.; Ahmad F.; Kuznetsov S. A. (2009) Annexin A1 as a functional linker between actin systems and Phagosome in mouse macrophages, European Molecular Biology Organization (EMBO), Amsterdam, The Netherlands, 28-1 August. (Poster presentation)

Patel, D. M.; Hoffmann E.; Ahmad F.; Kuznetsov S. A. (2008) Plasma membrane receptors define annexin-dependent interaction of mature phagosomes with F-actin. Advanced Microscopy Techniques for Immunanoscopy conference, Barcelona, Spain, 15-16 October. (Oral and Poster presentation)

Ahmad, S.F., Chtcheglova L.A., **Patel D. M.**, Wildling, L., Hinterdorfer, P. and Kuznetsov, S. A (2008) Mapping of macrophage receptors using latex bead system and atomic force microscopy. Advanced Microscopy Techniques for Immunanoscopy conference, Barcelona Spain, 15-16 October. (Poster Presentation)

Patel, D. **M.** and Kuznetsov S. (2008) New proteins involved in phagosome - F-actin interaction during the late stage of phagosome maturation. European Life Scientist Organization (ELSO) conference, Nice, France, 30 August - 2 September (Poster Presentation)

Patel, D. M. (2008) Identification of new proteins involved in F-Actin medicated transport of phagosome. Annual Phagosome Meeting, 2008, Titisee, Germany (Oral presentation)

Patel, D. **M.** and Peiris, P. (2003) Cellulolytic enzyme production from sorghum waste in submerged fermentation by *Trichoderma reesei*. Fermentation and Bio-processing Interest Group (FBIG) conference, Australia's Biotechnology Organization, Sydney 14-15 April (Poster Presentation)

Declaration

Selbstständigkeitserklärung

Ich versichere hiermit an Eides statt, dass ich die vorliegende Arbeit selbstständig angefertigt und ohne fremde Hilfe verfasst habe, keine außer den von mir angegebenen Hilfsmitteln und Quellen dazu verwendet habe und die den benutzten Werken inhaltlich und wörtlich entnommenen Stellen als solche kenntlich gemacht habe.

Rostock, 30-09-10 _____

Devang Patel

Supplementary

No	Protein name	Accession numbers	molecular weight (Kda)	Probability	Unique Peptides	%spectra covered	Unique Spectra	Identified Spectra
1	Ahnak AHNAK nucleoprotein isoform 1	IPI00553798	604.2	100%	92	2.10%	106	175
2	Myh9 Myosin-9	IPI00123181	226.3	100%	66	2.10%	85	179
3	Flna Isoform 1 of Filamin-A	IPI00131138	281.2	100%	29	0.47%	29	39
4	Pkm2 Pyruvate kinase isozyme M2	IPI00407130	58.0	100%	20	0.62%	26	52
5	Anxa2 Annexin A2	IPI00468203	38.7	100%	15	0.53%	20	44
6	Pgk1;EG433594;EG668435 phosphoglycerate kinase 1	IPI00230002	44.5	100%	13	0.33%	15	28
7	Spnb2 spectrin beta 2 isoform 2	IPI00121892	251.4	100%	13	0.18%	13	15
8	Spna2 Adult male brain cDNA, RIKEN full-length enriched library, clone:3526403B12 product:Spectrin alpha chain, brain (Spectrin, non-erythroid alpha chain) (Alpha-II spectrin) (Fodrin alpha chain) homolog (Fragment)	IPI00651953	114.1	100%	10	0.13%	10	11
9	Eef2 Elongation factor 2	IPI00466069	95.3	100%	10	0.22%	11	18
10	Spna2 similar to Spectrin alpha chain, brain (Spectrin, non-erythroid alpha chain) (Alpha-II spectrin) (Fodrin alpha chain) isoform 10	IPI00660522	235.3	100%	10	0.16%	10	13
11	Myh11 Isoform 1 of Myosin-11	IPI00114894	227.0	100%	8	0.29%	11	24
12	Msn Moesin	IPI00110588	67.8	100%	8	0.14%	8	12
13	Tkt Transketolase	IPI00137409	67.6	100%	7	0.13%	8	11
14	Pdia3 protein disulfide isomerase associated 3	IPI00230108	56.7	100%	7	0.16%	7	13
15	Jup Junction plakoglobin	IPI00229475	81.8	100%	7	0.11%	7	9
16	Tagln2 MKIAA0120 protein (Fragment)	IPI00117007	24.2	100%	7	0.16%	7	13
17	Dsp desmoplakin isoform 1	IPI00553419	332.9	100%	7	0.12%	7	10
18	2900073G15Rik myosin light chain, regulatory B-like	IPI00109044	19.9	100%	6	0.30%	8	25
19	Aldoa Fructose-bisphosphate aldolase A	IPI00221402	39.3	100%	6	0.20%	7	17
20	Prdx1 Peroxiredoxin-1	IPI00121788	22.2	100%	6	0.17%	6	14
21	Yars Tyrosyl-tRNA synthetase	IPI00314153	63.0	100%	6	0.08%	6	7
22	Krt16 Keratin intermediate filament 16a	IPI00131209	52.0	100%	6	0.08%	6	7
23	Tuba1a Tubulin alpha-1 chain	IPI00110753	50.1	100%	6	0.13%	8	11
24	Tomm34 Mitochondrial import receptor subunit TOM34	IPI00165694	34.3	100%	6	0.13%	8	11
25	Actr3 Actin-like protein 3	IPI00115627	47.3	100%	6	0.08%	6	7

No	Protein name	Accession numbers	molecular weight (Kda)	Probability	Unique Peptides	%spectra covered	Unique Spectra	Identified Spectra
26	Tubb2b Tubulin beta-2B chain	IPI00109061	49.9	100%	6	0.12%	6	10
27	EG667952;LOC671953 similar to Myosin light polypeptide 6	IPI00264053	21.9	100%	6	0.22%	6	18
28	Krt5 Keratin, type II cytoskeletal 5	IPI00139301	61.8	100%	5	0.16%	5	13
29	Mtap4 Microtubule-associated protein 4	IPI00408119	117.5	100%	5	0.07%	5	6
30	Actr2 Actin-like protein 2	IPI00177038	44.7	100%	5	0.10%	5	8
31	Stip1 Stress-induced-phosphoprotein 1	IPI00121514	62.6	100%	5	0.06%	5	5
32	Eef1a2 Elongation factor 1-alpha 2	IPI00119667	50.4	100%	5	0.16%	6	13
33	Ptpn6 Isoform 2 of Tyrosine-protein phosphatase non-receptor type 6	IPI00225419	67.7	100%	5	0.06%	5	5
34	Krt19 Keratin, type I cytoskeletal 19	IPI00112947	44.5	100%	5	0.11%	5	9
35	Cacybp Calcyclin-binding protein	IPI00115650	26.5	100%	5	0.08%	5	7
36	Krt28 similar to Keratin, type I cytoskeletal 10	IPI00750213	106.7	100%	4	0.22%	7	18
37	Eea1 Early endosome antigen 1	IPI00453776	160.9	100%	4	0.05%	4	4
38	Eef1a1 Elongation factor 1-alpha 1	IPI00307837	50.7	100%	4	0.14%	5	12
39	Krt6b Keratin, type II cytoskeletal 6B	IPI00131366	60.3	100%	3	0.18%	5	15
40	- similar to Spectrin alpha chain, brain (Spectrin, non-erythroid alpha chain) (Alpha-II spectrin) (Fodrin alpha chain) isoform 38	IPI00137368	66.3	100%	3	0.05%	3	4
41	Arpc1b Arpc1b protein	IPI00125143	41.5	100%	3	0.05%	3	4
42	- 39 kDa protein	IPI00133580	39.4	100%	3	0.12%	3	10
43	Snx22;Ppib peptidylprolyl isomerase B	IPI00135686	23.7	100%	3	0.07%	4	6
44	Arpc4;Ttll3 Actin-related protein 2/3 complex subunit 4	IPI00138691	19.6	100%	3	0.07%	3	6
45	Krt14 Keratin, type I cytoskeletal 14	IPI00227140	52.9	100%	3	0.10%	3	8
46	Eef1b2 Elongation factor 1-beta	IPI00320208	24.7	100%	3	0.10%	4	8
47	Hmgb2 High mobility group protein B2	IPI00462291	24.1	100%	3	0.05%	3	4
48	Lrrfip1 Isoform 2 of Leucine-rich repeat flightless-interacting protein 1	IPI00117277	71.3	100%	3	0.05%	3	4
49	Hist1h1c Histone H1.2	IPI00223713	21.2	100%	3	0.04%	3	3
50	Anxa1 Annexin A1	IPI00230395	38.7	100%	3	0.05%	3	4
51	Fus RNA-binding protein FUS	IPI00117063	52.7	100%	3	0.04%	3	3
52	Thoc4 Isoform 1 of THO complex subunit 4	IPI00114407	26.9	100%	3	0.04%	3	3
53	Mdh2 Malate dehydrogenase, mitochondrial precursor	IPI00323592	35.6	100%	3	0.05%	4	4

No	Protein name	Accession numbers	molecular weight (Kda)	Probability	Unique Peptides	%spectra covered	Unique Spectra	Identified Spectra
54	Eef1g Elongation factor 1-gamma	IPI00318841	50.0	100%	2	0.04%	2	3
55	Acta1 Actin, alpha skeletal muscle	IPI00110827	42.0	100%	2	0.04%	3	3
56	Cct8 T-complex protein 1 subunit theta	IPI00469268	59.5	100%	2	0.04%	2	3
57	Coro1a Coronin-1A	IPI00323600	51.0	100%	2	0.02%	2	2
58	Rcc2 Protein RCC2	IPI00222509	56.0	100%	2	0.02%	2	2
59	Mtap4 Mtap4 protein	IPI00406741	91.4	100%	2	0.04%	2	3
60	Krt42 Type I keratin KA22	IPI00468696	50.1	100%	2	0.13%	3	11
61	Krt79 Keratin 79	IPI00124499	57.5	100%	2	0.10%	3	8
62	Krt1 Keratin, type II cytoskeletal 1	IPI00625729	65.6	100%	2	0.08%	3	7
63	Tcea1 Isoform 2 of Transcription elongation factor A protein 1	IPI00121887	33.9	100%	2	0.02%	2	2
64	Dync1i2 Cytoplasmic dynein 1 intermediate chain 2	IPI00131086	68.4	100%	2	0.04%	2	3
65	Krt13 Isoform 1 of Keratin, type I cytoskeletal 13	IPI00136056	47.7	100%	2	0.04%	2	3
66	Got2 Aspartate aminotransferase, mitochondrial precursor	IPI00117312	47.4	100%	2	0.02%	2	2
67	Krt17 Keratin, type I cytoskeletal 17	IPI00230365	48.1	100%	2	0.02%	2	2
68	Krt76 Adult female vagina cDNA, RIKEN full-length enriched library, clone:9930024P18 product:similar to Keratin 2p	IPI00346834	62.8	100%	2	0.07%	3	6
69	Krt6a Keratin, type II cytoskeletal 6A	IPI00131368	59.3	100%	2	0.04%	2	3
70	Hspa1l Heat shock 70 kDa protein 1L	IPI00133208	70.6	100%	2	0.04%	2	3
71	Tpr Nuclear pore complex-associated intranuclear coiled-coil protein TPR	IPI00177059	267.0	100%	2	0.02%	2	2
72	- 21 kDa protein	IPI00339996	20.5	100%	2	0.04%	2	3
73	Fen1 Adult male testis cDNA, RIKEN full-length enriched library, clone:4930584I03 product:flap structure specific endonuclease 1, full insert sequence	IPI00410836	45.8	100%	2	0.04%	2	3
74	Lrrfip1 Isoform 1 of Leucine-rich repeat flightless-interacting protein 1	IPI00654388	79.2	100%	2	0.04%	2	3
75	Krt42 ES cells cDNA, RIKEN full-length enriched library, clone:2410129K01 product:similar to RADIATED KERATINOCYTE MRNA 266	IPI00420316	26.3	99%	2	0.05%	2	4
76	Actb Actin, cytoplasmic 1	IPI00110850	41.7	89%	2	0.05%	2	4

No	Protein name	Accession numbers	molecular weight (Kda)	Probability	Unique Peptides	%spectra covered	Unique Spectra	Identified Spectra
77	Krt73 Keratin 73	IPI00347110	58.9	100%	1	0.11%	2	9
78	Hspa8 Heat shock cognate 71 kDa protein	IPI00323357	70.9	100%	1	0.01%	1	1
79	Arpc2 Actin-related protein 2/3 complex subunit 2	IPI00661414	34.3	100%	1	0.02%	1	2
80	Eif4h Isoform Long of Eukaryotic translation initiation factor 4H	IPI00124742	27.3	100%	1	0.01%	1	1
81	EG433073 similar to actin related protein 2/3 complex subunit 2	IPI00461936	21.4	100%	1	0.01%	1	1
82	Ube2i SUMO-conjugating enzyme UBC9	IPI00119227	18.0	100%	1	0.02%	1	2
83	Eif5a Eukaryotic translation initiation factor 5A-1	IPI00108125	16.8	100%	1	0.02%	1	2
84	Psat1 Phosphoserine aminotransferase	IPI00115620	40.5	100%	1	0.01%	1	1
85	LOC213079 similar to High mobility group protein 1	IPI00355265	20.3	100%	1	0.01%	1	1
86	Krt2 keratin complex 2, basic, gene 17	IPI00622240	70.9	100%	1	0.05%	1	4
87	Hn1l Hematological and neurological expressed 1-like protein	IPI00107958	20.0	100%	1	0.01%	1	1
88	Pin4;EG628161 Peptidyl-prolyl cis-trans isomerase NIMA-interacting 4	IPI00109696	13.8	100%	1	0.02%	1	2
89	Tubb5 Tubulin beta-5 chain	IPI00117352	49.7	100%	1	0.02%	1	2
90	EG622339 similar to Glyceraldehyde-3-phosphate dehydrogenase	IPI00123176	36.5	100%	1	0.02%	1	2
91	Rbmx Heterogeneous nuclear ribonucleoprotein G	IPI00124979	42.3	100%	1	0.01%	1	1
92	Arpc5 Actin-related protein 2/3 complex subunit 5	IPI00399943	16.3	100%	1	0.01%	1	1
93	Calm2;Calm3;Calm1 12 days pregnant adult female placenta cDNA, RIKEN full-length enriched library, clone:I530005B05 product:calmodulin 1, full insert sequence	IPI00467841	21.5	100%	1	0.01%	1	1
94	Nefh Neurofilament triplet H protein	IPI00114241	117.0	100%	1	0.02%	1	2
95	1700009N14Rik RIKEN cDNA 1700009N14 gene	IPI00127109	24.3	100%	1	0.01%	1	1
96	Myo1e myosin IE	IPI00330649	126.8	99%	1	0.01%	1	1
97	Aldoc Fructose-bisphosphate aldolase C	IPI00119458	39.4	99%	1	0.01%	1	1
98	Prdx2 Peroxiredoxin-2	IPI00117910	21.8	99%	1	0.02%	1	2
99	Gfap Isoform 1 of Glial fibrillary acidic protein, astrocyte	IPI00117042	49.9	98%	1	0.12%	2	10
100	Cct5 T-complex protein 1 subunit epsilon	IPI00116279	59.6	98%	1	0.01%	1	1
101	Dnahc6 similar to Dynein heavy chain at 16F CG7092-PA	IPI00408085	468.6	98%	1	0.01%	1	1
102	Icam2 Intercellular adhesion molecule 2 precursor	IPI00117424	31.4	94%	1	0.01%	1	1
103	Krt2 Keratin (Fragment)	IPI00463282	25.3	89%	1	0.14%	2	12

No	Protein name	Accession numbers	molecular weight (Kda)	Probability	Unique Peptides	%spectra covered	Unique Spectra	Identified Spectra
104	Sytl3 Isoform 1 of Synaptotagmin-like protein 3	IPI00118098	68.5	89%	1	0.02%	2	2
105	Krt25 Keratin 25	IPI00122621	48.9	89%	1	0.10%	1	8
106	Arpc3 Actin-related protein 2/3 complex subunit 3	IPI00124829	20.5	89%	1	0.04%	2	3
107	Try4;1810049H19Rik Pancreatic trypsin	IPI00128108	26.3	89%	1	0.08%	2	7
108	Prss1 Trypsinogen 16	IPI00130391	26.1	89%	1	0.05%	2	4
109	Myl6b Myosin light polypeptide 6B	IPI00261638	22.7	89%	1	0.04%	1	3
110	Krt72 Type-II keratin Kb35	IPI00347096	56.7	89%	1	0.06%	2	5
111	Krt78 keratin Kb40	IPI00348328	89.8	89%	1	0.07%	2	6
112	Myl6 Isoform Smooth muscle of Myosin light polypeptide 6	IPI00354819	16.9	89%	1	0.02%	1	2
113	Ddef2 Isoform 1 of Development and differentiation-enhancing factor 2	IPI00355808	106.8	89%	1	0.05%	2	4
114	Ahnak Ahnak protein	IPI00408251	18.7	89%	1	0.02%	2	2
115	Hmgb1 High mobility group protein B1	IPI00420261	24.9	89%	1	0.02%	1	2
116	Prdx4 Peroxiredoxin-4	IPI00116254	31.0	89%	1	0.04%	1	3
117	Was Wiskott-Aldrich syndrome protein homolog	IPI00108084	54.2	89%	1	0.01%	1	1
118	LOC629750;LOC639383 similar to ubiquitin A-52 residue ribosomal protein fusion product 1	IPI00108590	15.4	89%	1	0.01%	1	1
119	Tubb4 Tubulin beta-4 chain	IPI00109073	49.5	89%	1	0.01%	1	1
120	Psma8 Proteasome subunit alpha type 7-like	IPI00109122	27.8	89%	1	0.01%	1	1
121	Hnrpa0 12 days embryo head cDNA, RIKEN full-length enriched library, clone:3010025E17 product:Heterogeneous nuclear ribonucleoprotein A0 (hnRNP A0) homolog	IPI00109813	30.5	89%	1	0.01%	1	1
122	Naca Nascent polypeptide-associated complex subunit alpha, muscle-specific form	IPI00111831	220.6	89%	1	0.01%	1	1
123	Fabp5 Fatty acid-binding protein, epidermal	IPI00114162	15.1	89%	1	0.01%	1	1
124	Ndph Norrin precursor	IPI00114341	14.7	89%	1	0.02%	1	2
125	Fnbp1 Formin binding protein 1	IPI00116278	64.6	89%	1	0.01%	1	1
126	- 18 kDa protein	IPI00116718	17.9	89%	1	0.01%	1	1
127	Tuba1b Tubulin alpha-2 chain	IPI00117348	50.1	89%	1	0.02%	1	2
128	Mapre1 Microtubule-associated protein RP/EB family member 1	IPI00117896	30.0	89%	1	0.01%	1	1

No	Protein name	Accession numbers	molecular weight (Kda)	Probability	Unique Peptides	%spectra covered	Unique Spectra	Identified Spectra
129	Snrpd3 Small nuclear ribonucleoprotein Sm D3	IPI00119224	13.9	89%	1	0.02%	1	2
130	Sprr2b Small proline-rich protein 2B	IPI00119361	10.7	89%	1	0.04%	1	3
131	Plek Pleckstrin	IPI00119551	39.9	89%	1	0.01%	1	1
132	Hvcn1 hydrogen voltage-gated channel 1	IPI00120788	31.2	89%	1	0.01%	1	1
133	Tmem40 Transmembrane protein 40	IPI00122469	24.9	89%	1	0.01%	1	1
134	Rasl2-9 GTP-binding nuclear protein Ran, testis-specific isoform	IPI00126133	24.4	89%	1	0.01%	1	1
135	Mtcp1 P8 MTCP-1 protein	IPI00127299	7.7	89%	1	0.01%	1	1
136	Cspg4 Isoform 1 of Chondroitin sulfate proteoglycan 4 precursor	IPI00128915	252.4	89%	1	0.01%	1	1
137	Cdh16 Cadherin-16 precursor	IPI00129960	89.8	89%	1	0.01%	1	1
138	2210010C04Rik trypsinogen 7	IPI00131674	26.4	89%	1	0.04%	1	3
139	Psma6 Proteasome subunit alpha type 6	IPI00131845	27.4	89%	1	0.01%	1	1
140	Ran GTP-binding nuclear protein Ran	IPI00134621	24.4	89%	1	0.01%	1	1
141	Uba52;LOC669193;LOC676687;LOC666586 Uba52 protein	IPI00138892	14.7	89%	1	0.01%	1	1
142	4933402J07Rik Adult male testis cDNA, RIKEN full-length enriched library, clone:4933402J07 product:weakly similar to HYPOTHETICAL 30.8 kDa PROTEIN	IPI00222019	31.2	89%	1	0.01%	1	1
143	Gpr128 Probable G-protein coupled receptor 128 precursor	IPI00222961	87.7	89%	1	0.01%	1	1
144	Srebf1 Isoform SREBP-1A-W42 of Sterol regulatory element-binding protein 1	IPI00223219	116.2	89%	1	0.01%	1	1
145	Man2a2 N-glycan processing alpha-mannosidase IIx	IPI00224294	130.6	89%	1	0.01%	1	1
146	Hmgb1l;LOC625781 HMG-L6	IPI00229570	23.1	89%	1	0.02%	1	2
147	- 18 kDa protein	IPI00277450	18.1	89%	1	0.04%	1	3
148	Chchd2 Coiled-coil-helix-coiled-coil-helix domain-containing protein 2	IPI00284925	15.6	89%	1	0.01%	1	1
149	Kcnab2 Voltage-gated potassium channel subunit beta-2	IPI00315359	41.0	89%	1	0.01%	1	1
150	Ewsr1 Ewing sarcoma homolog	IPI00322492	69.0	89%	1	0.01%	1	1
151	Myh10 Myosin, heavy polypeptide 10, non-muscle	IPI00338604	232.6	89%	1	0.01%	1	1
152	Trim40 Adult male cecum cDNA, RIKEN full-length enriched library, clone:9130003O04 product:hypothetical Zn-finger, B-box/Zn-finger, RING containing protein, full insert sequence	IPI00355276	27.9	89%	1	0.01%	1	1

No	Protein name	Accession numbers	molecular weight (Kda)	Probability	Unique Peptides	%spectra covered	Unique Spectra	Identified Spectra
153	Lyst Isoform 1 of Lysosomal-trafficking regulator	IPI00399954	425.4	89%	1	0.01%	1	1
154	6330407J23Rik Uncharacterized protein C6orf174 homolog precursor	IPI00403618	103.5	89%	1	0.01%	1	1
155	Armet Armet protein	IPI00404019	19.0	89%	1	0.01%	1	1
156	Osbpl1a RCB-0545 OHTA cDNA, RIKEN full-length enriched library, clone:G430090F17 product:similar to OSBP-RELATED PROTEIN 1	IPI00404881	44.3	89%	1	0.01%	1	1
157	EG229574 Filaggrin 2	IPI00406870	251.4	89%	1	0.02%	1	2
158	Slc1a1 Solute carrier family 1 (Neuronal/epithelial high affinity glutamate transporter, system Xag), member 1	IPI00420244	56.7	89%	1	0.01%	1	1
159	Psma2 In vitro fertilized eggs cDNA, RIKEN full-length enriched library, clone:7420458H06 product:proteasome (prosome, macropain) subunit, alpha type 2, full insert sequence	IPI00420745	27.5	89%	1	0.01%	1	1
160	BC033915 Isoform 1 of Serine/threonine-protein kinase QSK	IPI00453673	145.8	89%	1	0.04%	1	3
161	- 18 kDa protein	IPI00458341	18.1	89%	1	0.01%	1	1
162	Dmn Synemin isoform H	IPI00469184	173.2	89%	1	0.01%	1	1
163	Eif2s1 Eukaryotic translation initiation factor 2 subunit 1	IPI00474446	36.1	89%	1	0.01%	1	1
164	Ppia Peptidyl-prolyl cis-trans isomerase A	IPI00554989	18.0	89%	1	0.02%	1	2
165	Spna2 similar to Spectrin alpha chain, brain (Spectrin, non-erythroid alpha chain) (Alpha-II spectrin) (Fodrin alpha chain) isoform 14	IPI00661701	278.2	89%	1	0.01%	1	1
166	Lgr4 Leucine-rich repeat-containing G protein-coupled receptor 4	IPI00667018	101.3	89%	1	0.01%	1	1
167	Myh9 15 days pregnant adult female amnion cDNA, RIKEN full-length enriched library, clone:M421002E03 product:myosin heavy chain IX, full insert sequence	IPI00788324	226.4	89%	1	0.04%	1	3
168	Krt14 Type I epidermal keratin (Fragment)	IPI00828528	10.6	89%	1	0.02%	1	2
169	Gzma Isoform HF2 of Granzyme A precursor (Fragment)	IPI00229002	28.5	89%	1	0.01%	1	1
170	Zcchc5 Zinc finger, CCHC domain containing 5	IPI00345024	61.4	87%	1	0.01%	1	1
171	9130023D20Rik RIKEN cDNA 9130023D20 gene	IPI00453534	63.4	87%	1	0.01%	1	1
172	Gan similar to gigaxonin	IPI00749533	33.2	85%	1	0.01%	1	1
173	BB220380 Isoform 1 of Phosphoinositide 3-kinase regulatory subunit 6	IPI00169971	84.6	76%	1	0.04%	1	3
174	Gpr126 Developmentally regulated G-protein-coupled receptor	IPI00461962	129.7	67%	1	0.01%	1	1

No	Protein name	Accession numbers	molecular weight (Kda)	Probability	Unique Peptides	%spectra covered	Unique Spectra	Identified Spectra
175	- Endogenous murine leukemia virus polytropic provirus DNA, complete cds	IPI00761472	63.9	58%	1	0.01%	1	1
176	Hivep2 Human immunodeficiency virus type I enhancer-binding protein 2 homolog	IPI00115900	266.7	56%	1	0.01%	1	1
177	Inhba Inhibin beta A chain precursor	IPI00112347	47.4	53%	1	0.01%	1	1
178	Prrx1 Isoform PMX1-B of Paired mesoderm homeobox protein 1	IPI00118248	27.3	46%	1	0.01%	1	1
179	Alg13 Probable glycosyltransferase GLT28D1	IPI00108727	18.3	43%	1	0.02%	1	2